VNIVERSITAT DE VALÈNCIA

Relationship of morphokinetics and gene expression in the generation of aneuploidies in the human embryo

Author

María Vera Rodríguez

Supervisors

Dra. Carmen Rubio Lluesa

Dr. Carlos Simón Vallés

Facultad de ciencias biológicas
Departamento de bioquímica y biología molecular
Programa de doctorado en biomedicina y biotecnología

Relationship of morphokinetics and gene expression in the generation of aneuploidies in the human embryo

Relación de la morfocinética y la expresión génica en la generación de aneuploidías en el embrión humano

Author
María Vera Rodríguez

This dissertation is submitted for the degree of
Doctor of Philosophy
at the University of Valencia

Supervisors
Dra. Carmen Rubio Lluesa
Prof. Carlos Simón Vallés

Advisor
Prof. Antonio Pellicer Martínez

April 2017

La Dra. Carmen Rubio Lluesa, Doctora en Biológicas por la Facultad de Ciencias en la Universidad de Valencia, y el Prof. Carlos Simón Vallés, Catedrático de Obstetricia y Ginecología de la Facultad de Medicina en la Universidad de Valencia y Profesor Asociado de la Universidad de Stanford,

CERTIFICAN que la Licenciada en Biotecnología MARÍA VERA RODRÍGUEZ ha realizado bajo su dirección el trabajo que lleva por título "Relationship of morphokinetics and gene expression in the generation of aneuploidies in the human embryo", y autorizan a su presentación y defensa para optar al grado de doctor en Biomedicina y Biotecnología de la Facultad de Ciencias Biológicas de la Universidad de Valencia.

Y para que así conste, expiden y firman el presente certificado en Valencia, a 3 de Abril de 2017.

Dra. Carmen Rubio Lluesa

Prof. Carlos Simón Vallés

A mi padre,
el mayor científico que conozco.
A Juanma,
por enseñarme a ver más allá.

Agradecimientos

A Carmen Rubio, por acompañarme a lo largo del camino, siempre a mi lado, enseñándome y escuchándome. Por mostrarme que la actitud es, de hecho, lo más importante y contagiarme así su filosofía de vida. Su sonrisa y su afán por seguir aprendiendo me los llevo como un tesoro encontrado a la orilla del mar.

A Carlos Simón, por darme alas para llegar lejos, literalmente. Por confiar en mí y hacerme sentir valorada; por hacer así que yo también confiara en mí.

A mis compañeros de *PGS*, por orden alfabético en honor a la lista del acta, Asun, Chiti, Emi, Lorena, Miguel, Nasser, Sandra y Vanessa, con quienes todo empezó. Gracias por enseñarme que trabajar, mucho, no está reñido con reír, mucho. Os quiero. Luego llegaron Tantra, Pilar, Lucía y Azarina, para hacer el departamento aún más especial si cabía. Y aunque nos desperdigamos, ya sabéis, "la Rubio" hace escuela, por lo que siempre estaremos conectados, aunque sea leyendo el horóscopo a final de cada año, y aquí también entra Eva.

Al resto de compañeros de *Igenomix*, a los de los comienzos y a los que llegaron después, pero parecían de los de siempre. A los que me han enseñado durante todos estos años, y a los que se han limitado a sacarme sonrisas. Porque en mi tesis hay escritos experimentos, pero entre las líneas os leo a todos vosotros.

A mis maestras embriólogas del IVI, por orden de aparición, MJ Escribá, MJ Santos, Laura, Amparo, Pili, Txuki y Diana, por contagiarme vuestras inquietudes, por alargar vuestras jornadas para enseñarme, por vuestra paciencia y por ayudarme.

To Renee, for taking me in her group and making me feel part of it from the very first day. For sharing your enthusiasm for science and filling my notebook with her inspirational quotes. To Shawn, for holding my hand and being my partner in crime, "holy cow!". To Mark, for sharing hours *in & out* the lab, for

brainstorming, for the frozen yogurts, for belaying me, for your advices, and a long etcetera. To the rest of the *RRP* lab, Jenny, Bahareh, Sonya, Vittorio, Antonia, and others, you filled my stay with great science, and more importantly, with great memories, which make me miss California every single day.

A mi padre, por enseñarme desde pequeña que para todo hay una respuesta. Por contagiarme con sus experimentos a ras de la tierra. Por ser una fuente inagotable de sabiduría.

A mi madre, por leerse mis libros de clase mientras yo dormía. Por sacrificarse sin esperar nunca nada a cambio. Por enseñarme que la ciencia más sincera está intrínseca en ella.

A mis hermanas, porque las ramas siempre permanecen unidas por muy alto que lleguen. Por apoyarme por el camino, por escucharme, por permitirme ser siempre yo, sin filtros.

A Juanma, por creer en mí, el que más. Por saltar conmigo al vacío, sin mirar si quiera cuan alto es el precipicio. Esta tesis es tan tuya como mía.

Y a Vera, por sentarse en la balanza de mi vida y enseñarme, tan pronto, tanto.

Gracias

Summary

Over the last 20 years, the number of assisted reproduction procedures has drastically increased, and this trend is expected to continue as parenthood is postponed. In Europe, more than half a million in vitro fertilization (IVF) cycles are performed annually, resulting in 100,000 newborns. With the increased use of assisted reproduction, a concomitant increase in success rates would also be expected. However, the pregnancy rate per cycle has remained constant over the same 10-year range, despite important progress in the field. The majority of women using assisted reproduction are over 35 years old, and this needs to be taken into consideration since the rate of chromosomal abnormalities in the oocytes increases with age. As a consequence, advanced maternal age may result in an increase in the number of aneuploid embryos, which would be translated into high miscarriage rates and low live-birth rates. Since we are not able to modify the IVF population or to change embryo quality, our goal should be to focus on improving IVF techniques. Such improvement necessitates a better understanding of the etiology of embryo aneuploidies. Recent advances in imaging and molecular and genetic analyses are postulated as promising strategies to unveil the mechanisms involved in aneuploidy generation. Thus, our goal was to analyse, simultaneously in the same human embryo, morphology, kinetics, transcriptomics and genetics to find a correlation between these parameters in the origin of aneuploidies.

Here we combine time-lapse, complete chromosomal assessment and single-cell real-time quantitative PCR to simultaneously obtain information from all cells that compose a human embryo until the approximately eight-cell stage. Our data indicate that the chromosomal status of aneuploid embryos correlates with significant differences in the kinetic pattern when compared with euploid embryos, especially in the duration of the first mitotic phase. We also demonstrate that embryo kinetics is affected by the existence of irregular

divisions during development, and this should be taken into consideration for future studies. Gene expression analyses reveal that embryonic genome activation starts as early as the zygote stage. Moreover, gene expression profiling suggests that a subset of genes is differentially expressed in aneuploid embryos during the first 30 hours of development. Thus, we propose that the chromosomal fate of an embryo is likely determined as early as the pronuclear stage and may be predicted by a 12-gene transcriptomic signature. Finally, the atlas generated from the data obtained in this study shows the high variability underlying human embryo development. While euploid embryos seem to follow a uniform development without high variability for morphokinetics, aneuploid embryos may follow different pathways, overlapping with and mimicking euploid embryos in some cases, making them hard to differentiate.

Resumen

Introducción

Durante los últimos veinte años, el número de procedimientos de reproducción asistida ha aumentado drásticamente e, igualmente, se espera que continúe aumentando debido al retraso existente en la maternidad. En Europa se realizan más de medio millón de ciclos de fecundación *in vitro* (FIV) cada año, dando lugar a aproximadamente 100.000 recién nacidos, lo cual equivale al 1.5% de niños nacidos en Europa.

Junto con la expansión en el campo de la reproducción asistida, el número de avances, tanto técnicos como científicos, también ha ido en aumento. Sin embargo, a pesar de los esfuerzos, las tasas de embarazo por ciclo han permanecido constantes durante los últimos diez años. Las características de la población que hace uso de estos tratamientos, cuya edad sobrepasa los 35 años en más del 70% de los casos, puede estar correlacionada con la existencia de este techo de cristal, ya que se ha descrito que la tasa de anomalías cromosómicas aumenta significativamente con la edad materna. Como consecuencia, los embriones fecundados *in vitro* a partir de ovocitos de mujeres de edad materna avanzada tienen una mayor probabilidad de ser cromosómicamente anormales, lo cual tiene como consecuencia un aumento en las tasas de aborto y una disminución en las de recién nacido vivo.

Puesto que no existe la posibilidad de modificar las características de la población que requiere tratamientos de FIV, al menos desde un punto de vista clínico, ni tampoco la de modificar la calidad embrionaria a nivel genético, el objetivo actual debería estar dirigido a mejorar las técnicas empleadas durante los tratamientos de FIV para minimizar el posible efecto sobre la calidad embrionaria. Para el desarrollo de nuevas herramientas de cultivo y selección embrionaria es necesario un mejor conocimiento de la biología de los

embriones humanos. Sin embargo, debido al uso limitado de estos para fines científicos, el número de estudios en embriones completos y de buena calidad es muy limitado. Y esto, junto a la naturaleza multifactorial de las anomalías cromosómicas, ha hecho aún más complejo encontrar los mecanismos relacionados con las causas y consecuencias de la existencia de aneuploidías durante el desarrollo embrionario.

Los avances tecnológicos más recientes en análisis de imagen, análisis molecular y genético se presentan como una prometedora estrategia para desvelar la maquinaria implicada en la generación de aneuploidías. Así, nuestra hipótesis es que tanto la morfología, la cinética, como la transcriptómica del embrión están relacionados con la existencia de aneuploidías, ya sea como causa o como efecto, y un estudio simultáneo de todos estos parámetros en un mismo embrión podría permitir entender mejor la biología del desarrollo preimplantacional humano.

Objetivos

El objetivo general de este estudio fue investigar en detalle el origen y las consecuencias de la aparición de aneuploidías durante el desarrollo preimplantacional del embrión humano. Para ello, se llevaron a cabo los siguientes objetivos específicos:

- **O1.** Realización de un análisis descriptivo del embrión humano a cuatros niveles diferentes: morfología, cinética, transcriptómica y tasa de aneuploidías.

- **O2.** Estudio de las posibles relaciones entre morfología, patrones cinéticos, expresión génica y existencia de aneuploidías.

- **O3.** Desarrollo de un modelo de predicción de aneuploidías basado en las diferencias más significativas encontradas entre embriones aneuploides y euploides.

- **O4.** Integración de los datos sobre morfocinética, transcriptómica y aneuploidías para crear un atlas único sobre el desarrollo preimplantacional humano.

Métodos

Se descongelaron ciento diecisiete (117) cigotos humanos donados a investigación provenientes de 19 parejas con una edad media materna de 33.7 ± 4.3 años. De ellos, sobrevivieron Ochenta y cinco cigotos, los cuales fueron cultivados usando la tecnología de *time-lapse,* que permite crear una película del desarrollo embrionario a partir de fotografías tomadas cada 5 minutos. Los embriones fueron cultivados durante diferentes tiempos incluyendo el estadio pronuclear y las siete primeras divisiones mitóticas. Tras el cultivo, cada embrión se desagregó en células individuales, incluyendo los corpúsculos polares en aquellos en estadio de cigoto. La mitad de las células de cada embrión se amplificaron usando la técnica de WGA (*Whole* Genome Amplification), que permite la amplificación de ADN a nivel de célula única, para ser analizadas posteriormente mediante *arrays* de CGH (*Comparative genomic hybridization*) y determinar así su dotación cromosómica. Por otro lado, la otra mitad de las células de cada embrión se analizaron mediante PCR cuantitativa mediante un sistema de microfluidos que permitía el análisis a nivel de célula única. Así, se estudió la expresión de 86 genes relacionados con la existencia de aneuploidías en la bibliografía previa para determinar el perfil transcriptómico de los embriones. Finalmente, se correlacionaron los parámetros morfocinéticos, obtenidos en las películas de *time-lapse*, el estadio cromosómico y los niveles de expresión génicos para cada embrión.

Conclusiones

C1. Los parámetros morfológicos pueden tener un comportamiento dinámico durante el desarrollo embrionario. En concreto, los fragmentos celulares, los cuales aparecen mayoritariamente durante la primera división mitótica del embrión pueden dividirse, fusionarse a otros fragmentos o ser reabsorbidos por blastómeras.

C2. Los parámetros cinéticos se ven alterados por la existencia de divisiones irregulares durante el desarrollo embrionario, por lo cual estos deben calcularse de manera independiente según el tipo de división para evitar conclusiones confusas.

C3. Más de la mitad de los embriones humanos en este estudio, provenientes de pacientes de técnicas de reproducción asistida fueron aneuploides. Además, según los resultados, la incidencia de aneuploidías está correlacionada con la existencia de multinucleación, aunque no con la existencia de fragmentación o vacuolas en el embrión.

C4. Durante el desarrollo embrionario, encontramos grupos de genes con diferentes patrones de expresión según su origen de transcripción: materno, embrionario o ambos. Además, se observó que la activación embrionaria ocurre desde el estadio más temprano del embrión humano, el cigoto.

C5. La cinética de los embriones aneuploides está alterada en comparación con los euploides. En concreto, el tiempo entre la desaparición pronuclear y el comienzo de la primera citocinesis fue más largo en los embriones aneuploides. Además, el tiempo entre los estadios de tres y cuatro células fue también más largo en los embriones aneuploides, aunque esta diferencia se debió a la mayor proporción de embriones aneuploides con divisiones irregulares, las cuales alteran el patrón cinético embrionario.

C6. El perfil transcriptómico de los embriones aneuploides mostró diferencias estadísticamente significativas durante las primeras 30 horas de desarrollo frente al de los embriones euploides. Gracias a estas diferencias, se comprobó que la existencia de aneuploidías en los embriones en estadio de células se puede predecir haciendo uso de una firma transcriptómica basada en 12 genes.

C7. El atlas del embrión humano generado con los datos de este estudio muestra una alta variabilidad durante el desarrollo preimplantacional embrionario. Mientras que los embriones euploides parecen seguir una única ruta para desarrollarse satisfactoriamente sin mucha variabilidad en su morfocinética, los embriones aneuploides siguen múltiples rutas, solapándose y camuflándose en ocasiones con el comportamiento de los embriones euploides, dificultando así su diferenciación mediante técnicas no-invasivas.

Table of contents

List of figures

List of tables

Abbreviations

aCGH Comparative genomic hybridization arrays
AKT1 V-akt murine thymoma viral oncogene homolog 1
AMA Advanced maternal age
ANOVA Analysis of variance
ART Assisted reproductive technology
AUC Area under the curve
AURKA Aurora kinase A
BRCA1 Breast cancer 1
BUB1 BUB1 mitotic checkpoint serine/threonine kinase
BUB3 BUB3 mitotic checkpoint protein
CASP2 Caspase 2
CCNA1 Cyclin A1
CCND1 Cyclin D1
CDH1 Cadherin 1
CDK7 Cyclin-dependent kinase 7
CFL1 Cofilin 1
COS Controlled ovarian stimulation
CRY1 Cryptochrome circadian clock 1
C_t Threshold cycle
CTNNB1 Catenin beta 1
DAPI 4',6-diamino-2-fenilindol
DDX20 DEAD-box helicase 20
DDX4 DEAD-box helicase 4
DIAPH1 Diaphanous related formin 1
DNA Deoxyribonucleic acid
DNMT1 DNA methyltransferase 1
DNMT3B DNA methyltransferase 3b
DPPA3 Developmental pluripotency associated 3
E2F1 E2F transcription factor 1

EGA Embryonic genome activation
EPI Epiblast
ET Embryo transfer
FASLG Fas ligand
FISH Fluorescence *in situ* hybridization
GADD45A Growth arrest and DNA-damage-inducible alpha
GAPDH Glyceraldehyde-3-phosphate dehydrogenase
GO Gene ontology
GV Germinal vesicle
h Hours
HA Human albumin
ICM Inner cell mass
ICSI Intracytoplasmic sperm injection
IQR Interquartile range
IVF *In vitro* fertilization
k-NN K-nearest neighbors algorithm
M Molar
MCC Matthews correlation coefficient
MCL1 Myeloid cell leukemia 1
MI Metaphase I
MII Metaphase II
min Minutes
mL Milliliter
mRNA Messenger ribonucleic acid
ms Milliseconds
MSH2 Muts homolog 2
MSH3 Muts homolog 3
MSH6 Muts homolog 6
MSY2 Mouse Y-box protein
MZT Maternal-zygotic transition
NADPH Nicotinamide adenine dinucleotide phosphate
NGS Next-generation sequencing
NLRP5 NLR family, pyrin domain containing 5
NPM2 Nucleophosmin/ nucleoplasmin 2
OOEP The oocyte expressed protein
PADI6 Peptidyl arginine deiminase type VI
PBS Phosphate-buffered saline

PCR Polymerase chain reaction
PDCD5 Programmed cell death 5
PE Primitive endoderm
pET Personalized embryo transfer
PER1 Period circadian clock 1
PGS Preimplantation genetic screening
PN Pronuclei
PNa Pronuclear appearance
PNd Pronuclear disappearance
POU5F1 POU Class 5 Homeobox 1
PTTG1 Pituitary tumor-transforming 1
PVP Polyvinylpyrrolidone
QACM Quinn's Advantage® Cleavage Medium
QAM Quinn's Advantage Medium with HEPES
RB1 RB transcriptional corepressor 1
RCC2 Regulator of chromosome condensation 2
RMSE Root mean squared error
RT-qPCR Real-time quantitative PCR
s Seconds
SET Single-embryo transfer
SNP Single nucleotide polymorphism
SOX2 SRY-box 2
SPS Serum Protein Substitute
TE Trophectoderm
TP53 Tumor protein p53
TSC2 Tuberous sclerosis 2
WGA Whole genome amplification
WOI Window of implantation
XPA DNA damage recognition and repair factor
YBX2 Y-box-binding protein 2
YY1 Yin Yang 1 transcription factor
ZAR1 Zygote arrest 1
ZSCAN4 Zinc finger and SCAN domain containing 4
µL Microliter
˚C Degrees Celsius

INTRODUCTION

1 | Introduction

1.1 Assisted reproduction overview

Over the last 20 years, the number of assisted reproduction procedures has drastically increased. This trend is expected to continue as parenthood is postponed. In Europe, more than half a million *in vitro* fertilization (IVF) cycles are performed annually, resulting in 100,000 newborns, or 1.5% of all babies born in Europe (Sullivan *et al.*, 2013). The number of IVF cycles registered in Spain increased 1.7-fold over 10 years, from 63,215 in 2004 to 108,492 in 2013 (**Figure 1**). Similarly, over the same time period, the annual number of cycles in the United States increased 1.5-fold, from 128,216 to 190,773 **(Figure 1)**.

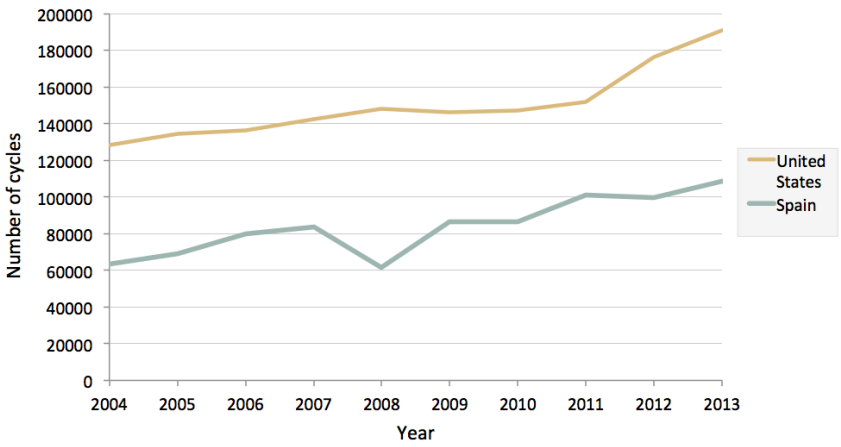

Figure 1 | Number of assisted reproduction cycles registered in Spain and the United States from 2004 to 2013.
Data were obtained from the annual reports created by the Spanish society of fertility (Sociedad Española de Fertilidad, SEF; www.registrosef.com) and the United States Centers for Disease Control and Prevention (CDC, www.cdc.gov/art/reports).

With the increased use of assisted reproduction, a concomitant increase in success rates would also be expected. However, the pregnancy rate per cycle has remained constant over the same 10-year range, despite important progress in the field **(Figure 2)**.

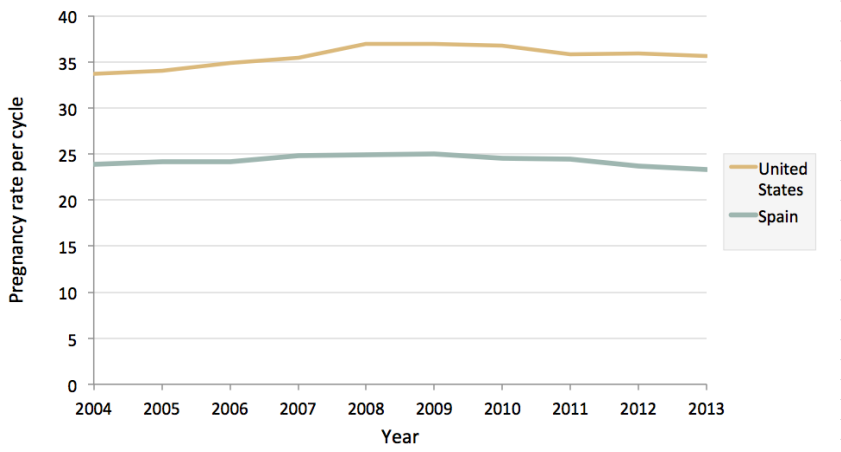

Figure 2 | Pregnancy rate per cycle started in Spain and the United States from 2004 to 2013.
Data were obtained from the annual reports created by the Spanish society of fertility (Sociedad Española de Fertilidad, SEF; www.registrosef.com) and the United States Centers for Disease Control and Prevention (CDC, www.cdc.gov/art/reports). The pregnancy rate per cycle from the United States was derived from fresh non-donor cycles since pregnancy rates from frozen and/or donor cycles were not available. The pregnancy rate from Spanish data was calculated including fresh and frozen cycles, as well as non-donor and donor cycles.

To understand the origin of the slow progress in IVF success rates, it is important to understand the type of populations that require these techniques. In 2013, the population undergoing IVF and intracytoplasmic insemination (ICSI) in Spain was mostly over 35 years old (72.3%), with a significant percentage of women over 40 years old (28.9%, **Figure 3a**). Furthermore, the age distribution for 2013 in the United States assisted reproduction technology (ART) population indicates 64.6% of patients were over 35 years old, and 23.1% over 40 years old **(Figure 3b)**. Both countries' populations showed a similar age distribution in the same year, with a slight increase in younger patients (<35 years) in the United States. This majority of women using ART at over 35 years old needs to be taken into consideration since it is well known that the rate of chromosomal

abnormalities increases with age (Hassold and Hunt, 2001). As a consequence, the advanced maternal age (AMA) may result in an increase in the number of aneuploid embryos (Demko *et al.*, 2016), which would be translated into high miscarriage rates and low live-birth rates (Schoolcraft *et al.*, 2009; Rubio *et al.*, 2013a).

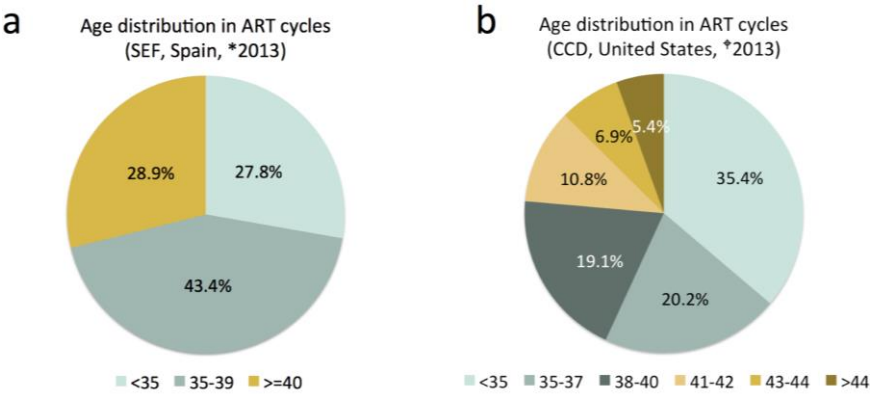

Figure 3 | Age distribution in assisted reproduction cycles in Spain and the United States in 2013.
(a) In the Spanish ART population, almost 29% of the patients are 40 years and older. Data obtained from the annual reports created by the Spanish society of fertility. *Based on 67,754 cycles. **(b)** In the United States population using ART, 23.1% of the registered patients were over 40 years old. Data obtained from the annual reports generated by the Centers for Disease Control and Prevention. *Based on 190,773 cycles.

Once we characterize the population that needs IVF treatments, a better understanding of the human embryo is also crucial. We need to know how infertility affects embryo biology and how frequent embryos will fail in development with the possible causes: aneuploidies, abnormal pool of inherited transcripts, fail in embryonic genome activation (EGA) or others.

Finally, since we are not able to modify the IVF population nor to possibly change the embryo quality, our goal should be mainly to focus on improving the IVF techniques by developing new physiological stimulation protocols, better culture systems and more effective selection methods. This knowledge and improvements, together with proper endometrial synchronization, would help to guarantee the success of ART as resulting in a healthy newborn.

1.2 The molecular inner life of the human embryo

For a complete understanding of the influence of each *in vitro* procedure on embryo biology, it is important to understand the underlying biological processes. Notably, most knowledge related to the preimplantation embryo relies on *in vitro* models due to the difficulties in observing it in natural conditions.

1.2.1 Meiosis and mitosis

Meiosis in humans varies considerably between males and females **(Figure 4).** In females, meiosis begins somewhat synchronously in all oocytes during fetal development, but then arrests before birth. Resumption of meiosis occurs asynchronously after puberty, at the time of ovulation, but arrests again until fertilization (Vera *et al.*, 2012). In contrast, male meiosis does not begin until puberty and occurs continuously throughout adulthood. Primary spermatocytes divide into two secondary spermatocytes through meiosis I, and each secondary spermatocyte divides into two spermatids, which will differentiate and maturate into sperm. The main difference between the male and female production of gametes is that oogenesis only leads to the production of one final ovum from each primary oocyte; in contrast, in males four sperm result from each primary spermatocyte **(Figure 4).** Three events can lead to aneuploidy during MI: failure to resolve chiasmata, resulting in a true non-disjunction; no chiasma formation or early disappearance of one, resulting in an achiasmate non-disjunction; and, finally, a premature separation of sister chromatids (Hassold and Hunt, 2001). In meiosis II the only cause of aneuploidy is non-disjunction of sister chromatids (Hassold and Hunt, 2001).

After fertilization, the zygote undergoes multiple rounds of mitosis to further develop. In human embryos, mitotic errors occur frequently; their origins have been attributed to the non-disjunction of some chromosomes or to a failure in separating during anaphase, creating one daughter cell with an extra chromosome and another with a missing chromosome (Mantikou *et al.*, 2012; Carbone and Chavez, 2015). In general, mitotic errors will then produce mosaic embryos, with different chromosomally distinct cells, whereas meiosis errors will produce aneuploid embryos in which every blastomere will be affected

with the same alteration, unless subsequent mitotic errors have modified the chromosome complement of some blastomeres, or some aneuploidy-correcting mechanism have taken place. The rates of aneuploidies from meiotic or mitotic origin in the bibliography are very varied, as they will be modified by the maternal age, sperm quality or culture conditions between others (Voullaire *et al.*, 2000; Chavez *et al.*, 2012; Capalbo *et al.*, 2013a; Chow *et al.*, 2014).

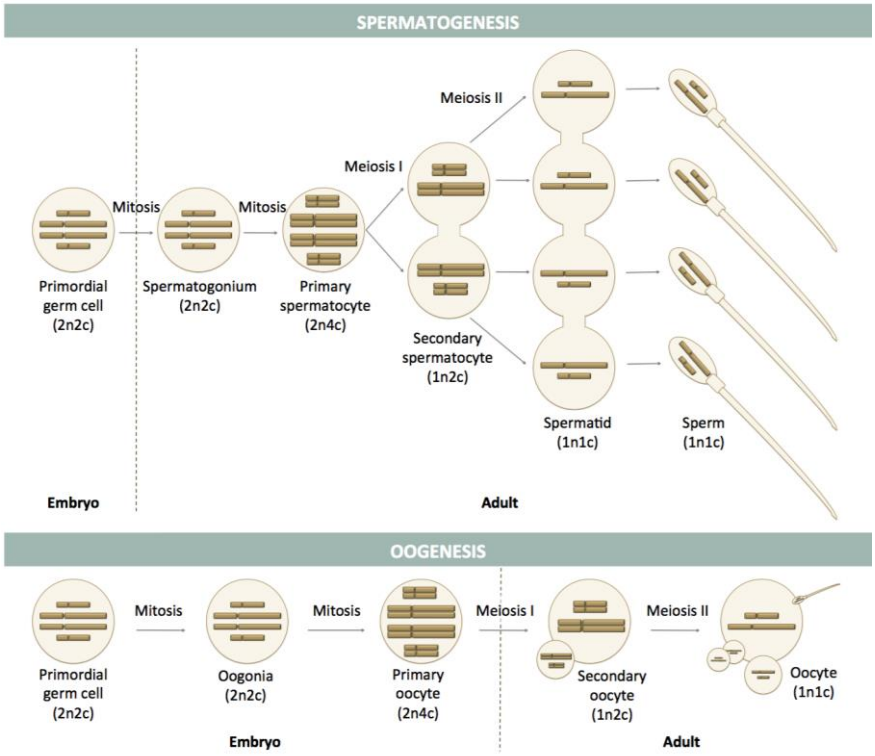

Figure 4 | Gamete formation in males (spermatogenesis) and females (oogenesis). During spermatogenesis, the primordial germ cell will suffer a series of mitotic and meiotic divisions that will originate four spermatozoa from each primary spermatocyte. By contrary, during oogenesis, each primary oocyte will develop into a single oocyte, since the rest of the daughter cells will correspond to the polar bodies, that are not destined to further develop. n, number of chromosomes; c, number of chromatids.

1.2.2 Embryo transcriptomics

One unique process that takes place during embryonic development is the maternal-zygotic transition (MZT). During the last part of oogenesis, the oocyte accumulates a series of transcripts and proteins to support very early development, before the embryonic genome is activated. Although the average life span of a messenger ribonucleic acid (mRNA) is estimated at around 10 hours (Schwanhausser *et al.*, 2011), maternal transcripts can last longer thanks to a protection mechanism that stabilizes them, as it has been described in mouse (Yu *et al.*, 2003).

Studies of embryo transcriptomics have been limited, especially for good-morphology embryos, as embryo availability is very limited. Nevertheless, several reports have contributed to a better understanding of the MZT and embryonic genome activation **(Table 1)**. The major wave of embryonic transcription occurs at the six- to eight-cell stage, though there is minor transcription of certain genes beginning at the two-cell stage (Dobson *et al.*, 2004; Zhang *et al.*, 2009; Galan *et al.*, 2010; Vassena *et al.*, 2011) **(Table 1)**. A subset of genes is potentially activated as early as the zygote stage (Xue *et al.*, 2013). These observations suggest that, contrary to a longstanding hypothesis, there is not a punctual activation by the embryo genome, but it is rather a gradual process in which different genes start their transcription according to the moment in which they are required in development. This would not undermine the maternal transcripts, which may still play an important role in guaranteeing the necessary machinery for fertilization and to escort the zygote/embryo to start its development with a minimal support is provided, allowing the embryo to become molecularly independent in a gradual manner.

An interesting study with human embryos showed that the embryonic genome activation and maternal transcript degradation are independent processes of cell division (Dobson *et al.*, 2004). More specifically, arrested embryos showed similar transcriptomic status to embryos with similar developmental time, instead of embryos at a similar cell-stage (Dobson *et al.*, 2004). This information provides a question mark for the reliability of performing comparative studies of embryos according to their number of cells. It remains

Table 1 | Transcriptomic studies in human embryo development

	Technique	Embryo stage	N	Main outcomes
Dobson et al. 2004	Microarrays from whole embryos	6 stages: GV, MI, MII, 2-c, 4-c, 8-c	22	• Arrested embryos are not linked to EGA failure
Zhang et al. 2009	Microarrays from pool of embryos	6 stages: GV, MI, MII, 4-c, 8-c, blastocyst	12	• Two EGA waves • Embryo development genes are very conserved
Galan et al. 2010	Microarrays from single cells	4 stages: 5-c, 6-c, 8-c, blastocysts (TE and ICM)	49	• Blastomere fate is not committed for ICM or TE at the cleavage stage.
Vassena et al. 2011	Microarrays from whole embryos	7 stages: oocyte, 2-c, 4-c, 6-c, 8/10-c, morula, blastocyst	19	• Three EGA waves at 2-c, 4-c and 8/10-c • Activation of pluripotency genes
Shaw et al. 2013	Microarrays from whole embryos	3 stages: oocyte, 4-c, blastocyst	9	• High variability between embryos from same stage
Xue et al. 2013	Single-cell RNAseq	6 stages: oocyte, zygote, 2-c, 4-c, 8-c, morula	36	• EGA starts already at zygote stage • Detection of monoallelic expression genes
Yan et al. 2013	Single-cell RNAseq	7 stages: oocyte, zygote, 2-c, 4-c, 8-c, morula and blastocysts (ICM and TE)	90	• Patterns of alternative splicing during development • Description of novel long noncoding RNAs • EPI, PE, and TE lineage segregation

GV, germinal vesicle; MI, metaphase I; MII, metaphase II; 2-c, two-cell; 4-c, four-cell; 5-c, five-cell; 6-c, six-cell; 8-c, eight-cell; TE, trophectoderm; ICM, inner cell mass; EGA, embryonic genome activation; EPI, epiblast; PE, primitive endoderm.

to be known if this feature would also be similar at different biological levels, such as cell fate decisions, cell communications or embryonic metabolic needs.

1.2.3 Early embryo metabolism

Once the oocyte has been fertilized and starts the process of transcription, the embryo also activates its own metabolism to provide energy for the cell, to maintain intracellular homeostasis and to provide all necessary metabolites for growth and development. Under *in vitro* conditions, the human embryo obtains ATP, the main energy source, by non-oxidative and also by oxidative metabolism. Thus, the importance of oxygen during *in vitro* embryo culture, whose consumption would increase with development.

As the human embryo development is a series of subsequently cell divisions, deoxyribonucleic acid (DNA) synthesis and replication are crucial processes that require energy consumption. The pentose phosphate pathway generates ribose-5-phosphates that are the nucleotides involved for all DNA-related processes. This pathway also generates nicotinamide adenine dinucleotide phosphate (NADPH), which is necessary in the majority of anabolic pathways, such as glycolysis. After EGA, the glucoses are a key component for embryo development, as they are essential for the synthesis of lipids, amino acids and nucleic acids. It has been suggested that the ratio between different amino acids is more relevant than the concentration, as they compete with each other for the different membrane transport systems (Baltz, 2012).

For proper homeostasis and pH regulation in the cells, a correct balance of electrolytes is also crucial. Similarly, vitamins are necessary for some metabolic processes, such as methylation, by folic acid and vitamin B12; or for redox system, by vitamins C and E. Finally, the role of the growth factors *in vitro* is still unclear, although they seem to have a positive effect on the cell number and embryo quality.

In summary, for *in vitro* embryo development, the composition of the embryo culture media is essential and needs to be very carefully designed, as this is the main source from which the embryo has to obtain all necessary molecules for growth.

1.3 *In vitro* fertilization procedures

The regular natural process of reproduction involves the ovulation of a single oocyte by the woman, which needs to be fertilized by a single sperm from the semen of the man. Both gametes, oocyte and sperm, are haploid, thus their union creates a diploid cell that will develop into a healthy newborn. When there is a problem of infertility, an IVF process is needed, preceded by a controlled ovarian stimulation (COS) and followed by a supervised embryo development to select the best embryo to be transferred at the right timing for a correct synchronization with the endometrium. Each step of the process is crucial for the final success of the procedure, and therefore the reproductive medicine community should work toward the improvement of all of them.

1.3.1 Controlled ovarian stimulation

The human ovulation system involves, in most cases, the availability of only one oocyte per cycle, meaning a unique possibility for pregnancy every 28 days. If we add to this an infertility situation, the chances of success diminish significantly. This observation resulted in COS being established as a procedure to bypass the low expectations of natural cycles once infertility is present, enabling production of a higher number of mature follicles per cycle and, therefore, a higher number of oocytes capable of being fertilized. Nevertheless, recent studies have shown that lower gonadotrophin doses increase embryo quality (Rubio *et al.*, 2010) and that only when the stimulation is mild the aneuploidy rate is comparable to natural cycles, 40.6% and 34.8% aneuploid embryos, respectively (average female age: 25.4 ± 4 years) (Labarta *et al.*, 2012). Indeed, in assessing the events occurring in the oocyte during gonadotrophin stimulation **(Figure 5)**, the differences in aneuploidy rates between stimulation protocols may have a biological explanation. In natural cycles, during follicle recruitment, meiosis I is resumed with the extrusion of the first polar body and the selection of only one follicle; whereas in COS cycles, this resumption and maturation occurs in multiple follicles simultaneously.

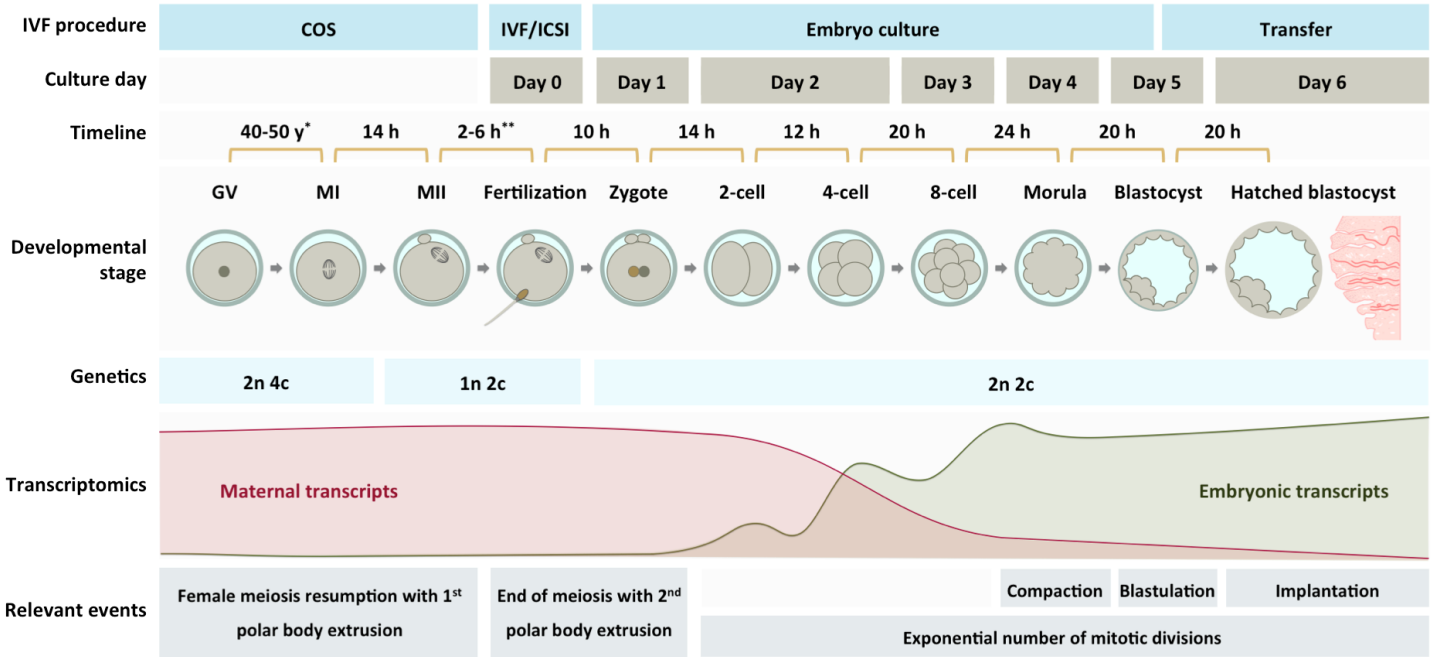

Figure 5 | Stages and events of human embryo development during *in vitro* fertilization procedures.
From top to bottom, the different procedures that are performed during IVF,the equivalence of day of culture, the timing between stages according to the literature (Hyun *et al.*, 2007; Wong *et al.*, 2010; Strassburger *et al.*, 2010; Meseguer *et al.*, 2011; Escrich *et al.*, 2012; Alvarez *et al.*, 2013; Desai *et al.*, 2014; Chawla *et al.*, 2015), the developmental stages, the chromosomal content in the individual nucleus –with *n* being the number of chromosomes and *c* the number of chromatids per chromosome-, the transcripts maternal-zygotic transition, and the most relevant molecular events of embryo development. COS, controlled ovarian stimulation; IVF, *in vitro* fertilization; ICSI, intracytoplasmic sperm injection; 2n, two copies per chromosome; 1n, one copy per chromosome; 2c, two chromatids; 4c, four chromatids. * Average maximum time on arrest. ** Average recommended time in clinical routine.

1.3.2 *In vitro* fertilization process

Once good-quality mature oocytes are obtained, we then need to focus on their proper fertilization, with two possible techniques to achieve this: conventional IVF or ICSI, which are chosen according to the seminal and clinical background of the patients.

Conventional IVF is recommended for patients with good-quality sperm (Bhattacharya *et al.*, 2001) and it involves the incubation of the oocyte, generally overnight, with sperm of good motility (ESHRE Guideline Group on Good practice in IVF, December, 2015). The sperm concentration is the main factor to control: if is too low it can decrease the chances of fertilization, and if is too high, it can cause polyspermia and polyploid embryos (Fukuda and Chang, 1978). The recommended sperm concentration for conventional IVF ranges from 0.1 to 0.5 million/mL of motile sperm (ESHRE Guideline Group on Good practice in IVF, December, 2015).

In contrast, ICSI involves the manual injection of a single spermatozoon into a mature oocyte. Thus, it is specifically recommended for severe male infertility cases. The selection of a spermatozoon to inject is crucial for the later embryonic development since it has been correlated with aneuploidies in the sperm (Rodrigo *et al.*, 2011). Selection of a motile and good morphology spermatozoon is critical to reduce the chances to introduce an abnormal chromosomal content (Collodel *et al.*, 2007). The spermatozoon not only contributes to half of the embryonic chromosomal content, but also contributes one of the most essential cell organelles, the centrioles (Sathananthan *et al.*, 1991). The centrioles are tubulin structures that, together with the pericentriolar material, will create the centrosome, which has a crucial role in cell division by helping organize the mitotic spindle. Further, ICSI requires careful attention to the way in which the spermatozoon is injected into the embryo to avoid damage of internal structures of the embryo, such as the spindle. For that, it is recommended to place the polar body in the opposite site to the injection site, as it is an indicator of spindle position (ESHRE Guideline Group on Good practice in IVF, December, 2015).

Additionally and independently of the technique selected, the introduction of the sperm inside the oocyte will start the resumption of meiosis II, triggering the extrusion of the second polar body **(Figure 5).** Thus, the evaluation of correct fertilization includes the observation of the two pronuclei, one maternal and one paternal, and the first and second polar bodies. According to the number of polar bodies and pronuclei, abnormalities can be attributed to female meiosis errors or fertilization failures (Flaherty *et al.*, 1998). This evaluation is recommended to be performed 16-18 hours (h) post insemination (ESHRE Guideline Group on Good practice in IVF, December, 2015).

1.3.3 Embryo culture

The preimplantation embryo development comprises multiple mitotic divisions starting from the zygote stage. The cell number then increases exponentially, since each daughter cell´s mitosis takes place in parallel, producing double the number of daughter cells. Thus, the normal mitosis rate of an embryo would be from 1 to 2 cells, from 2 to 4 cells, from 4 to 8 cells, from 8 to 16, etc. reaching in only five days of development around 250 cells (Niakan *et al.*, 2012).

During this *in vitro* development we can differentiate at least three stages according to the cell-number and morphology **(Figure 5)**: (1) The cleavage-stage, when the embryo has between 2 to 8 individual cells and corresponding to the first 3 days of development. At this stage, each cell is called a blastomeres; (2) The morula, approximately 4 days after fertilization, when all cells of the embryo start to fuse their cytoplasm in a process called compaction, creating a syncytium; (3) The blastocyst stage, when, thanks to the Na^+/K^+ channels, the morula will start to accumulate fluid inside the embryo. This process is known as cavitation and creates a space inside the embryo called the blastocoel. The embryo, now known as a blastocyst, contains two different cell lineages: the trophectoderm, whose cells form a hollow sphere; and the inner cell mass, that will form a cluster inside the trophoblastic cells.

During the first two stages of development, cleavage and morula, the embryo divides without a significant change in size; at blastocyst stage, due to

different collapsing movements, the embryo starts increasing its size. Eventually, the zona pellucida will develop a crack, in which the blastocyst will start hatching until, after multiple collapsing movements, the embryo leaves the zona pellucida.

Sometimes an embryo does not follow the whole developmental process and arrests at a certain stage, eventually dying. This phenomenon of the embryo has been correlated with failures in embryo biology, such as transcriptomic alterations (Wong *et al.*, 2010), but also with metabolic problems (Leese *et al.*, 2008) and an increased rate of chromosomal abnormalities (Munne *et al.*, 1995).

The main goal of *in vitro* embryo culture is to replicate the natural conditions of the endometrial cavity in more optimal way. For this, the embryo culture must be done under very well monitored conditions (temperature, oxygen levels, humidity, etc.) by using incubators and heated surfaces, and by selecting the best culture media according to the stage and the nutritional requirements of the embryo, choosing between single embryo culture or co-culture of multiple embryos of the same patient. Depending on these parameters, each IVF laboratory develops different protocols for embryo culture to achieve the best success rates, which also implies the existence of substantial differences between centers that create difficulties in comparisons between them.

1.3.4 Implantation

Finally, after a high-quality blastocyst is obtained, we would expect to have a correct implantation, but at this step, a new actor comes into scene, the endometrium. For implantation to occur, the endometrium needs to be receptive, and this is only possible during a limited period of time known as the window of implantation (WOI) that could be different among patients from day 19 to 23 of their natural cycle or from progresterona+3 to progresterone+7 in hormonal replacement cycles (Diaz-Gimeno *et al.*, 2011). This is different to what has been always established, being the reason for standard embryo transfer (ET) to fail, as different women would need a personalized embryo transfer (pET).

In clinical practice, it was common to transfer two embryos at the same time. This increases the pregnancy rates up to approximately 70% (Gardner *et al.*, 2000). However, although it increases slightly the pregnancy rates, it also increases the chances of a twin pregnancy (McLernon *et al.*, 2010). To avoid this, SET has been proposed as an effective strategy to decrease the incidence of twins (McLernon *et al.*, 2010; Gianaroli *et al.*, 2012). However, to maintain similar pregnancy rates, especially for bad-prognosis patients, improvements on the embryo selection are needed.

1.4 How to select the best embryo

The purpose of embryo selection is to reduce the number of transfer needed to achieve a pregnancy from a pool of embryos. Considering the best embryo—the one having the highest probabilities to implant and to develop into a healthy newborn—its selection should be based on all those embryonic parameters that have been demonstrated to be correlated with success rates in the clinical routine. Although this set of parameters is very wide, here we wish to discuss those that have gained greater popularity among the clinical community: morphology, kinetics and aneuploidies. We have also added transcriptomics since, although still experimental, it can provide some biological answers to support clinical observations.

1.4.1 Morphology evaluation

Morphology is the most traditional way to evaluate an embryo since there is no need for additional equipment beyond a heated surface and an inverted microscope. With the increase in IVF treatments and research, this type of evaluation has evolved toward selecting the most predictive parameters, such as fragmentation, cell number, symmetry, and multinucleation, and relying less on least predictive parameters like vacuole existence, cytoplasm anomalies and zona pellucida alterations (Alpha Scientists in Reproductive Medicine and ESHRE Special Interest Group of Embryology, 2011).

1.4.1.1 Fragmentation

Fragmentation is one of the main morphological parameters used in embryo assessment. Fragments appear when part of the blastomere's cytoplasm protrudes. Embryos with a high degree of fragmentation have lower implantation rates (Alikani *et al.*, 1999).

Although the origin of the fragmentation remains unknown, it has been correlated to multiple inner events. One the most extended findings is that embryos with a higher percentage of fragments have a higher percentage of chromosomal abnormalities (Magli *et al.*, 2001; Magli *et al.*, 2007; Chavez *et al.*, 2012). Indeed, one recent publication reported for the first time the existence of DNA in fragments of cleavage-stage embryos (Chavez *et al.*, 2012).

Fragmentation has also been correlated with alterations in the expression of some genes, especially with increased expression of tumor protein p53 (*TP53*) transcription factor in DNA repair pathways and apoptosis (Wells *et al.*, 2005). A relationship between embryo fragmentation and telomere shortening has also been found, which is related to *TP53*-mediated pathways and other precursors of aneuploidy abnormalities (Keefe *et al.*, 2005; Treff *et al.*, 2011). Furthermore, lower mitochondrial DNA copy number in embryos with a high fragmentation degree that could result in decreased ATP production, which is necessary for proper embryo development (Lin *et al.*, 2004). Many other factors such as apoptosis (Jurisicova *et al.*, 1996; Liu *et al.*, 2000; Chi *et al.*, 2011), cytoskeleton abnormalities (Neganova *et al.*, 2000; Liu and Keefe, 2002; Alikani *et al.*, 2005) and toxic substances (Keltz *et al.*, 2006; Hutt *et al.*, 2010) have been correlated with fragmentation.

1.4.1.2 Cell number and symmetry

The number of cells in the embryo is the main indicator of the number of cell divisions it has undergone. In conventional morphology evaluation, it is expected to observe one cell at day 1 (zygote stage), two to four cells at day 2, six to eight cells at day 3 and fourteen to sixteen cells before compaction at day 4 **(Figure 5).** When the number of cells at one stage is lower or higher than expected, it means that the embryo cleavage rate is either too slow or too fast, which has a negative impact on the implantation rate (Ziebe *et al.*, 1997; Van Royen *et al.*, 1999). A higher cell number may also be related with the previous existence of irregular divisions from one to more than two cells. Thus, there is a correlation between the cell number and the chromosomal constitution of the embryo (Magli *et al.*, 2007).

Similarly, the uneven size of blastomeres can originate from asynchronous divisions or from irregular divisions, as 1 to 3 divisions in which one blastomere is bigger or smaller than the others. Blastomere asymmetry is correlated with a higher percentage of aneuploidies (Hardarson *et al.*, 2001; Munne, 2006) and with a decrease in the pregnancy rate (Racowsky *et al.*, 2003).

1.4.1.3 Multinucleation

In the cleavage-stage, an embryo is considered multinucleated when at least one of its blastomeres contains more than one nucleus. It is normally differentiated between binucleation, when two nuclei are present, and multinucleation when we can observe more than two nuclei, also called micronuclei.

The origin of multinucleation has been related to nuclear membrane anomalies (Webster *et al.*, 2009), DNA damage (Norppa and Falck, 2003) or to an asynchrony between karyokinesis and cytokinesis (Pickering *et al.*, 1995). This is in concordance with the correlation found between multinucleation and a higher rate of aneuploidies (Pickering *et al.*, 1995; Hardarson *et al.*, 2001; Munne *et al.*, 2006). Thus, transfer of multinucleated embryos is not recommended (Alpha Scientists in Reproductive Medicine and ESHRE Special Interest Group of Embryology, 2011), although some studies have reported healthy newborns from multinucleated embryos (Balakier and Cadesky, 1997; Jackson *et al.*, 1998; Fauque *et al.*, 2013).

Finally, multinucleation has been also correlated with other morphological parameters, such as high degree of fragmentation (Van Royen *et al.*, 2003; Chavez *et al.*, 2012) or asymmetric divisions (Hnida *et al.*, 2004). As a consequence, multinucleated embryos have been shown to reach less frequently the blastocyst stage, when it occurs at day 2/3 (Alikani *et al.*, 2000), and have a lower implantation potential (Jackson *et al.*, 1998; Van Royen *et al.*, 2003; Chavez *et al.*, 2012).

1.4.1.4 Other morphological parameters

There are also different parameters that, due to the low frequency in which they are found or to slight effect on embryo development, are considered to have secondary roles in the morphological evaluation. They include vacuole existence, cytoplasm anomalies or zona pellucida alterations, among others. If we focus on vacuoles, it seems crucial to differentiate the time of appearance, between oocyte, ICSI or embryo arrest, to estimate the consequences on success rates, being the latest the one with more detrimental effect (Ebner *et*

al., 2005). Nevertheless, vacuoles have been shown to not correlate with aneuploidies (Magli *et al.*, 2001).

1.4.2 Morphokinetics by time-lapse

The incorporation of time-lapse culture systems for the evaluation of human embryo development has been an important achievement in the field during the last decade. Although these systems had been previously employed for embryo culture (Payne *et al.*, 1997), new improvements such as a decrease in the light exposure or a decrease in the size of the microscopes allowed them to be incorporated into the clinical routine. The two studies that raised the popularity of this system were published by Wong and colleagues in 2010 and by Meseguer *et al.* in 2011. These studies agreed on the existence of certain kinetic parameters that enable prediction of the success of embryo development, either at the blastocyst stage (Wong *et al.*, 2010) or at the implantation level (Meseguer *et al.*, 2011). Since, the use of time-lapse technologies has gradually increased.

1.4.2.1 The technology

Time-lapse systems consist of the incorporation of a microscope inside a standard incubator, enabling observation of the embryo at any time without opening the incubator. Thus, this system avoids the disruption of culture conditions that occurs when taking the embryos out of the incubator for standard morphological assessment, such as temperature or pH variations that can negatively affect the embryo development. A camera takes pictures every 5-20 minutes (min), depending on the commercial system, from right after fertilization to the latest stage before ET, on day 3, day 5 or day 6. To avoid light damage to the embryo, time-lapse systems use either dark-field illumination, as Eeva™ (Auxogyn, CA, USA) or really short exposure times, as Embryoscope™, the one with the lowest aperture (<0.032s) (Schatten, 2016). With dark-field technology, it is estimated that the embryos would be exposed during the whole recording process to the light equivalent to the one used in less than a minute under typical bright-field microscopes (Wong *et al.*, 2010). Indeed, no differences were observed in embryo development, blastocyst rate

or gene expression between embryos observed by this technique compared with the standard assessment (Wong *et al.*, 2010; Kirkegaard *et al.*, 2012).

In addition, time-lapse systems normally include software that allows image analysis algorithms and some additional features depending on the commercial system employed. For instance, Eeva™ system (Auxogyn, CA, USA) includes an automatic cell identification that allows the software to calculate kinetic parameters by itself and to automatically score each embryo according to the predictive potential. Nevertheless, Embryoscope™ (Unisense Fertilitech, Denmark) offers the possibility to change the focus plane for each picture, which is especially useful for the evaluation of some spatial parameters like fragmentation. Other systems, like the BioStation IM-Q (Nikon, Japan), even allow the taking of fluorescence images, although this is more useful for research purposes.

1.4.2.2 Morphology evaluation

The significant improvement of time-lapse technology versus previous evaluation methods is that it provides a non-invasive alternative to the morphological assessment of embryos. The creation of whole-development movies for each embryo allows a more extensive morphological analysis of the embryo, enabling the observation of cellular events that would otherwise remain undetected by conventional methods, such as irregular divisions, also known as direct-cleavage divisions. Normal mitotic divisions are expected to give two daughter cells, nevertheless abnormal divisions to 3, 4 or even 5 cells have been reported in human embryo development (Schatten, 2016). The probability of identifying these types of divisions through classical evaluation is very low, since the division needs to take place in the moment that the embryo is being evaluated, to be detected. In some cases, the occurrence of irregular divisions may be hypothesized by the number of cells during conventional evaluation, but time-lapse allows the complete identification of them by just playing the final movie of the whole embryo development (Rubio *et al.*, 2012; Athayde Wirka *et al.*, 2014; Desai *et al.*, 2014). This novel characterization in human embryo development has allowed correlating this feature with a decrease in blastocyst rate and implantation potential (Rubio *et al.*, 2012; Athayde Wirka *et al.*, 2014). Additionally, time-lapse has allowed the

identification of blastomere fusion, also known as reverse cleavage (Desai *et al.*, 2014). This type of event typically occurs, although not necessarily, after an irregular division as an attempt to correct it. Both direct and reverse cleavage have been correlated with the existence of multinucleation (Desai *et al.*, 2014).

Finally, time-lapse allows analysis of a new dimension of fragmentation: fragment divisions and reabsorption. More specifically, fragments can be reabsorbed by the same or a different blastomere (Hardarson *et al.*, 2002; Chavez *et al.*, 2012), and this process may be the consequence of an embryonic response to aneuploidies (Chavez *et al.*, 2012).

1.4.2.3 Kinetic parameters

In time-lapse, each time range between two different events that occur in routine of the human embryo can be considered as a kinetic parameter. Kaser and Racowsky (2014) performed in an extended review of time-lapse studies and compared the reported timings for each one **(Figure 6)**. Depending on the interval selected, kinetic parameters allow the study of cell cycle duration, when measuring the time between one blastomere is generated and the same blastomere divides; cytokinesis duration, when measuring the time between the appearance of a cleavage furrow to complete daughter-cell separation (Hlinka *et al.*, 2012); interphase duration, when measuring the time between the nucleus appears to the nucleus disappearance (Sundvall *et al.*, 2013); or blastocyst-related events, such as the compaction duration, the time between the start of compaction until the time in which the embryo is totally compacted (Campbell *et al.*, 2013). Additionally, kinetics allows determining the synchrony between daughter cells by calculating the difference between both cell cycles (Wong *et al.*, 2010; Meseguer *et al.*, 2011).

Note that most of the time-lapse studies calculate the kinetic parameters using ICSI time as the reference (Kaser and Racowsky, 2014), and this has two disadvantages: first, there is no option to use frozen zygotes, although this is not a common practice as it is more frequent to freeze oocytes; and second, late parameters calculated from the ICSI time will be affected by earlier parameters, producing a bias in the analysis.

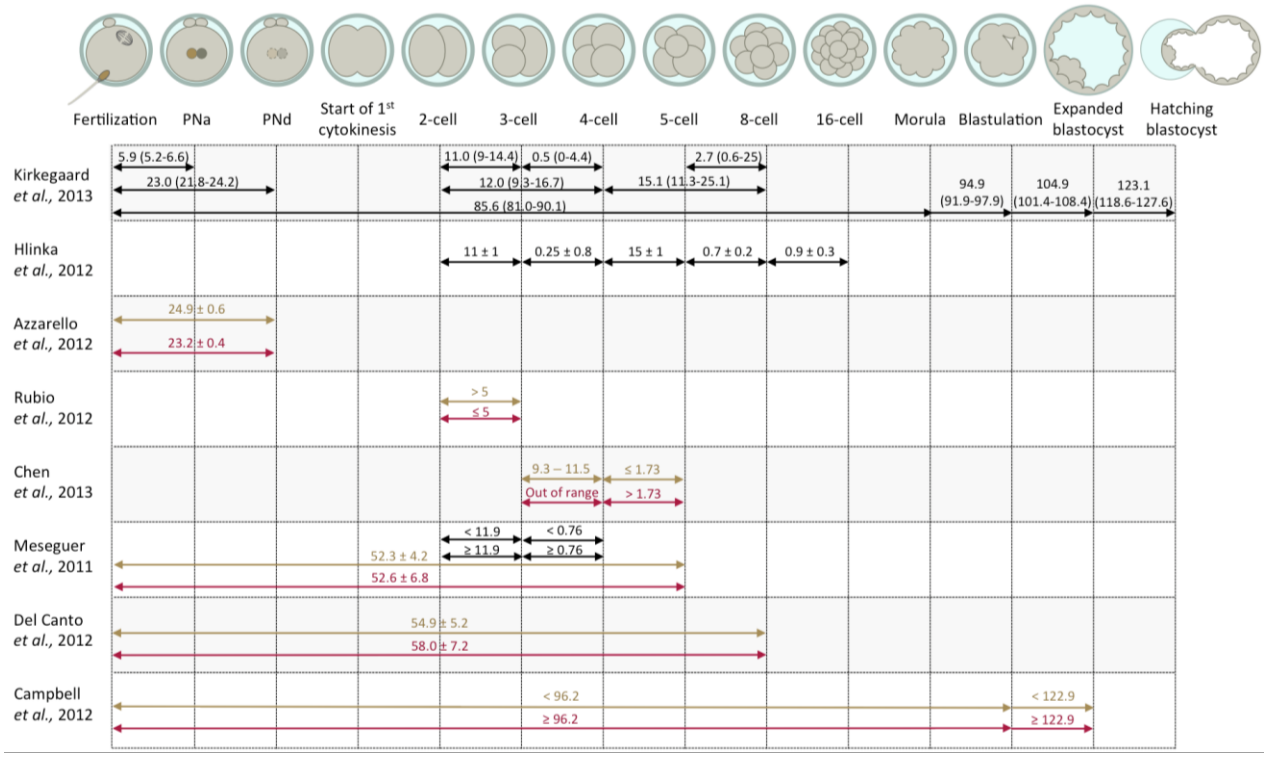

Figure 6 | Summary of reported timing for time-lapse parameters between fertilization and hatching blastocyst.
Parameters that were not significantly different between implanted and non-implanted embryos are represented in black. When significant differences were reported, the implanted embryo timing is in orange, and the non-implanted in red. Values are expressed in hours, as mean for normally distributed populations, and median for non-normally distributed. PNa, pronuclei appareance. (Adapted from Kaser and Racowsky, 2014).

1.4.2.4 Prediction models

Concomitant with the increased use of time-lapse, an increase in the prediction models for different success rates have occurred. New knowledge about embryonic cell cycles and development has resulted in new models showing higher accuracy than the traditional scoring using exclusively morphology parameters (Yang *et al.*, 2014; Aparicio-Ruiz *et al.*, 2016).

- **Predicting blastocyst formation**

One of the first attempts that was made by time-lapse was to create a model for blastocyst formation prediction based on kinetic parameters until day 3 with high sensitivity and specificity (Wong *et al.*, 2010). This type of model would allow transferring those embryos with the highest probability to develop into a blastocyst already on day 3. Some other studies went one step further to create a model that not only predicts the blastocyst formation, but also the good-quality one with 80% success (Kirkegaard *et al.*, 2013; Cetinkaya *et al.*, 2015). Finally, in general, shorter kinetic parameters are linked to better blastocyst quality (Cruz *et al.*, 2012). Interestingly, the kinetic dynamics of embryos with the highest probability to reach a blastocyst have less dispersion, compared to those embryos with lower chances to successfully develop (Milewski *et al.*, 2015).

- **Predicting clinical success rates**

Apart from obtaining high-quality blastocysts, it is important to understand their implantation potential, since aneuploid embryos can similarly develop into beautiful blastocysts (Alfarawati *et al.*, 2011). The first study reporting a model for implantation was exclusively based on early kinetic parameters, which is relevant for prediction in case of day-3 ET (Meseguer *et al.*, 2011). From these results, multiple studies tried later to test this model for their embryos or tried to develop their own algorithm for implantation prediction **(Figure 6)**. The majority found significant differences between the kinetics of implanted embryos versus non-implanted (Meseguer *et al.*, 2011; Azzarello *et al.*, 2012; Dal Canto *et al.*, 2012; Rubio *et al.*, 2012; Chen *et al.*, 2013; Campbell *et al.*, 2013), and most of those were concordant in that non-implanted embryos had longer parameters than one that implanted (Meseguer *et al.*, 2011; Dal Canto *et al.*, 2012; Campbell *et al.*, 2013; Chen *et al.*, 2013).

One study found a shorter kinetic parameter, the time between the two- and the three-cell stage, for the non-implanted embryos (Rubio *et al.*, 2012), contrary to previous reports (Meseguer *et al.*, 2011) in which embryos with direct cleavage were excluded. Only one study was focused on live-birth rate, finding that embryos resulting in live birth showed shorter time to pronuclear disappearing (PNd) than the no birth group (Azzarello *et al.*, 2012).

- **Predicting ploidy status**

Several studies have combined chromosomal analysis technologies to generate a ploidy prediction model based on embryo kinetics **(Table 2)**. Most of the studies found significant variations between the kinetics of euploid embryos versus aneuploid embryos, although no parameter resulted in a reliable predictor (Chavez *et al.*, 2012; Campbell *et al.*, 2013; Basile *et al.*, 2014; Chawla *et al.*, 2015; Nogales *et al.*, 2017).

The first study comparing kinetics for ploidy groups was performed at the four-cell stage with the main goal of doing the prediction as soon as possible in development (Chavez *et al.*, 2012). Aneuploid embryos had a higher variability in the duration of cell cycles and also presented a higher incidence of fragments. Campbell *et al.* published the first model for embryo aneuploidy prediction at the blastocyst stage, based on the time between insemination to initiation of blastulation and the time from insemination to full blastulation (Campbell *et al.*, 2013). Embryos were categorized according to the kinetics in a low-, medium-, or high-risk category. The chances of an aneuploid embryo in the low-risk group (0.37) were still too high to consider this method as an alternative to preimplantation genetic screening (PGS). Only the high-risk group of the model could be considered reliable, with a 0.97 probability of being aneuploid, although the proportion of embryos fitting in this category was as low as 12.4%. A similar later study performed by a different group did not find the same results as Campbell *et al.* (Kramer *et al.*, 2014) and attributed the discordances to differences between clinic procedures and even to a variability among patients. The only parameter that was found as statistically significant between euploid and aneuploid embryos was the duration of compaction, with an area under the curve (AUC) of 0.674, although they concluded that this parameter was still poorly predictable for ploidy detection.

The published ploidy model based on kinetics with a higher number of embryos (n=504) found that prediction was possible by using the time between the two- and the five-cell stage and the time between the two- and the five-cell stage (Basile *et al.*, 2014). It is important to note that the selected parameters for the model are multicollinear, and variability in the first one would produce variability in the second one. These results were confirmed by a second study in 460 embryos, but in this case, they performed one different model for each parameter with similar accuracy (Chawla *et al.*, 2015). Additionally, a recent report showed that the kinetics is altered differently depending on the type of chromosomal abnormality (Nogales *et al.*, 2017).

In summary, we can conclude that with the current data, morphokinetic classification by time-lapse technique is not accurate enough to predict ploidy, although it would be optimal to use when PGS is not possible, for instance due to legal reasons, or in combination with PGS to increase the success rates. In relation to this last option, one prospective study comparing the selection of embryos for transfer based only in PGS versus time-lapse plus PGS showed that time-lapse significantly increased the chances of getting a euploid embryo to implant and to obtain a clinical and ongoing pregnancy (Yang *et al.*, 2014).

1.4.3 Preimplantation Genetic Screening

The chromosomal component in an embryo is a key factor to determine its developmental fate. It is well known that aneuploid embryos that can reach the blastocyst stage, implant, and even produce a pregnancy ending in a miscarriage or in an affected newborn (Rubio *et al.*, 2005; Alfarawati *et al.*, 2011; Campos-Galindo *et al.*, 2015). Thus, PGS was introduced in clinical routine practice, based on the assumption that the high aneuploidy rate frequently found in cleavage-stage embryos was responsible for the low pregnancy rate after ART.

Table 2 | Ploidy prediction models based on kinetic parameters reported in the literature.

	N	Average maternal age	Stage of ploidy assessment	Model parameters	Accuracy
Chavez et al. 2012	45	33.5	4-cell	• Duration 1st cytokinesis • Time from 2- to 3-cell stage • Time from 3- to 4-cell stage	100% sensitivity 66% specificity
Campbell et al. 2013	97	38.6	Blastocyst	• Time from insemination to initiation of blastulation • Time from insemination to full blastulation	AUC 0.720
Kramer et al. 2014	145	37.3	Blastocyst	• Duration of compaction	AUC 0.674
Basile et al. 2014	504	36.1	Day 3	• Time from 2- to 5-cell stage • Time from 3- to 5-cell stage	AUC 0.634
Chawla et al. 2015	460	32.9	Day 3	• Model (A): Time from 2- to 5-cell stage • Model (B): Time from 3- to 5 cell stage	(A): AUC 0.632 (B): AUC 0.631
Nogales et al. 2017	485	35.5	Day 3	• Time from 2- to 5-cell stage • Time from insemination to 3-cell stage	NA

AUC, area under the curve; NA, not available.

1.4.3.1 Clinical approach

- **Indications for PGS**

The chromosomal analysis of preimplantation embryos is highly relevant for patients with certain indications that have been previously correlated with high aneuploid rates, such as low implantation rates and/or high miscarriage rates. Advanced maternal age is the most common indication for PGS since maternal age is highly correlated with the prevalence of aneuploidy (Hassold, 1982). A recent study reported that the rate of mis-segregation for the most clinically relevant aneuploidies (chromosomes 13, 16, 18, 21, 22) increased from 20% to 60% in women between the ages of 35 and 43 years (Kuliev *et al.*, 2011). Nevertheless, the use of PGS in patients with AMA have shown contrary results between studies detecting no improvement in the clinical success rates (Mastenbroek *et al.*, 2011) versus studies showing an increase in live-birth rates or a decrease in miscarriage rates when using PGS (Rubio *et al.*, 2013b; Rubio *et al.*, 2017).

In addition to AMA, patients with recurrent miscarriages—two or more consecutive miscarriages—are also recommended to undergo PGS, as some studies have reported an increase of aneuploid products of conceptions in this type of patient (Nybo Andersen *et al.*, 2000; Marquard *et al.*, 2010). Similarly, when there is a repetitive implantation failure, although the cause is still poorly defined, some authors argue that these couples produce more aneuploid embryos (Pagidas *et al.*, 2008) and exhibit a trend to higher live-birth rates with PGS (Rubio *et al.*, 2013a).

Another clinical indication for PGS would be male factor, as an increased incidence of chromosome abnormalities in the sperm of these patients has been reported (Rubio *et al.*, 2001) producing low implantation and high miscarriage rates (Egozcue *et al.*, 2000; Bernardini *et al.*, 2004). Furthermore, couples with a previous trisomic pregnancy are also encouraged to follow PGS due to an increased risk versus a control group (Al-Asmar *et al.*, 2012).

Finally, PGS has also been applied for good-prognosis patients with the goal of reaching a healthy newborn in a shorter period of time or to promote single-

embryo transfer (SET), which has been shown to have higher pregnancy rates when combined with PGS (Yang *et al.*, 2012)

- **Sample collection**

PGS requires a sample of the embryo, which would be representative of the whole for its diagnosis. According to the developmental stages to analyze, different types of biopsies have been used. First, polar body biopsy would be performed the day of fertilization, allowing the detection of genetic diseases or chromosome abnormalities related to the oocyte. Nevertheless, this type of biopsy would not give information about the father/sperm or about embryonic de-novo alterations, which is an important drawback for chromosomal screening (Salvaggio *et al.*, 2014).

As an alternative, cleavage-stage embryos can be biopsied at day 3 by taking one or two blastomeres for analysis. Normally, only embryos with good morphology are recommended to be biopsied (Harton *et al.*, 2011). Day-3 biopsy allows detection of both maternal and paternal contributions, as well as de novo mitotic alterations. Furthermore, this type of biopsy permits transferring the embryo in a fresh cycle after getting the results.

Finally, blastocyst biopsy is performed on day 5 or 6 of development by taking a group of cells (4-10 cells) from the trophectoderm. In comparison with day-3 biopsy, this option also allows detection of mitotic errors in development that take place between day 3 and day 5. On the other hand, unless the diagnosis can be obtained within 24 hours, the blastocyst needs to be cryopreserved. Additionally, it is important to note that, in case of mosaicism, trophectoderm biopsy could allow the detection since several cells are obtained for the analysis. The development of new vitrification protocols with very high survival rates together with recent reports showing high concordance between the chromosomal component of the inner cell mass and the trophectoderm have made day-5/6 biopsy the most common practice for PGS (Johnson *et al.*, 2010a; Capalbo *et al.*, 2013b).

1.4.3.2 Technology in the laboratory

Several methods currently allow for the study of aneuploidies in human embryos, including fluorescence *in situ* hybridization (FISH), single nucleotide polymorphism (SNP) arrays, comparative genomic hybridization arrays (aCGH) and, the most recent, next-generation sequencing (NGS). The evolution of the techniques for aneuploidy screening has allowed having more information about the genetics status and faster results that allow transferring the euploid embryos during the same cycle.

- **Fluorescence *in situ* hybridization**

FISH assay was the most widely applied methodology for aneuploidy screening for many years. It uses fluorescent nucleic acid probes complementary to DNA to visualize regions of interest (Rubio *et al.*, 2013a). However, FISH cannot be performed for all chromosomes simultaneously (Abdelhadi *et al.*, 2003) and is therefore exclusively used for those chromosomes in which aneuploidies are commonly implicated in spontaneous miscarriages or compatible with affected live births (Stephenson *et al.*, 2002) such as chromosomes 3, 15, 16, 17, 18, 21, 22, X and Y. FISH assays required the studied cell to be fixed by using Carnoy solution, and the quality of the fixation may vary with cell integrity, operator experience or room humidity, making the later hybridization quality also a variable factor to be considered. For this reason, the biopsy of 2 cells from the same embryo is a common procedure when aneuploidy screening is performed by FISH. Thus, the main disadvantages for FISH have been the high percentage of embryos with no results and the high false-positive rate (Uher *et al.*, 2009), although one study reported an increase in the accuracy of the technique by the reanalysis of doubtful signals (Mir *et al.*, 2010).

- **Array comparative genomic hybridization**

Fortunately, new technologies were developed, like array-based platforms, which facilitated the transition from the study of a limited number of chromosomes by FISH, to the analysis of all 23 chromosome pairs simultaneously in a single cell (Rodrigo *et al.*, 2014). Array-based technologies give the opportunity to have the result in less than 24 hours and with less than 3% of non-informative rate (Gutierrez-Mateo *et al.*, 2011). One of the most used platforms is aCGH, which requires the placement of the sample,

blastomere or trophectoderm biopsy, in a sterile polymerase chain reaction (PCR) tube in which whole genome amplification will be performed. Amplification quality needs to be ensured (e.g., by gel electrophoresis), and then samples and control DNA are labeled with fluorophores (Rubio *et al.*, 2013b). Labeling mixes are combined and hybridized on the arrays. Each probe in the array is specific to a different chromosomal region and occupies a discrete spot on the slide. Chromosomal loss or gain is revealed by the color adopted by each spot after hybridization, this is because this technique involves the competitive hybridization of differentially labeled test and reference euploid DNA samples. Fluorescence intensity is detected with the use of a laser scanner, and specific software is used for data processing. Therefore, embryo transfer and vitrification of surplus euploid embryos can be scheduled on day 5 when day-3 biopsies are performed, or on day 6 for trophectoderm biopsies (Rubio *et al.*, 2013b).

- **Next-generation sequencing**

Finally, NGS has been developed as an effective technique for the analysis of copy number variation in single cells (Zhang *et al.*, 2013). The decrease of the cost of sequencing has made NGS one of the most promising platforms for the study of not only aneuploidies, but also mitochondrial DNA or gene disorders in a simultaneous analysis (Yan *et al.*, 2015). Most NGS protocols share the first steps with aCGH, starting with a whole genome amplification from a single cell. This is followed by a barcoding procedure, in which the different samples are labeled with unique sequences, in the way that they can be mixed later and sequenced at a time as they can be individually identified. This pooling step is the one that has contributed to significantly reducing the cost of the technique and its transfer into the clinical routine. The deepness of the sequencing is also an important aspect to consider, especially for the simultaneous study of aneuploidies and gene disorders, which would need high coverage on those regions of interest. An alternative is the parallel study of the mitochondrial DNA, which has been related to embryo quality (Diez-Juan *et al.*, 2015). In addition, sequencing has been shown to detect lower mosaicism degrees in trophectoderm biopsies than previous technologies (Ruttanajit *et al.*, 2016; Vera-Rodriguez *et al.*, 2016). Nevertheless, it would be important to consider

the relevance of mosaicism in the trophectoderm, as there are no studies related to the effect of different percentages of aneuploid cells in the blastocyst.

- **Non-invasive PGS**

The coming technologies for aneuploidy screening should be focused on non-invasive techniques; currently, all clinical methods require the biopsy of a blastomere, when the embryo is on day 3 of development, or trophectoderm, if the embryo is on day 5 or 6. The first studies performing non-invasive PGS by the exclusive use of spent culture medium (Xu *et al.*, 2016; Shamonki *et al.*, 2016) show concordant results with traditional PGS. Nevertheless, these studies have important issues to resolve, such a high non-informative rate, false negative and false positive results, or a methodological design that includes assisted hatching and therefore arises doubts about whether embryos without the zona pellucida altered would produce the same results. Thus, although this technology is not ready for clinical routine, new improvements in the method, as a more efficient removal of granulosa cells to avoid contamination with DNA of maternal origin, would allow the non-invasive technologies to be translated into the clinic for aneuploidy screening.

1.4.3.3 Aneuploidy rates in the human embryo

Aneuploidies are not a common feature in embryonic development for all mammals. For instance, aneuploidy rates in mouse embryos are really low, around 1% (Bond and Chandley, 1983). Nevertheless, the frequency of aneuploidies in humans is much higher than in any other species (Hassold and Hunt, 2001) resulting in low pregnancy rates.

Although aneuploidy existence in the human embryo has been tightly linked to infertility, high rates are still reported in embryos from fertile couples (Wells *et al.*, 2015). Furthermore, the chromosome segregation error rate increases drastically with the maternal age (Franasiak *et al.*, 2014) with percentages between 30% and 60% of aneuploidies in oocytes (Obradors *et al.*, 2011; Fragouli *et al.*, 2011). If we consider also the mitotic errors that occur in later embryonic development, aneuploidy rates reach percentages as high as 70% (Vanneste *et al.*, 2009; Mertzanidou *et al.*, 2013).

In general, a wide range of abnormalities has been reported, in some instances even from similar populations. This variability derives from different factors, such as culture conditions, the quality of the biopsied embryos (Harton *et al.*, 2011), the quality of the biopsied cells, or the methods of assessment. In addition, another important factor to consider is mosaicism. Mitotic errors during embryo development can result in chromosomally distinct cell populations producing mosaic embryos. Mosaicism at day 3 or day 5 can produce misdiagnoses, since the PGS analysis performed of a embryonic sample, one blastomere or several trophectoderm cells, does not necessarily represent the embryo as a whole.

1.4.4 Embryonic transcriptomics

The transcriptomics of the embryo reflect what is happening at a biological level, since the response of a cell to any new situation often implies new gene transcription. Due to technical limitations, previous transcriptomic studies of human embryo development analyzed only a select group of genes (Taylor *et al.*, 2001; Tachataki *et al.*, 2003) and/or large pools of embryos (Zhang *et al.*, 2009), which can be confounded by potential embryo heterogeneity. As real-time quantitative PCR (RT-qPCR) techniques have evolved and become more sensitive, gene expression analysis of individual human embryos followed (Wong *et al.*, 2010; Shaw *et al.*, 2013). More recently, single-cell RT-qPCR analysis has become a reality (Wong *et al.*, 2010; Yan *et al.*, 2013; Xue *et al.*, 2013) allowing analysis at a minimum level.

Embryo transcriptomics have been previously correlated with morphology. One study in 42 embryos analyzed 9 different genes versus different morphological parameters (Wells *et al.*, 2005). They found that expression of certain genes was correlated mainly with multinucleation and fragmentation(Wells *et al.*, 2005), suggesting an apoptotic activation of the fragmented embryos by a chromosomal abnormality that may be correlated with multinucleation. Additional studies have supported that fragmented embryos have an altered transcriptomic profile linked to telomere maintenance genes (Keefe *et al.*, 2005; Treff *et al.*, 2011)

To date, only a couple of studies have correlated gene expression patterns with aneuploidy in human embryos, one of which observed differential expression of certain epigenetic mediators in euploid versus aneuploid embryos (Chavez *et al.*, 2014) and the other examining DNA repair genes in embryos with single over complex aneuploidies (Bazrgar *et al.*, 2014). However, the latter study did not include euploid embryos, only evaluated 6 chromosomes via FISH, and analyzed 15-20 pooled day-4 embryos rather than individual embryos or single cells.

1.5 Hypothesis

Aneuploidies are a frequent alteration during the *in vitro* development of the human embryo, contributing to the low clinical success rates that are found in assisted reproductive technology. A better understanding of embryo biology remains necessary for the improvement of selection tools that could allow transfer of the embryo with the best chance to develop into a healthy newborn. However, due to the restricted availability of human embryos for research purposes, few studies have been able to combine different analyses within the same embryo. This, in combination with the multifactorial nature of aneuploidies, has made difficult the understanding of its causes and consequences.

Here, we propose that morphology, kinetics and gene expression alterations are correlated with the presence of aneuploidy in the human embryo. This knowledge could be used for explaining the etiology of chromosomal alterations in the human embryo and aiding in the improvement of IVF techniques, embryo selection methods and clinical success rates.

OBJECTIVES

2 | Objectives

The aim of this work was to better understand the causes and consequences of aneuploidy generation during human embryo development. To this end, the following specific objectives were addressed:

O1. The descriptive analysis of the human embryo at four different levels: morphology, kinetics, transcriptomics and aneuploidy incidence.

O1. The study of the relationship between morphology, kinetic behavior, gene expression and aneuploidy existence.

O2. The development of a ploidy predictive model based on the most significant differences between aneuploid and euploid embryos.

O3. The integration of morphokinetics, transcriptomics and aneuploidy data to create an atlas of the preimplantation human embryo.

METHODS

3 | Methods

3.1 Experimental design

One hundred-seventeen (117) human zygotes originating from 19 couples with an average maternal age of 33.7 ± 4.3 years were thawed for this study. Eighty-five embryos survived and were cultured under time-lapse imaging **(Figure 7)**, for a survival rate of 72.6%, which is a normal value for cryopreserved human embryos at the pronuclear stage (Reed *et al.*, 2010; Pavone *et al.*, 2011). Embryo retrieval was performed at continuous times throughout embryonic development at the pronuclear stage and during mitotic divisions 1 to 7; the number of the cells varied depending on the division types: 1 to 2, 1 to 3, or 1 to 4 cells. After embryo culture, embryos were disassembled into single blastomeres, including polar bodies from zygotes. Half of the cells of each embryo underwent whole genome amplification (WGA) and were analyzed by aCGH to determine their chromosomal status at a single-cell level. The other half were analyzed by RT-qPCR for 86 genes to evaluate the specific transcriptome signature in each cell. Kinetic parameters, chromosomal status and expression levels were compared and analyzed for individual embryos.

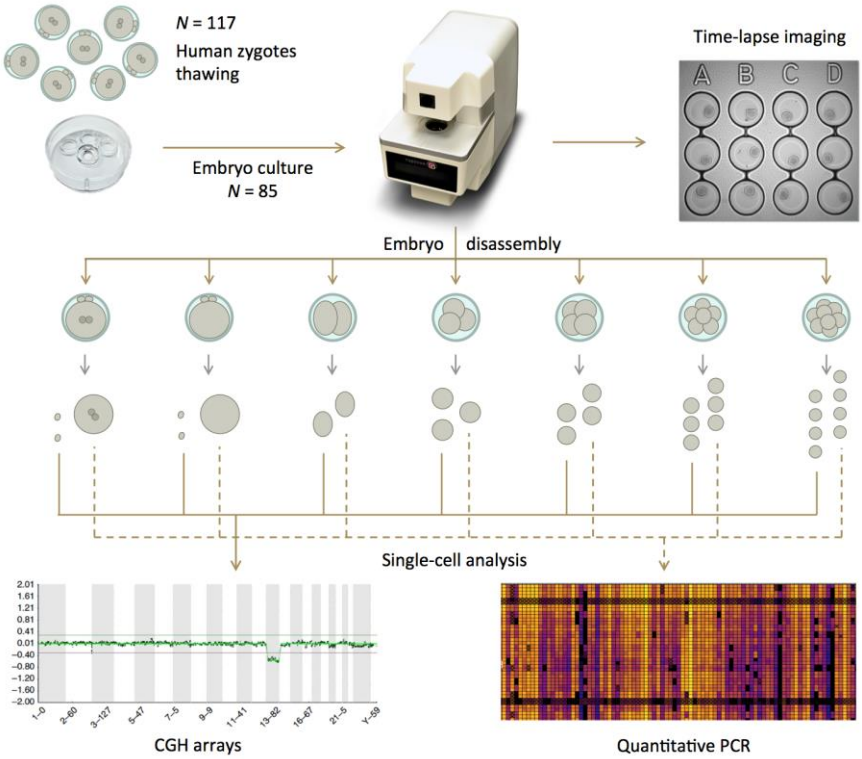

Figure 7 | Experimental design of the study.
One hundred-seventeen human embryos at the zygote stage were thawed; eighty-five of them survived and were cultured in nine different experiments. Embryo culture was performed in alphanumeric-labelled Petri dishes to allow embryo tracking during time-lapse imaging. Embryos were removed at different times until approximately the eight-cell stage. The number of cells varied depending on the type of divisions: one to two, one to three or one to four. Embryos were disaggregated into individual cells. Half of the cells from each embryo were analyzed using aCGH to determine the ploidy status, and the other half were analyzed using RT-qPCR to study gene expression. Time-lapse movies were generated for each embryo and kinetic parameters were analyzed.

3.2 Embryo manipulation

3.2.2 Embryo source

Human embryos from successful IVF cycles, subsequently donated for research, were obtained with written informed consent from the Stanford University RENEW Biobank. This cohort of embryos was cryopreserved at the pronuclear stage before the assessment of quality. Embryos in the RENEW Biobank are received from several IVF clinics across the United States. De-identification was performed according to the Stanford University Institutional Review Board-approved protocol #10466 entitled 'The RENEW Biobank' and molecular analysis of the embryos were in compliance with institutional regulations. No protected health information was associated with individual embryos.

3.2.2 Embryo thawing and culture

Human embryos at the two-pronucleus stage stored by slow-freezing were thawed by a two-step process using Quinn's Advantage Thaw Kit (CooperSurgical, CT, USA) as recommended by the manufacturer. In brief, cryocontainers were removed from the liquid nitrogen and placed in a 37 degrees Celsius (°C) water bath after being held in the air for approximately 30 seconds (s). Once thawed, liquid contents were transferred to an empty petri dish under a microscope to locate the embryos. The embryos were quickly picked and transferred to a 0.5 molar (M) sucrose solution for 10 min and then placed in a 0.2 M sucrose solution for 10 min more. Then, embryo survival was evaluated by visual observation; zygotes that did not survive were disregarded for further procedures. Dead zygotes were identified by a dark cytoplasm appearance. Only intact zygotes were washed in Quinn's Advantage® Cleavage Medium (QACM; CooperSurgical) supplemented with 10% Quinn's Advantage® Serum Protein Substitute (SPS; CooperSurgical) and cultured in 100-microliter (µL) drops of shared medium under mineral oil (Sigma, MO, USA). Embryos were cultured in custom polystyrene petri dishes (Auxogyn, CA, USA) with 12 individual microwells in the center **(Figure 8)**. Small markers (letters and numbers) were located at the edges to help with embryo identification. The dishes were prepared at least 5 h in advance and placed in the incubator to pre-equilibrate. The embryos were cultured at 37°C with 6% CO_2, 5% O_2 and 89%

N_2, standard human embryo culture conditions in accordance with current clinical IVF practice.

Figure 8 | Culture plate and individual labelled wells.
Custom petri dish with three top wells for embryo washes and one centered well for embryo culture. In the center, 12 microwells labelled with numbers and letters for individual embryo identification. Culture media was shared for all embryos.

3.2.3 Embryo disassembly and collection

The embryos were collected at different times and stages. For this purpose, the dish was removed from the incubator for not more than 5 minutes to avoid affecting either the culture of the remaining embryos or the time-lapse imaging intervals. Embryos were individually transferred to 50-µL drops of Quinn's Advantage Medium with HEPES (QAM; CopperSurgical) plus 10% human albumin (HA; CooperSurgical), at 37°C under mineral oil. Each procedure was performed with one single embryo at a time to maintain embryo identification and tracking. The zona pellucida was removed from each embryo by transferring the embryos to 200-µL drops of Acidified Tyrode's Solution (Millipore, MA, USA) briefly and then washing in QAM plus 10% HA at 37°C under mineral oil. To weaken the cellular junctions between blastomeres, embryos were incubated in 60-µL drops of Quinn's Advantage Ca^{++}/Mg^{++}-Free Medium with HEPES (CooperSurgical) plus 10% HA for 10 minutes at 37°C under mineral oil. Embryos were disaggregated using gentle mechanical pipetting in the same medium **(Figure 9)**. Once disaggregated, counting and identification of blastomeres and polar bodies was performed. Not all blastomeres from each embryo could be harvested. Annotations referring the cell appearance such as visible nuclei, membrane integrity and cytoplasmic anomalies, were recorded during the

tubing. Each sample was washed three times in 5-µL drops of phosphate-buffered saline (PBS) 1% polyvinylpyrrolidone (PVP) buffer and transferred to a sterile 0.2 milliliter (mL) PCR tube. All tubes were stored at -80°C until subsequent analysis.

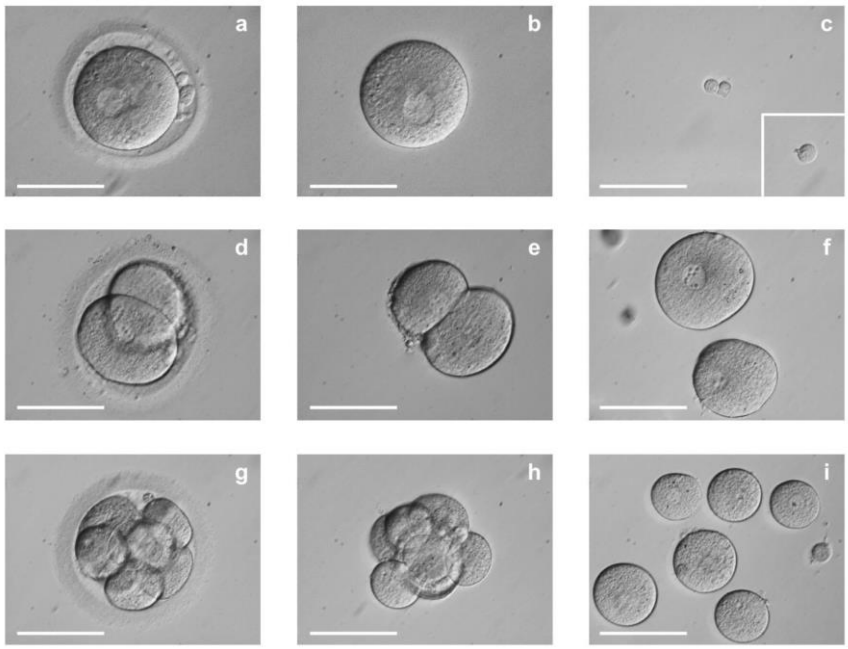

Figure 9 | Representative images of embryo disassembly at different stages.
Embryos were removed and disaggregated at different times during development. An embryo at the one-cell stage **(a)** was detached from its zona pellucida and separated into zygote **(b)** and polar bodies **(c)**. Note that the differentiation between first and second polar bodies was not possible. Another embryo at the two-cell stage **(d)** had its zona pellucida removed **(e)** and was disassembled into individual blastomeres **(g)**. An embryo at the eight-cell stage **(g)** was released from the zona pellucida **(h)** and disaggregated into individual cells **(i)**. Note that in fragmented embryos, fragments were separated from blastomeres by mechanical pipetting since they may potentially interfere in the results. Scale bar, 100 µm

3.3 Time-lapse imaging

3.3.1 Image taking

Embryos were monitored continuously using a microscope system (Auxogyn) **(Figure 10)** inside a standard tri-gas incubator (Sanyo, Japan). The system consisted of an inverted digital microscope with light-emitting diode illumination, X10 Olympus objective, automatic focus knob and 5 megapixel CMOS camera. Three types of images were collected during culture: darkfield and brightfield images were taken automatically every 5 min and at 1 s and 500 milliseconds (ms) of exposure time, respectively. In addition, brightfield images were also taken at 10 equidistant planes at several points throughout culture to capture images of the whole embryo. The time between multiplane captures varied depending on when the embryo was collected and one last capture was taken just before taking each embryo out of the incubator.

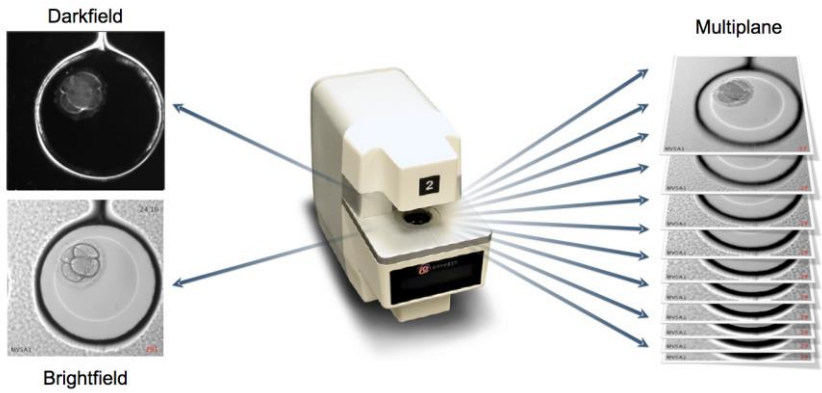

Figure 10 | Time-lapse imaging technology.
Time-lapse microscope took three types of pictures: darkfield images every 5 minutes, useful for a clear detection of cell membranes and embryo divisions; brightfield images every 5 minutes for the evaluation of cytoplasm related events, such as pronuclear disappearance, vacuole existence or blastomere multinucleation; and multiplane captures at 10 equidistant distance for a three-dimensional perception of the embryo, useful to measure spatial parameters such as percentage of fragmentation.

3.3.2 Image processing

After each experiment, all images were processed using ImageJ software (Schneider *et al.*, 2012). Brightfield and darkfield images were cropped to get individual images from each embryo. Contrast and color balance were modified

to allow an easier identification of cytoplasmic events. All images from one single embryo were compiled into time-lapse movies. Identification labels and timestamps were included to facilitate the measurement of the imaging parameters. In addition, multiplane images of every embryo were assembled in a multi-stack file using ImageJ. For this, images from one embryo were grouped into consecutive stacks of 10 pictures. Each stack was equivalent to a different time point, and each picture of a stack corresponded to a different plane of the embryo, from the bottom to the top.

3.3.3 Parameter evaluation

Developmental kinetics of each embryo were translated from frames to hours on the basis that an image frame was captured every 5 min. All timing intervals between the one- and nine-cell stages were measured for each embryo unless removed for molecular or chromosomal analysis before reaching this stage of development (**Figure 11** and **Supplementary Movie 1)**. These intervals corresponded to the kinetic parameters to study. In addition, the existence of irregular divisions was also annotated, as the exact time in which the division took place and the type: direct division from 1 to 3 cells or 1 to 4 cells.

Morphological parameters were also annotated, such as fragmentation, multinucleation or vacuole existence. We recorded the fragmentation percentage in each embryo according to the total cytoplasmic volume that the fragments were representing. In case of fragmentation existence, we also annotated when they appeared for the first time (one-cell stage, 1st division, two-cell stage or later). We also noted multinucleation when more than one nucleus was visible in a blastomere. We added all additional comments that could be useful for later embryo evaluation, such as vacuole existence, cytoplasm polarization, division attempts or uneven blastomere size.

Multiplane captures were used to confirm brightfield and darkfield imaging observations and to assist in the measurement of certain parameters such as PNd or percentage of fragmentation, which may be difficult to determine using just one single plane. Embryo development evaluation was completed before ploidy and gene expression analyses to ensure blinded parameter measurements.

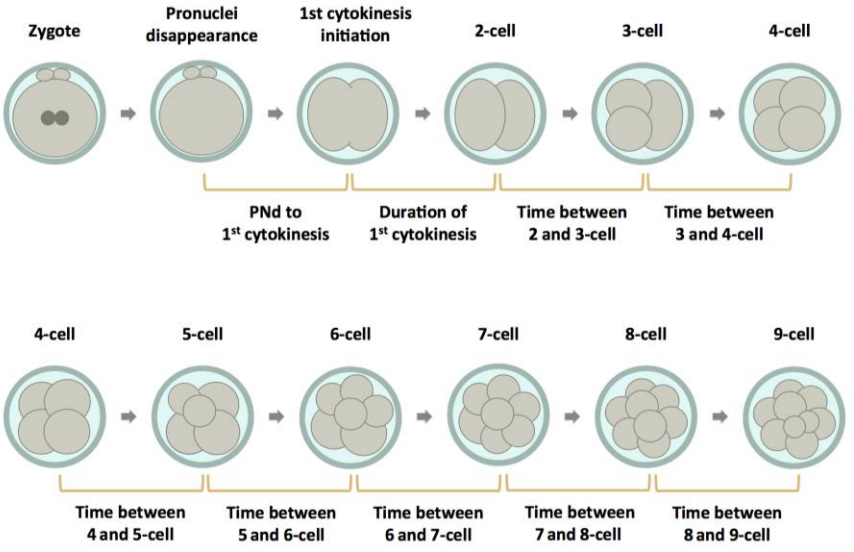

Figure 11 | Kinetic parameters.
The standard kinetic parameters that were evaluated in the embryos included times between divisions. Due to the importance of the first mitosis the time from pronuclear disappearance to the start of the first cytokinesis and the duration of the first cytokinesis was also measured. The number of parameters analyzed depended on the final stage in which the embryo was retrieved. The nine-cell stage was included for those embryos in which divisions were faster than normal due to irregular divisions.

3.3.4 Embryo classification

Because an important part of our study was to analyze gene expression, a reliable manner to classify embryos was necessary to make proper comparisons between embryos. In the clinical routine, embryos are classified according to the number of cells, but since irregular divisions during development produce a greater number of faster-dividing cells, the number of blastomeres was disregarded as a method to stage embryos. As an example, an embryo with four blastomeres could result from three consecutive regular divisions, but it could also be produced during one direct cleavage from 1 to 4 cells. In both cases, the embryos would be at the four-cell stage and it would be inappropriate to make transcriptomic comparisons between them. Thus, the time from PNd was chosen as the best reference for the starting point to define embryo stage for all studies; PNd is the first event observed post-thaw and before mitotic divisions.

3.4 Detection of chromosomal abnormalities in single cells

Aneuploidy screening for the detection of chromosomal abnormalities for all 24 chromosomes was accomplished by aCGH. The completed protocol was performed in less than 24 h with five different steps: whole genome amplification, labelling, combination, hybridization and scanning **(Figure 12).** Arrays CGH was the chosen method not only for being the most popular technique inside PGS clinical programs, but because its efficiency and accuracy for the analysis of not only blastomeres, but also polar bodies, had been widely supported(Geraedts *et al.*, 2011; Gutierrez-Mateo *et al.*, 2011; Christopikou *et al.*, 2013; Rubio *et al.*, 2013b; Rodrigo *et al.*, 2014).

3.4.1 Whole genome amplification

Single-cell DNA extraction and WGA was accomplished using the Sureplex Kit (Illumina, Cambridge, UK) in a three-step protocol: cell lysis, pre-amplification and amplification process. For cell lysis, 3 µL of Cell Extraction Buffer, 4.8 µL Extraction Enzyme Dilution Buffer and 0.2 µL of Cell Extraction Enzyme were added to each individual sample. A positive control (1 µL of genomic control DNA) and a negative control (2 µL of PBS 1% PVP buffer) were included. This first step was accomplished by incubated the samples 10 min at 75°C following by 4 min at 95°C. For pre-amplification step, 4.8 µL of SurePlex Pre-amp Buffer and 0.2 µL of SurePlex Pre-amp Enzyme were added to each lysed sample, following by an incubation process at 95°C for 2 min, followed by 12 cycles of 95°C for 15 s, 15°C for 50 s, 25°C for 40 s, 35°C for 30 s, 65°C for 40 s, and 75°C for 40 s. Final amplified DNA was obtained by adding 34.2 µL of Nuclease-free Water, 25 µL of SurePlex Amplification Buffer and 0.8 µL of SurePlex Amplification Enzyme to each pre-amplified sample. Samples were incubated at 95°C for 2 min, followed by 15 cycles of 95°C for 15 s, 65°C for 1 min, and 75°C for 1 min. To determine the success of the whole genome amplification process, all amplified samples and controls were tested using the FlashGel™ system (catalog # 57067; Lonza Ltd., Switzerland) by loading 1 µL of each DNA together with 4 µL of loading mix (3 µL water : 1 µL loading buffer) in each well of the cassette **(Figure 12).**

3.4.2 Labelling

WGA products and reference DNA (normal male and female controls) were labelled with either Cy3 or Cy5 fluorophores using random primers according to manufacturer´s protocol (Illumina). An automatic template was created to distribute all samples into two groups: half were labelled by Cy3, and half by Cy5 **(Figure 12).** Male and female DNA references were also included, and distributed into different slides, top and bottom subarrays, and Cy3/Cy5 fluorophores, for an accurate paralleling process. For labelling, 5 µL of Primer Solution and 8 µL of DNA (either sample or reference) were first combined and then incubated at 94°C for 5 min and -20°C for 5 min. Afterwards, 12 µL of labelling mix (5 µL Reaction Buffer, 5 µL dCTP mix, 1 µL Cy3/Cy5, and 1 µL Klenow) were added to each sample following the template. Finally, samples were incubated for 2 h at 37°C.

3.4.3 Combination, precipitation, and hybridization

Labelled control and samples DNAs were combined by mixing one Cy3 labelled sample together with one Cy5 labelled sample, and by adding 25 µL of COT Human DNA **(Figure 12)**. The resultant mix was reduced by centrifugal evaporation at 75°C for 1 h. The pellet was resuspended with 21 µL Hybridization Buffer (15% dextran sulphate) and incubated for 10 min at 75°C. Subsequently, 18 µL from each well were loaded in each subarray hybridization area (24sure, Illumina) and covered with a coverslip **(Figure 12)**. All slides were placed inside a hybridization chamber containing a tissue saturated in 6 mL 2X SSC/50% formamide. Finally, hybridization chambers were incubated for 6-12 h in a 37°C water bath.

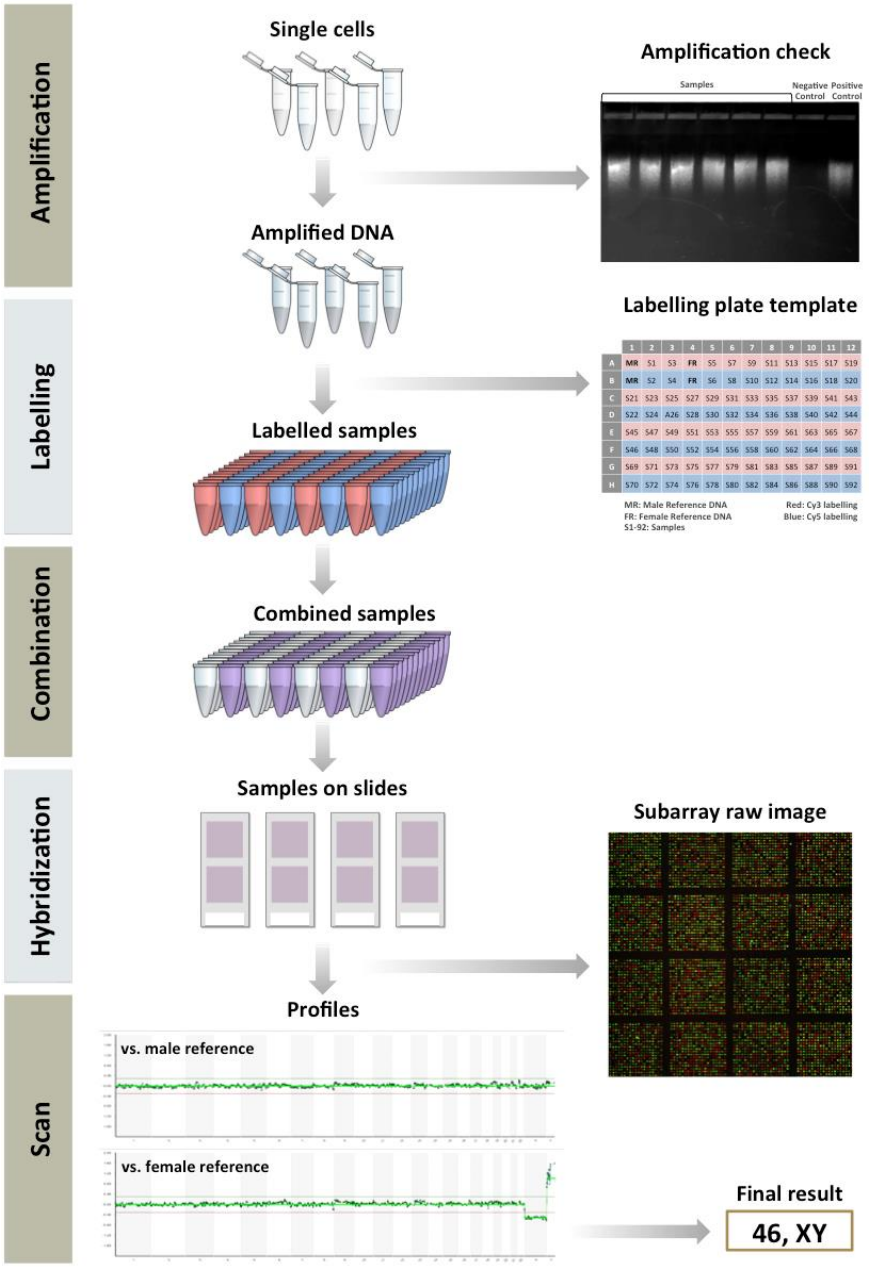

Figure 12 | Comparative genomic hybridization arrays illustrative protocol.
For the detection of chromosomal abnormalities single cells were amplified and labelled with either Cy3 (red) or Cy5 (blue) fluorophores. Reference and sample labelled DNAs were combined and co-hybridized on 24sure arrays for a minimum of 4 h. After washing, slides were scanned and the data analyzed using the BlueFuse Multi software (Illumina).

3.4.4 Post-hybridization washes and scan

Before scanning, coverslips were removed carefully by immersion of the slides in a coplin jar containing 2X SSC/0.05% Tween20. Then slides were washed in the same solution and with agitation for 10 min. Afterwards, slides were quickly transferred to a 1X SSC solution for 10 min, then a 0.1X SSC solution at 60°C for 5 min, and finally a 0.1X SSC solution for 1 min. After washes, slides were dried by centrifugation at 170 x *g* for 3 min. The scanning process was performed using Innoscan 710 (Innopsys, Carbonne, France) **(Figure 12)**.

3.4.5 Array CGH results interpretation

All aCGH data were analyzed using the BlueFuse Multi software (Illumina). The software produces two profiles from each sample: one versus a female reference and another versus a male reference **(Figure 12)**. Both profiles were evaluated to have an unequivocal evaluation of the sex chromosomes (X and Y). The X separation (log2 value) was a key parameter to know the quality of the experiment. Other quality parameters were the percentage of included clones and the confidence values for individual chromosomes results. Results obtained from questionable samples, such as fragmented polar bodies or those with inconsistent profiles, were disregarded **(Figure 13).**

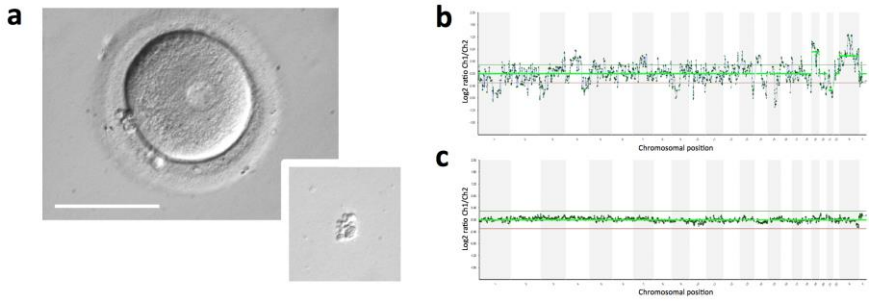

Figure 13 | Ploidy exclusion criteria.
Ploidy results were discarded in cases of a zygote with polar body fragmentation **(a)** since DNA from fragmented polar bodies may be degraded and show an aCGH profile with amplification failure **(b)** rather than the typical aCGH profile **(c)**. Scale bar, 100 µm

3.5 High-throughput single-cell gene expression analysis

3.5.1 Gene selection and primer design

A total of 86 genes were selected on the basis of their previously reported importance in the literature (Liu *et al.*, 2000; Jurisicova *et al.*, 2003; Wells *et al.*, 2005; Ma *et al.*, 2006; Bultman *et al.*, 2006; Jaroudi and SenGupta, 2007; Wan *et al.*, 2008; Jaroudi *et al.*, 2009; Wong *et al.*, 2010; Kiessling *et al.*, 2010; Galan *et al.*, 2010; Tashiro *et al.*, 2010; Mantikou *et al.*, 2012; Choi *et al.*, 2012; Shaw *et al.*, 2012; Galan *et al.*, 2013; Baran *et al.*, 2013). The biological processes in which the genes were involved included, but were not limited to, cell cycle regulation, apoptosis, telomere maintenance and DNA methylation **(Table 3).** Primers were designed to span exons and detect all gene isoforms whenever possible **(Supplementary Table 1).** Primers were first tested in single blastomere and redesigned when nonspecific amplification was observed.

3.5.2 Complementary DNA synthesis

The procedure for gene expression analysis was adapted from the Advanced Development Protocol for Single-Cell Gene Expression Using EvaGreen DNA Binding Dye (Fluidigm, CA, USA). cDNA was prepared by adding to each individual sample: 9 µL RT-STA Solution [5 µL Cells Direct 2X Reaction Mix (Invitrogen, CA, USA); 0.2 µL SuperScript III RT Platinum Taq Mix (Invitrogen); 2.5 µL 4X Primer Mix (200 nM); and 1.3 µL DNA Suspension Buffer (Teknova, CA, USA)]. Reverse transcription and pre-amplification was accomplished by incubating the samples at 50°C for 15 min and 95°C for 2 min, followed by 18 cycles of 95°C for 15 s and 60°C for 4 min. Exonuclease I treatment method was used to remove unincorporated primers by adding 3.6 of Exo I Reaction Solution (2.52 µL purified water, 0.36 µL Exonuclease I Reaction Buffer, 0.72 µL Exonuclease I at 20U/µL) to each sample, and incubating at 37°C for 30 min followed by 15 min at 80°C. The final volume was diluted two-fold before RT-qPCR.

Table 3 | Main functions for the studied genes.

Gene Name	Function	Gene Name	Function
ACTB	Cytoskeleton organization	*GATA4*	Transcription regulation
AHR	Apoptosis	*INCENP*	Centromere
AKT1	Apoptosis	*KHDC3L*	Genomic imprinting
ALKBH2	DNA repair	*MAD2L1*	Spindle checkpoint
APC	Apoptosis	*MBD4*	Methylation
ATM	Cell cycle checkpoint	*MCL1*	Apoptosis
AURKA	Spindle stabilization	*MLH1*	DNA repair
AURKB	Chromosome segregation	*MRE11A*	DNA repair
BAD	Apoptosis	*MSH2*	DNA repair
BCL2	Apoptosis	*MSH3*	DNA repair
BRCA1	Genomic stability	*MSH6*	DNA repair
BRCA2	DNA repair	*NLRP5*	Oocyte biology
BUB1	Cell cycle checkpoint	*NPM2*	Histone chaperone
BUB3	Cell cycle checkpoint	*OOEP*	RNA binding
CASP2	Apoptosis	*PADI6*	Cytoskeleton organization
CCNA1	Cell cycle regulation	*PCNT*	Centrosome organization
CCND1	Cell cycle regulation	*PDCD5*	Apoptosis
CCNE1	Cell cycle regulation	*PER1*	Cyrcadian regulation
CCT3	Protein folding	*PLK1*	Cell cycle checkpoint
CDH1	Apoptosis	*POT1*	Telomeres maintenance
CDK1	Cell cycle regulation	*POU5F1*	Pluripotency
CDK2	Cell cycle regulation	*PRMT1*	Histone methylation
CDK7	Cell cycle regulation	*PTTG1*	Chromatid separation
CETN2	Centrosome organization	*RAD51*	DNA recombination
CFL1	Cytoskeleton organization	*RAD52*	DNA recombination
CHEK1	DNA damage checkpoint	*RB1*	Cell cycle regulation
CHEK2	Cell cycle checkpoint	*RCC2*	Cell cycle regulation
CLOCK	Cyrcadian regulation	*RPL10L*	Ribosome
CRY1	Cyrcadian regulation	*RPLP0*	Ribosome
CTCF	DNA methylation	*RPS24*	Ribosome
CTNNB1	Adherens junctions	*SMARCA4*	Transcription regulation
DDX20	RNA secondary structure	*SOX2*	Pluripotency
DDX4	RNA secondary structure	*TERF1*	Telomere regulation
DIAPH1	Actin polymerization	*TERF2*	Telomere regulation

DNMT1	Methylation	*TERT*	Telomere maintenance
DNMT3A	Methylation	*TP53*	Cellular stress
DNMT3B	Methylation	*TSC2*	Cell cycle arrest
DPPA3	Maternal factor	*TUBG1*	Centrosome organization
E2F1	Cell cycle regulation	*XPA*	DNA excision repair
ECT2	Cytokinesis	*YBX2*	mRNA stabilization
FASLG	Apoptosis	*YY1*	Transcription regulation
GADD45A	DNA repair	*ZAR1*	Embryogenesis
GAPDH	Metabolism	*ZSCAN4*	Telomere maintenance

3.5.3 Real-time quantitative PCR

For RT-qPCR, 2 µL of STA and Exo I-treated sample was mixed with Sample Mix solution [2.5 µL 2X Taqman Gene Expression Master Mix (Applied Biosystems, CA, USA); 1.25 µL 20X DNA Binding Dye Sample Loading Reagent (Fluidigm); 1.25 µL 20X EvaGreen DNA binding dye (Biotium, CA, USA)]. Gene assay mix solutions were prepared by adding 1.25 µL of 40 µM primer pairs with 2.5 µL 2X Assay Loading Reagent (Fluidigm) and 1.25 µL DNA Suspension Buffer. Both sample and assay mixes were loaded into 96.96 Dynamic Arrays for RT-qPCR on a BioMark System (Fluidigm). The same technical replicates were included on each dynamic array to check for variability between arrays and ensure reliable data. Data Collection and Real-Time PCR Analysis software (Fluidigm) were used to calculate threshold cycle (C_t) values from the melt curve of each gene assay.

3.5.4 Raw data processing

Raw data were normalized to avoid variability between chips and allow comparison between blastomeres from different developmental stages. As gene activation during embryo development may not be simultaneous in embryos of similar stage or between blastomeres within the same embryo, normalization using housekeeping genes was not performed. Instead, a quantile normalization method was applied using *limma* package (Smyth, 2005) for R (R Core Team, 2013). This method was chosen to highlight expression differences rather than absolute expression values. Other normalization methods do not distinguish between genes with different dynamic range. We call dynamic range as the

distance between the minimal and the maximal expression values of a gene. If we do not attend to the dynamic range, we consider similar ΔC_t to have the same biological relevance between two difference genes **(Figure 14a)**.

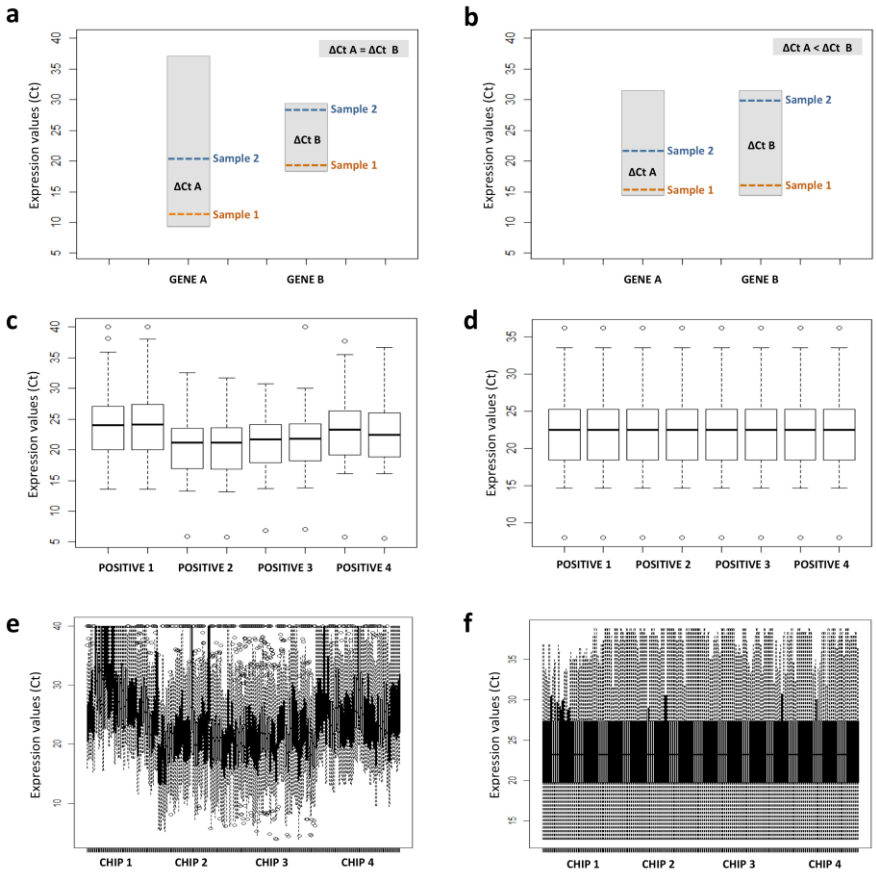

Figure 14 | Normalization process for gene expression data.
Similar differences in expression values from two samples between genes can be translated in a different biological meaning when they have different expression ranges **(a)**. With quantile normalization we can compare genes and samples between them since all genes acquire the same distribution **(b).** To evaluate the accuracy of data normalization, boxplots from each sample were generated. Each boxplot shows the median (black line), 25th percentile value (lower hinge), 75th percentile value (highest hinge), and the maximum and minimum values (whiskers) excluding outliers (circles). A common positive control was added to all chips to have a reference after normalization. Due to experimental variability, we observed different values in the raw data from positive control between chip data **(c)**; quantile normalization allowed to equalize them **(d).** Sample raw data also showed high variability between experiments **(e)**, but thanks to normalization they could all be compared by the acquisition of similar distributions **(f)**.

Nevertheless, quantile normalization makes data have equal distributions, meaning equal dynamic ranges, and allows comparison of C_t values between genes **(Figure 14b)**. This is also important since we compare samples different developmental stages. To detect experimental variability, the same positive control was run in all four chips **(Figure 14c)** and compared after normalization to confirm the efficacy **(Figure 14d)**. Afterwards and before secondary analysis, all raw data **(Figure 14e)** were also normalized **(Figure 14f)**.

An assumed baseline C_t value of 28 or below was included on the basis of previous findings (Guo *et al.*, 2010) and all C_t values higher than this value were called as no expression. Similarly, all samples with questionable results such as a disproportionately high number of failed gene assays or unusual melt curves were discarded **(Figure 15)**. Absolute expression levels were obtained by subtracting C_t values from the C_t baseline value of 28.

Finally, for group comparisons, relative expression was calculated by dividing each expression value between the average expression value of the reference group (Ex. non-vacuolated embryos, when comparing expression between embryos with and without vacuoles) to obtain a final fold-change value, which may be more informative in those cases.

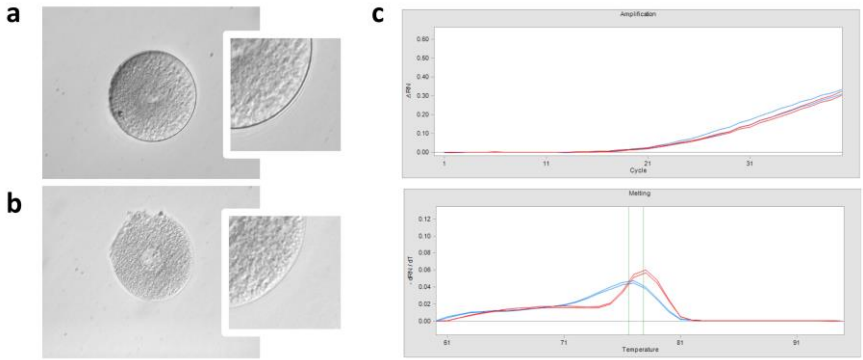

Figure 15 | Gene expression exclusion criteria.
Since the integrity of the cell membrane could alter gene expression results, only blastomeres with an intact membrane were included **(a)**; blastomeres with a compromised membrane **(b)** were disregarded in the analysis. This is on the basis of RT-qPCR curves from blastomeres with an intact membrane (**c**, red lines) and a compromised membrane (**c**, blue lines).

3.6 Statistical analysis of gene expression data

Data analyses including outliers, descriptive parameters and statistical tests were performed using IBM® SPSS® Statistics Version 21. For descriptive variables, Saphiro-Willg test was first performed to check for normal distribution. If they were normally distributed, *t*-test (for two groups) or one-way analysis of variance (ANOVA; for more than two groups) was performed to compare mean values. When not normally distributed, the medians were compared by the non-parametric Mann-Whitney *U*-test (for two groups) or by Kruskal Wallis test (for more than two groups). For categorical variables chi-square test was performed, except for variables with small sample size (one of the alternatives has a number smaller than 5) in which Fisher´s exact test was performed.

For gene regressions models, gene expression values were adapted to a quadratic curve (ax^2+bx+c) and the accuracy of the model was tested by ANOVA. For gene expression comparisons between groups of fragmentation, vacuoles, kinetics or ploidy, we first perform a *t*-test between the average collection times. In case of significant differences between groups ($P<0.05$) the comparison was discarded to avoid biased results.

Babelomics was the selected platform for the analysis of the gene expression data (Medina *et al.*, 2010). The functional analysis tool, FatiGO, was used to detect over-represented functional annotations in a cluster of genes and the class comparison tool assisted in the detection of genes differentially expressed between groups. Comparative expression between aneuploid and euploid embryos from the same time point was performed in the class comparison tool using the *limma* test in Babelomics (Medina *et al.*, 2010) and Benjamini and Hochberg test was selected to estimate the false discovery rate.

3.7 Ploidy predictor model

The prediction model was built using the *k*-nearest neighbors algorithm (k-NN) in the Babelomics platform (Medina *et al.*, 2010), which consists of a function for the measurement of distances between samples on the basis of gene expression profiles. To avoid bias during model generation, sample-split was performed. Two-thirds of the samples were randomly selected and grouped as a training set and the other one-third of the samples became the validation set, which was used to test the model once generated. Each sample from the training group was assigned a class: euploid or aneuploid. For a test sample, the model was assigned a class attending to the most represented among the closest *k* samples. Several models were generated on the basis of the number of neighbors that were evaluated for the prediction. To select the most accurate model, a *k*-fold cross-validation was performed. In this method, the data set was automatically split into *k* partitions and *k-1* was used for model training and error estimation, respectively. This process was complete when all samples were tested and repeated several times to improve prediction accuracy.

RESULTS AND DISCUSSION

4 | Results and discussion

4.1 Early human embryo developmental morphology

4.1.1 Fragmentation

A recent publication described for the first time the existence of chromosome content in embryo fragments (Chavez *et al.*, 2012). Therefore, we wanted to focus on fragmentation as the main morphological parameter to study for a possible relationship with aneuploidy generation. We evaluated the percentage and timing of fragmentation. The percentage of fragmentation was defined as the volume of an embryo that is occupied by fragments. Multicapture imaging was essential to obtain a three-dimensional picture of each embryo and an accurate measurement of the fragmentation degree **(Figure 16).**

The majority of embryos exhibited less than 25% fragmentation (n = 62), and no embryo showed fragmentation greater than 60% of the cytoplasmic volume **(Figure 17a).** Regarding the stage of the first appearance of fragmentation, we differentiated between three time points: before the first division, meaning the one-cell or zygote stage **(Supplementary Movie 2),** during the first division **(Supplementary Movie 3)**, or after the first division **(Supplementary Movie 4).** In the 64 embryos displaying fragmentation to any degree, most (68.8%) were initially fragmented during the first division, highlighting the importance of the first mitosis. Of the remainder, 21.9% fragmented before, and 9.4% after the completion of this division **(Figure 17b).** Additionally, in 3 embryos we could observe several events of fragment dynamics, such as fragment division, fusion of fragments, and fragments resorption by a blastomere (**Supplementary Movie 5).** These phenomena have been previously reported in the literature (Chavez *et al.*, 2012).

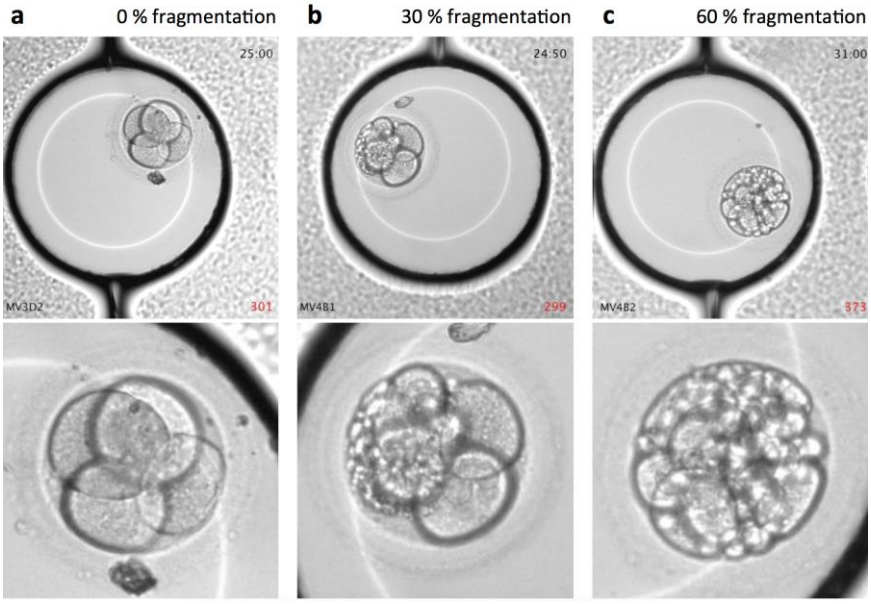

Figure 16 | Embryo fragmentation degree range.
Three human embryos showing different degrees of fragmentation at the four-cell stage. Some embryos did not show any fragmentation **(a)**, but some other embryos showed fragmentation from intermediate **(b)** to very high degrees **(c)**.

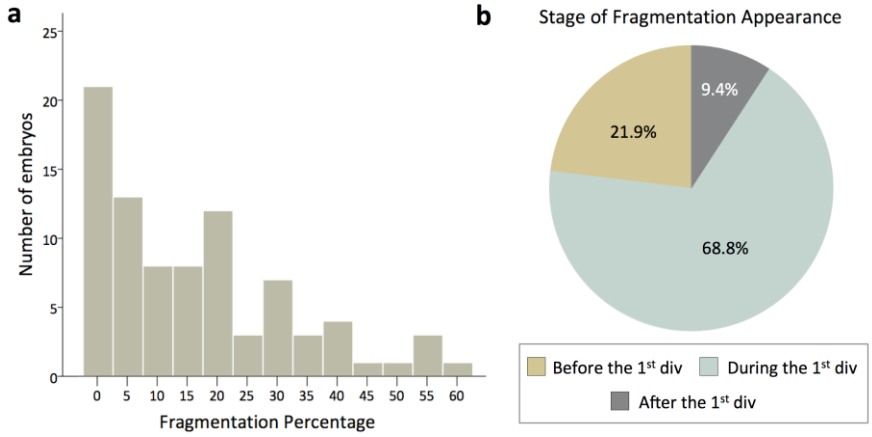

Figure 17 | Cellular fragmentation dynamics in embryos.
(**a**) The distribution of embryos according to the percentage of fragmentation at collection. Fragmentation was quantified at intervals of 5% and was confirmed via three-dimensional multi-plane imaging. (**b**) A pie graph showing that almost all fragmentation appears before (*n* = 14) or during the first division (*n* = 44) with a much smaller percentage appearing later (*n* = 6). Note that each embryo was annotated by the stage in which fragmentation appeared for the first time.

4.1.2 Other morphological parameters

In addition to fragmentation, we annotated any other morphological characteristic that may be relevant to aneuploidy, such as multinucleation. In total, 14% of the cultured embryos (*n* = 12) showed more than one nucleus at some cleavage stage, or more than two pronuclei at zygote stage. Most of the embryos (*n* = 9) were multinucleated at the two-cell stage (**Figure 18a**), but two of them had more than one nucleus in at least one blastomere at the four-cell stage. Another embryo also showed multinucleation at the one-cell stage after a failed division attempt **(Supplementary Movie 6).** This embryo had originally two pronuclei, which disappeared to start cytokinesis, but since the division did not end successfully, the embryo did not divide and the nuclei appeared again, but this time there were five nuclei, instead of two.

In the literature, multinucleation rates range from around 30% (Van Royen *et al.*, 2003; Ergin *et al.*, 2014; Desai *et al.*, 2014) to more than 40% (Aguilar *et al.*, 2016; Balakier *et al.*, 2016)of embryos. Those rates, which are much higher than our findings, include embryo culture until blastocyst stage; we cultured until eight-cell stage only, removing embryos at different times. As most of the multinucleation takes place during the two-cell stage (Van Royen *et al.*, 2003; Ergin *et al.*, 2014; Aguilar *et al.*, 2016), if we consider only embryos from this stage (n = 47), the adapted multinucleation rate is 25.5%, which is closer to the one described in the literature.

We also annotated other events such as cytoplasm polarization **(Figure 18b)**, different pronucleus sizes, cytoplasm anomalies, or vacuoles existence. We found two interesting dynamics in embryos with vacuoles. First, most of the embryos with vacuoles showed a decrease in the vacuole number right after the first mitosis (**Figure 18c**). Second, we observed the fusion between small vacuoles to give rise to a larger one **(Figure 18d and Supplementary Movie 7)**. Vacuole dynamics have been only reported in one previous study, in which the authors observed the vacuoles throughout embryo development. They described a vacuole frequency between 5 and 12% of the embryos, depending if the embryos were fertilized by IVF or ICSI, respectively, and around 28% of the vacuoles generated by ICSI disappeared by day 2. These data would explain why we saw a decrease in the number of vacuoles right after the first mitosis.

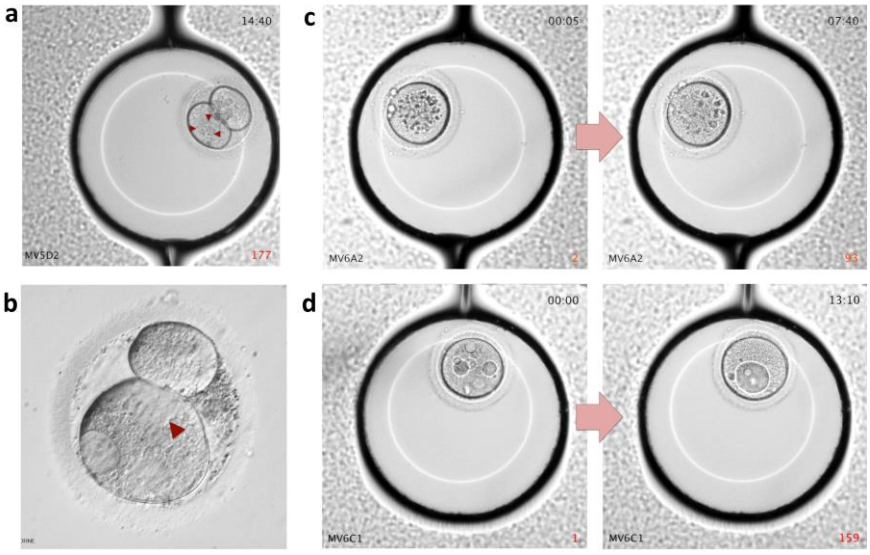

Figure 18 | Altered morphology in human embryos.
(**a**) Embryo at the two-cell stage showing multinucleation. Red arrows point at three nuclei in the bottom blastomere.
(**b**) Embryo at the two-cell stage showing cytoplasm polarization. Red arrow indicates the line between the two density areas from the cytoplasm in the bottom blastomere.
(c) Human zygote with a high number of vacuoles (left frame); most of them disappear right after the first mitotic division (right frame).
(d) Human zygote with several vacuoles of medium size (left frame) that fused to produce a larger vacuole (right frame). See also **Supplementary Movie 7**.

4.2 Kinetic behaviour of the early human embryo

4.2.1 Description of kinetic parameters

We began by examining previously reported parameters including the duration of the first cytokinesis (time between the appearance of a cleavage furrow and completion of daughter cell separation), the time between the two- to three-cell stages, and time between the three- to four-cell stages (Wong *et al.*, 2010; Meseguer *et al.*, 2011) **(Table 4)**. The median duration of the first cytokinesis was 20 min (range 15 min to 2.9 h), the time from two- to three-cell stages was 11.4 h (range 0-16.8 h) and the median time between the three- and four-cell stages was 1.3 h (range 0-22.1 h). Note that some parameters range from 0 hours, which is the result of the existence of an irregular division: if a zygote divides directly to three cells instead of two, the time between the two- and three-cell stages would be zero, and similar with the time between the three- and the four-cell stages when the zygote divides directly to four cells.

Wong *et al.* studied embryo morphokinetics of 242 frozen zygotes and defined these three parameters predictive of blastocyst formation with the average values of 14.3 ± 6.0 min for the duration of the first cytokinesis, 11.1 ± 2.2 h for the time between the two- and the three-cell stages, and 1.0 h ± 1.6 for the time between the three- and the four-cell stages (Wong *et al.*, 2010). Similarly, Meseguer *et al.* analyzed 2,120 fresh embryos and established the mean value for the parameters of those that implanted, with a time between the two- and three-cell stages (called as 'CC2') of 11.8 ± 1.2 h and a time between the three- and the four-cell stages (called as 'S2-') of 0.78 ± 0.73 h (Meseguer *et al.*, 2011). Although our morphokinetic data are in concordance with these two previous publications, small differences are expected due to different embryo populations, as it would be for the one with embryos that exclusively succeed in blastocyst formation or implantation; or due to different embryo origins, as for embryos from fresh cycles, instead of frozen.

Besides evaluating previously identified imaging parameters, we also measured the time between PNd and the start of the first cytokinesis, a recently described parameter that has been linked to human embryo viability (Athayde

Wirka *et al.*, 2014; Desai *et al.*, 2014), but not to chromosomal status. As shown in Table 1, the median for the time between PNd and the start of the first cytokinesis was 2.7 h (range 15 min-22.2 h) suggesting that the wide range of this parameter might reflect underlying differences in embryo developmental potential.

Table 4 | Kinetic parameters in all cultured embryos.

	N	Median	IQR
PNd to first cytokinesis (h)	48	2.71	(2.33;3.15)
First cytokinesis (min)	67	20.0	(15.0;30.0)
Two to three cells (h)	47	11.42	(0.92;14.5)
Three to four cells (h)	39	1.25	(0.58;4.42)
Four to five cells (h)	21	8.08	(0.71;12.25)
Five to six cells (h)	17	2.25	(0.46;7.29)
Six to seven cells (h)	16	1.54	(0.79;6.44)
Seven to eight cells (h)	14	0.79	(0.50;2.17)
Eight to nine cells (h)	3	1.58	(0.50;NA)

IQR, interquartile range (Q1;Q3);Q1, 25th percentile; Q3, 75th percentile; PNd, pronuclear disappearance; NA, not applicable

4.2.2 Irregular divisions and effect on kinetics

In addition to normal cell cycle divisions, we were able to detect irregular division events in certain embryos, including divisions from 1 to 3 cells or from 1 to 4 cells instead of the regular division from 1 to 2 cells. Irregular divisions, also called "direct cleavage", have been described in the literature with a frequency ranges from 14% to 26% (Rubio *et al.*, 2012; Campbell *et al.*, 2013; Desai *et al.*, 2014). In our study, these atypical events occurred in 23.6% (*n* = 20) of embryos with the majority dividing from 1 to 3 blastomeres (*n* = 17; **Supplementary Movie 8)** and a much smaller subset dividing from 1 to 4 cells (*n* = 3; **Supplementary Movie 9**). Notably, 85% (*n* = 17) of all irregular divisions occurred during the first mitosis, as previously reported (Campbell *et al.*,

2013), whereas only 15% (*n* = 3) occurred in either the second or third mitosis **(Supplementary Movie 10),** stressing the relevance of the first mitotic division.

It is important to note that one irregular division altered all subsequent kinetic parameters **(Figure 19).** Thus, we considered that kinetic parameters should be always calculated for regular and irregular division separately to avoid drawing misleading conclusions, as has already been established in the literature (Herrero *et al.*, 2013). In addition, this would be related with the use of developmental time instead of the cell stage to classify or compare embryos in a study, as two embryos with the same number of cells can proceed from very different origins, especially when irregular divisions are part of the process.

As expected, the time between two- and three-cell stages was shorter in embryos with irregular divisions, and together with the time between the four- and five-cells stage were the most statistically differential parameters versus embryos with regular divisions (**Table 5**). Also, it is important to notice that the time between the PNd and the first cytokinesis, and the duration of the first cytokinesis, were not statistically different between groups, since irregular divisions only affect kinetics after they have occurred.

The origin of direct cleavage during embryo development remains unknown. Different hypotheses have been postulated. The most accepted ones support that irregular divisions are originated from multipolar spindles that can be created during polyspermia (Kola *et al.*, 1987) or by anomalies in the inherited centrosome from the sperm (Sathananthan *et al.*, 1996). In our study, all embryos showed two polar bodies and two pronuclei, which are indicative of a proper fertilization, discarding polyspermia. Nevertheless, a previous study in rhesus monkey has shown that embryos from sperm that has been previously exposed to oxidative stress show higher proportions of irregular divisions (Burruel *et al.*, 2014). Surprisingly, DNA oxidation has been correlated with lower sperm motility in infertile males (Meseguer *et al.*, 2008), which would explain the high proportions of irregular divisions in embryos from IVF couples. Interestingly, a recent study has demonstrated that irregular divisions may create the segregation of the parental genomes in chimeric and/or mixoploid lineages inside the embryo (Destouni *et al.*, 2016).

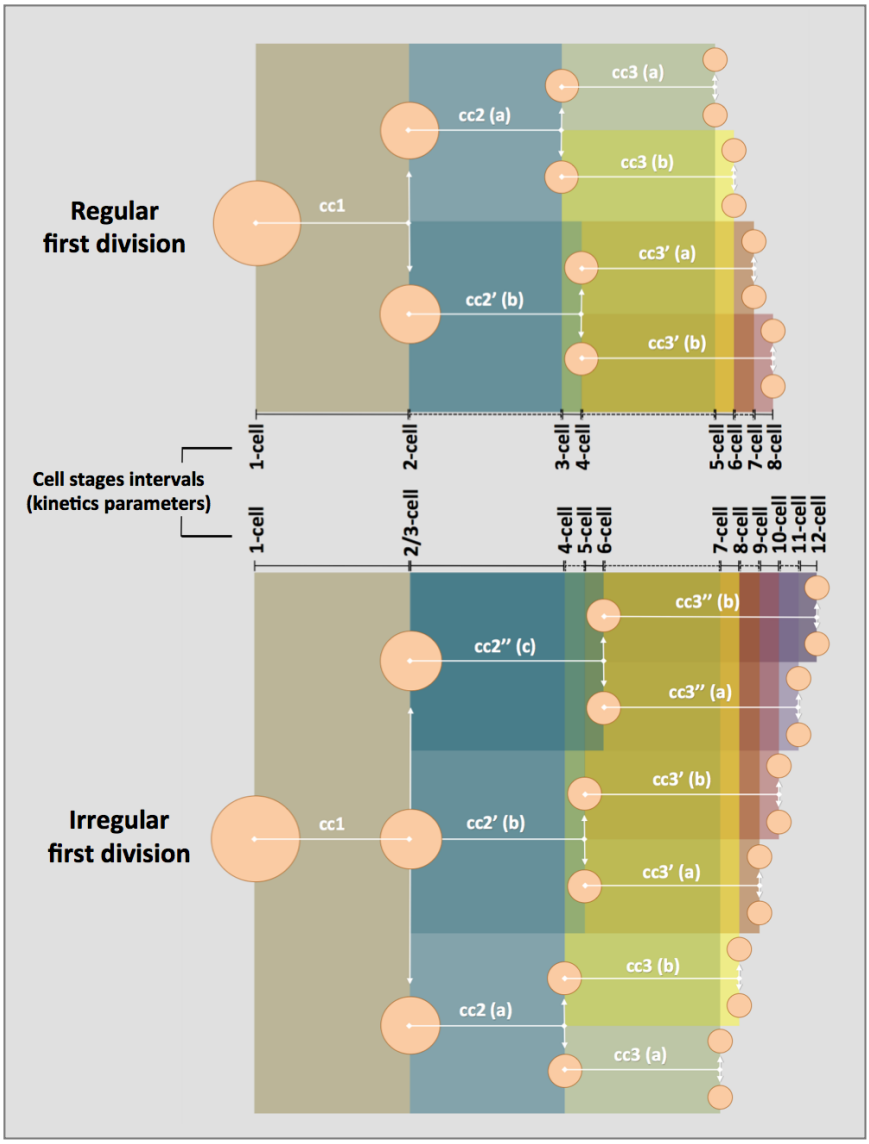

Figure 19 | Time ranges between the different cell stages according to the existence or non-existence of irregular divisions during embryo development.
Irregular divisions altered all subsequent kinetics parameters. When the irregular division takes place during the first mitosis (lower part of the image), the time between the 2- and the three-cell stages is nonexistent compared to the regular first division (top part of the image). Similarly, the time between the three- and the four-cell stages is be much longer when the irregular division occurs, the time between the four- and the five-cell stages is shorter, and the majority of the next parameters are altered. Also the number of the total cells of the embryo is greater at the same time point when an irregular division takes place. Cells resulting from the same division have been labeled as (a), (b), and (c), if necessary. cc, cell cycle.

Table 5 | Kinetic parameters in embryos with regular and irregular divisions.

	Regular divisions			Irregular divisions		
	N	Median	IQR	N	Median	IQR
PNd to 1st cytokinesis (h)	32	2.58	(2.25;3.06)	16	2.88	(2.46;3.17)
First cytokinesis (min)	47	0.25	(0.17;0.50)	20	0.42	(0.25;0.63)
Two to three cells (h)	27	**12.17** [a]	(11.58;12.92)	20	**0.88** [a]	(0.27;2.46)
Three to four cells (h)	27	**1.00** [b]	(0.42;1.67)	12	**7.58** [b]	(1.17;11.92)
Four to five cells (h)	10	**12.25** [c]	(9.19;14.65)	11	**0.75** [c]	(0.00;8.08)
Five to six cells (h)	10	2.08	(0.52;4.85)	7	2.75	(0.42;13.42)
Six to seven cells (h)	9	**1.25** [d]	(0.54;2.04)	7	**4.25** [d]	(1.25;12.25)
Seven to eight cells (h)	9	0.93	(0.50;2.42)	5	0.67	(0.33;3.54)
Eight to nine cells (h)	0	NA	NA	3	1.58	NA

IQR, interquartile range (Q1;Q3); NA, not applicable; PNd, pronuclear disappearance.
[a,c] $P<0.001$ [b,d] $P<0.05$ (Mann-Whitney *U*-test).

4.3 Aneuploidy incidence in the human embryo

We further performed the chromosomal analysis of all embryos. Informative results for chromosome content were obtained for 89 cells, specifically 71 blastomeres and 18 polar bodies, from a total of 57 embryos **(Supplementary Table 2)**. The percentage of informative data (67%) was lower in comparison with the published clinical rate (97%) (Rodrigo *et al.*, 2014), which may be caused by the freeze/thaw cycle of the embryos by slow freezing, which has been shown to be less efficient than vitrification (Fasano *et al.*, 2014); or by a possible lower quality of some of the embryos dedicated to the study, as in the clinical routine only embryos with good development and morphology are selected for biopsy.

The aneuploidy rate was 50.9% (n = 29; **Figure 20**), with no statistically significant differences according to the maternal age between euploid (33.4 ± 3.1 years) and aneuploid embryos (32.6 ± 3.4 years). This is in agreement with previous reports using different array-based approaches (Vanneste *et al.*, 2009; Johnson *et al.*, 2010b; Ata *et al.*, 2012; Chavez *et al.*, 2012) and further supports the notion that there is still an important incidence of aneuploidy at the cleavage-stage even with low maternal age (Munne *et al.*, 2004; Munne *et al.*, 2006).

Embryos were classified into different categories according to the aCGH results **(Figure 20).** Aneuploid embryos were differentiated according to the number of affected chromosomes between single aneuploid, when one chromosome was affected (n = 9; **Figure 21a),** complex aneuploid, when between 2 and 10 chromosomes were affected (n = 11), or chaotic if more than 10 chromosomes were aneuploid (n = 9; **Figure 20).** We wanted to differentiate the chaotic profiles since this type of pattern remains to be more deeply analyzed, as it has been hypothesized that lysed cells and damaged DNA may lead to this result. Rebiopsy of these embryos may show different chromosomal composition, pointing to possible initial artefactual results (Rubio *et al.*, unpublished data).

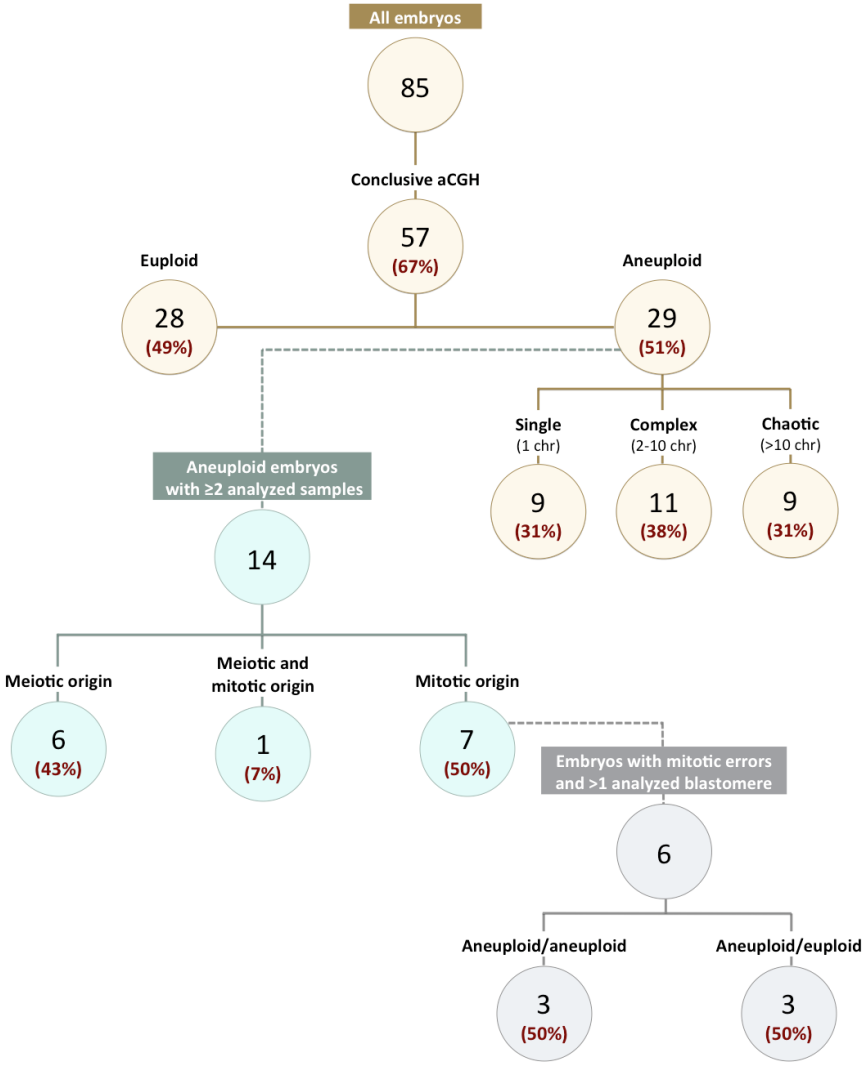

Figure 20 | Distribution of chromosome abnormalities according to aCHG results. Informative embryos were differentiated between euploid and aneuploid. 'Single' aneuploid embryos were considered when only one chromosome was affected, 'Complex' when 2-10 chromosomes were affected, and 'Chaotic' when more than 10 chromosomes were altered. In aneuploid embryos with 2 or more cells analyzed –including polar bodies- the origin was determined as meiotic, when all blastomeres shared the same alteration and/or the polar bodies were aneuploid; mitotic, when at least two blastomeres were aneuploid for different chromosomes and the polar bodies were euploid, if available; or both, when the altered chromosome(s) in blastomeres and polar bodies were different. Finally, in the aneuploid embryos from mitotic origin, they were classified according to the existence of only aneuploid blastomeres, or a mix of euploid and aneuploid blastomeres. aCGH, array-comparative genomic hybridization; chr, chromosome.

On the other hand, other authors support that chaotic aCGH patterns are caused by mosaic embryos (Le Caignec *et al.*, 2006), which will also support the finding of a different result by the second biopsy. Independent of the origin of this pattern, DNA damage or mosaicism, their frequency ranges between 15% and 20% of the analyzed embryos at cleavage stage (Le Caignec *et al.*, 2006; Rodrigo *et al.*, 2014), which is concordant with the percentage in our study (12.3%, 7/57), and high enough to be considered for future studies.

In some cases, when more than one sample from the same embryo was analyzed, it was also possible to infer the origin of the aneuploidy(s) (n = 14; **Figure 20).** Embryos with all blastomeres showing identical aneuploidies and/or with aneuploid polar bodies had most likely inherited meiotic errors. Unfortunately, we did not have information to differentiate between the first and the second polar body, as both of them were already extruded before freezing at pronuclear stage. In contrast, those embryos with different chromosomal constitution between blastomeres and euploid polar bodies had incurred mitotic errors. And embryos with aneuploid polar bodies and aneuploidy blastomeres, but for different chromosomes, were likely originated by meiotic and mitotic errors. According to these criteria, we proposed that 50% (7/14) of those aneuploid embryos originated from mitotic errors, 43% (6/14) from meiotic errors, and 7% from both **(Figure 20).** From the 7 embryos with mitotic errors, 6 displayed mosaicism among blastomeres –the other one only had information from one blastomere and one polar body-: in 3 of them, all blastomeres were chromosomally abnormal, but with different abnormalities and complementary abnormalities in some cases *(***Figure 21***b);* and three embryos exhibited a mixture of euploid and aneuploid blastomeres **(Figure 21c; Figure 20).** The rate of mosaic embryos in our embryo population was 10.5% (6/57), and the rate of "risky" mosaic embryos was 5.3% (3/57); considering "risky" embryos those with at least one euploid blastomere, with the probability of misdiagnosing in case of genetic analysis of a single blastomere. These rates are in concordance with the ones described in the literature, which have shown that day-3 aCGH diagnoses has a false positive rate of 2-3% (Gutierrez-Mateo *et al.*, 2011; Mir *et al.*, 2013). We have to consider that the false positive rate only includes those embryos that were originally diagnosed as aneuploid and were not fully aneuploid after all blastomeres were analyzed,

whereas our rate (5.3%) would also include the opposite situation, embryos diagnosed as euploid using a single blastomere, that would be mosaic if we could analyze all cells.

Finally, when we differentiated the aneuploidy rate at one-cell embryos versus cleavage-stage embryos, we obtained 37.5% versus 53% of aneuploid embryos, respectively. The percentage of aneuploidies at zygote stage would correspond to the meiotic error rate, whereas the increase in the aneuploidy rate throughout development would be caused by the appearance of aneuploidies due to errors in the subsequent mitotic cell divisions. This number similar to the one calculated in **Figure 20,** from embryos with 2 or more samples analyzed, so we could range meiotic error rate between 37.5% and 43% in this study. A previous publication in a similar population showed a meiotic error rate of 20% (Chavez *et al.*, 2012), although this value was inferred exclusively from cleavage-stage embryos. Since the aneuploidy rate at the zygote stage calculated in this study was also based on polar body results, we should consider these issues as a possible source for the discrepancy.

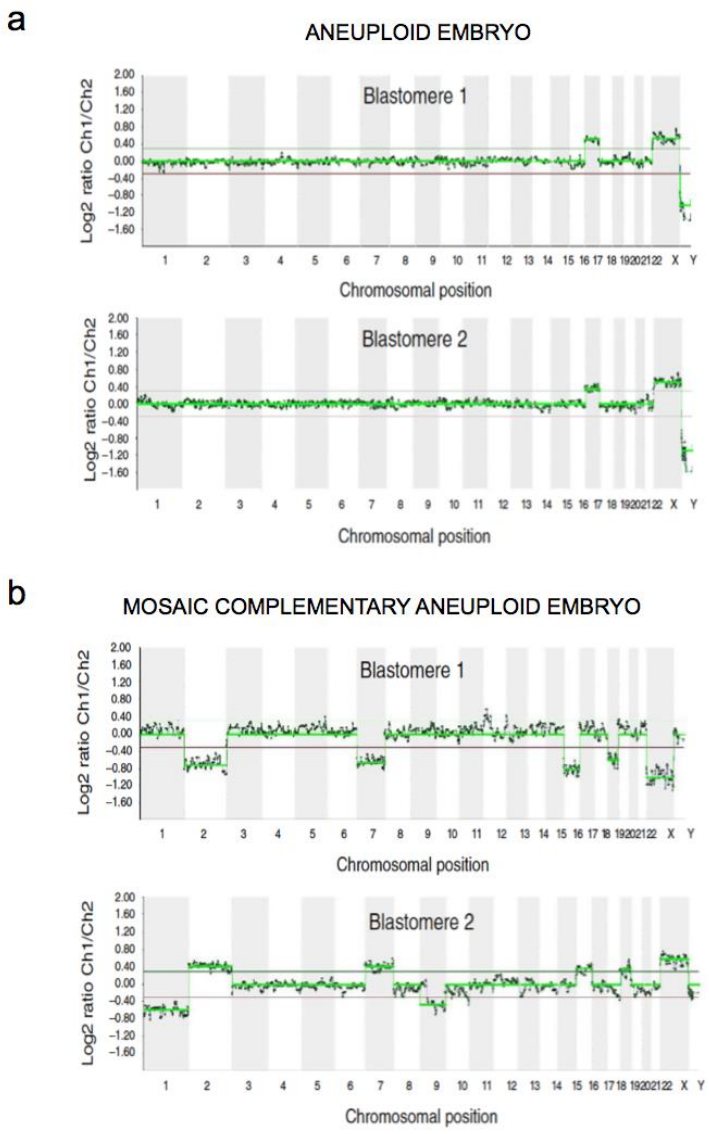

Figure 21 | Representative aCGH results.
(a) Two blastomeres from the same four-cell embryo showing chromosome 17 trisomy. **(b)** Two blastomeres from a chromosomally mosaic four-cell embryo with complementary aneuploidies for chromosomes 2, 7, 16, 19 and the sex chromosomes (Y0 and XXY). **(c)** Four blastomeres from a mosaic eight-cell embryo with two euploid blastomeres (46, XY), one blastomere with a trisomy for chromosome 18, and one blastomere with multiple aneuploidies (trisomies for chromosomes 10 and 21, and Y0). All profiles were compared with the male control DNA reference.

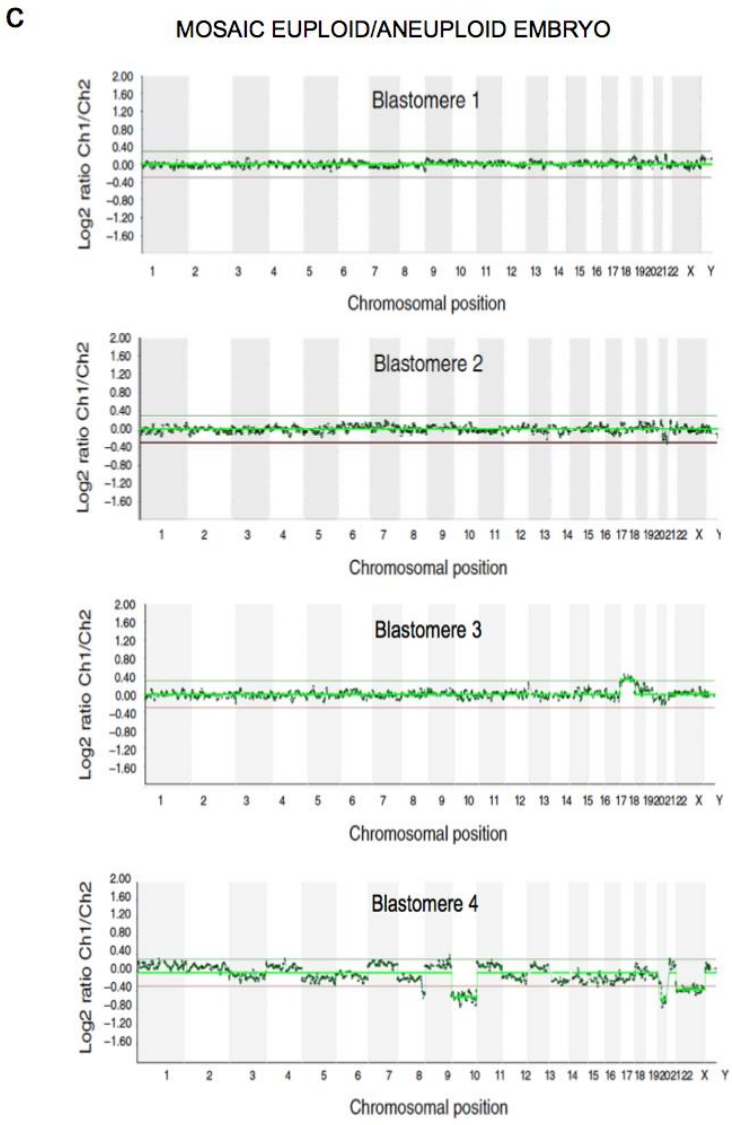

Figure 21 (continued)

4.4 Gene expression throughout embryo development

Besides assessing the chromosomal status and imaging behavior of each embryo, we also collected single-cell expression data from genes with relevant function during the first stages of human embryo development. Single-cell gene expression results were obtained for 119 blastomeres from 78 embryos. A total of 86 genes were selected on the basis of their previously reported importance to aneuploidies generation (Liu *et al.*, 2000; Jurisicova *et al.*, 2003; Wells *et al.*, 2005; Ma *et al.*, 2006; Bultman *et al.*, 2006; Jaroudi and SenGupta, 2007; Wan *et al.*, 2008; Jaroudi *et al.*, 2009; Wong *et al.*, 2010; Kiessling *et al.*, 2010; Galan *et al.*, 2010; Tashiro *et al.*, 2010; Mantikou *et al.*, 2012; Choi *et al.*, 2012; Shaw *et al.*, 2012; Galan *et al.*, 2013; Baran *et al.*, 2013). The biological processes in which the genes were involved included, but were not limited to, cell cycle regulation, apoptosis, telomere maintenance and DNA methylation (**Table 3**). Individual gene expression patterns were analyzed in each blastomere of a given embryo to determine developmental progression of expression levels during preimplantation development. To compare expression between embryos at different stages, we established a common start and end time point for all embryos. As mentioned above, PNd was designated as zero in the time scale and 56 h after was set as the final time point; no gene expression data were obtained beyond this.

4.4.1 Identification of gamete versus embryonic genome activated transcripts

Since the human embryo remains largely transcriptionally silent for the first few days of development, with only a small subset of genes activated before the six- to eight-cell stage (Dobson *et al.*, 2004; Zhang *et al.*, 2009; Vassena *et al.*, 2011; Xue *et al.*, 2013), normal development relies on mRNA inherited from the gametes for survival. It is estimated that approximately 70% of retained RNAs derive from the oocyte, and approximately 30% are inherited paternally (Zhang *et al.*, 2009). We aimed to definitively determine which transcripts from our study were from gametic origin or resulting from EGA. To accomplish this, we calculated the expression value at time zero for each gene using quadratic regression **(Supplementary Table 3).** Values higher than 2 indicated that the

transcript was present in the zygote and thus provided by the gametes. When the expression values were above 2 for the final time point **(Supplementary Table 3),** the transcript was considered activated by the EGA.

Y-box-binding protein 2 *(YBX2)* expression was selected as a double check for this procedure. *YBX2* has been described to be essential for the storage of the maternal mRNA in mouse embryos (Yu *et al.*, 2003). Our data showed high levels of *YBX2* transcripts at a pronuclear stage, but a gradual decrease along development, becoming at very low levels 56 hours from PNd **(Figure 22).** Relying on this, we stated that most maternal transcripts should be already degraded by that time and genes with transcripts have should have been activated by the embryonic genome.

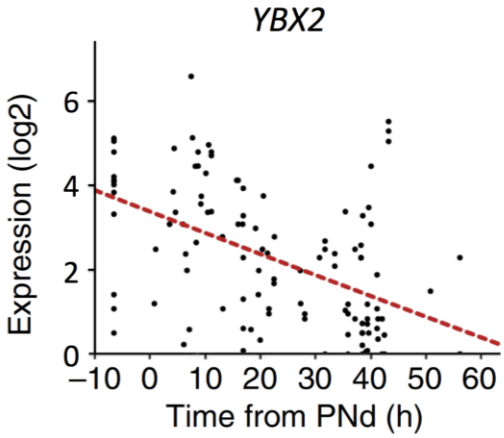

Figure 22 | Expression (log2) of *YBX2* in blastomeres during embryo development. Blastomeres coming from the same embryo are represented as independent events. Pronuclear disappearance was set as time zero. Zygotes analyzed before the PNd were placed in the time scale as -10 h.

From this analysis, we identified 40 genes that appeared to encode transcripts inherited from the gametes **(Figure 23).** In this group, aurora kinase A *(AURKA),* *BUB3* mitotic checkpoint protein *(BUB3),* cadherin 1 (*CDH1),* cyclin-dependent kinase 7 *(CDK7),* developmental pluripotency associated 3 *(DPPA3),* the oocyte expressed protein *(OOEP),* and peptidyl arginine deiminase type VI *(PADI6)* were the inherited transcripts with the highest levels of expression at the zygote

stage **(Supplementary Figure 1).** In contrast, a total of 44 genes were activated by the embryonic genome, 10 of which were undetectable in the zygote and, thus, not likely required during the earliest stages of embryo development **(Figure 23).** More specifically, glyceraldehyde-3-phosphate dehydrogenase *(GAPDH),* Cyclin A1 *(CCNA1), DPPA3*, and Yin Yang 1 transcription factor *(YY1)* were the most significant in this group and showed expression log2 values above 10 during the oocyte-to-embryo transition **(Supplementary Figure 1).**

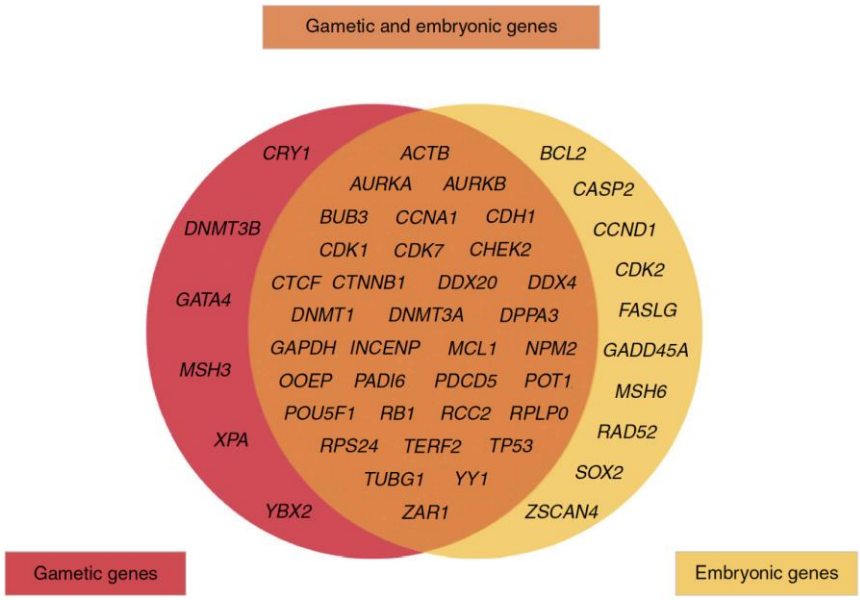

Figure 23 | Identification of gametic versus embryonic transcripts.
Gametic transcripts (*n* = 40) were highly expressed at time zero, whereas EGA genes (*n* = 44) were highly expressed at the final time point. The majority of these genes (n = 34) were originally inherited from the gametes and subsequently activated by EGA. See also Supplementary Figure 1.

Here, we demonstrate new potential maternally or paternally-derived gene products, including *CDH1*, which has been described as only expressed at the cleavage and blastocyst stage (Galan *et al.*, 2010). Other genes, such as *OOEP* and *PADI6,* identified as gametic in origin here, have been previously reported to represent maternal effect genes in murine embryos (Tashiro *et al.*, 2010; Li *et al.*, 2010), but our data suggest that they have a conserved function in early

human development. Note that, although we describe that many similarities exist between mouse and human embryos, with numerous studies in the former, important differences between the two species have been recently reported (Niakan *et al.*, 2012; Niakan and Eggan, 2013; Madissoon *et al.*, 2014). Therefore we should never rely on results from mouse without the corresponding replication study in human.

4.4.2 Gene expression patterns throughout development

To create a "best fit" model that allowed identification of statistically different gene profiles in embryos, a quadratic regression was performed for each gene as described in *Methods*. Using this regression, we observed statistically significant differences in 55 out of 86 genes analyzed ($P<0.05$, ANOVA test; **Supplementary Figure 1** and **Supplementary Table 3**).

We then grouped genes into different clusters according to their expression dynamics. For the interpretation of the clusters, we considered that the gene expression values for each time point were the result of inherited molecules from the gametes and/or newly synthesized molecules generated by the embryonic genome. Thus, inherited transcripts would be highly expressed at the pronuclear stage and decrease in expression as development proceeds unless they are activated by the embryonic genome. On the other hand, embryo transcribed genes would increase with development and would exhibit none or relatively minor transcriptional inheritance from the gametes.

Cluster 1 (n = 29) comprised genes inherited from the gametes and showed no evidence of transcriptional activation by the embryo since expression levels decreased throughout development **(Figure 24)**.

On further analysis of the cluster 1 genes, we determined that the most significant annotations obtained ($P\leq0.001$, Fisher´s exact test) were related to cell cycle regulation, DNA metabolism and chromosome organization (**Table 6).**

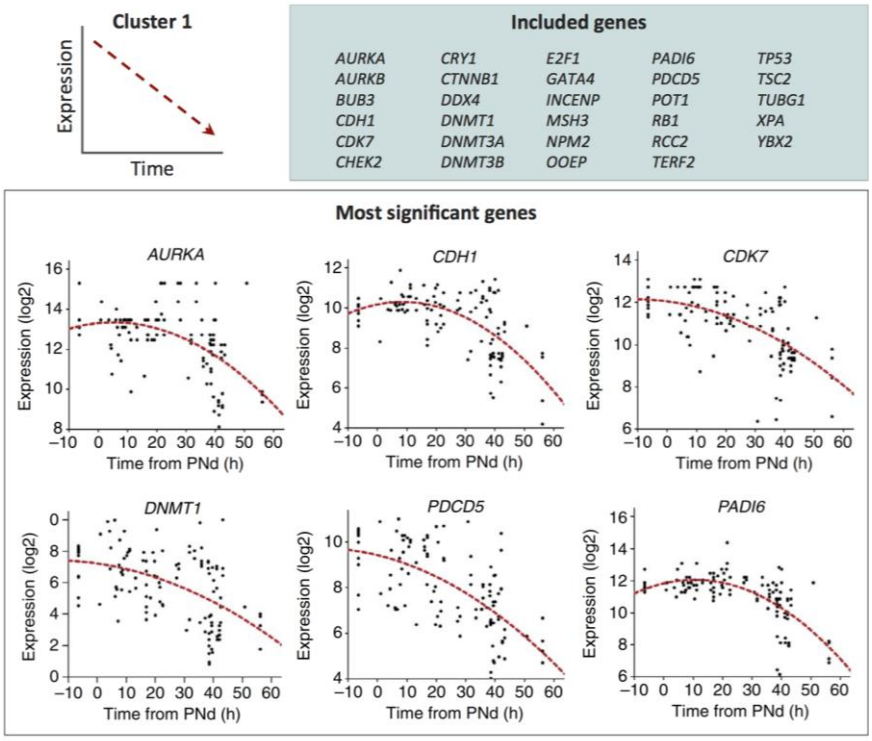

Figure 24 | Gene expression patterns in cluster 1 genes.
Significant quadratic regressions were classified into four different clusters according to the expression trend versus time. The majority of genes included in cluster 1 (n = 29) were expressed in the zygote stage but decreased in expression by at least twofold between the start and the final time. The most significant regressions were selected by ANOVA test with $P<1x10^{-6}$ and fold change>10. Each expression data point corresponds to the mean value obtained from three technical replicates. A baseline of C_t = 28 was used to obtained the shown expression values. For the rest of gene charts from this cluster see Supplementary Figure 1.

Our findings are in accordance with previous reports (Wong *et al.*, 2010), wherein *PDCD5*, the cell death-related gene that inhibits the degradation of DNA damage response proteins, was present in the zygote and decreased in expression until day 3. *AURKA*, which is involved in chromosome stabilization of the spindle, has been shown to be highly expressed at early stages and scarcely detected at the eight-cell stage (Kiessling *et al.*, 2010).

Table 6 | Most represented gene ontology terms for cluster 1.

GO:Term	Term name	C	G	Adjusted *P* value
GO:0007049	Cell cycle	15	937	1.09E-10
GO:0006259	DNA metabolic process	12	635	6.03E-09
GO:0022402	Cell cycle process	11	638	1.00E-07
GO:0009892	Negative regulation of metabolic process	11	707	2.20E-07
GO:0009890	Negative regulation of biosynthetic process	10	561	3.68E-07
GO:0051276	Chromosome organization	10	627	8.79E-07
GO:0009893	Positive regulation of metabolic process	11	858	9.03E-07
GO:0051726	Regulation of cell cycle	8	313	9.03E-07
GO:0000278	Mitotic cell cycle	9	469	9.03E-07
GO:0000279	M phase	8	386	3.88E-06
GO:0009790	Embryonic development	9	608	6.72E-06
GO:0033044	Regulation of chromosome organization	4	28	1.18E-05
GO:0001701	In utero embryonic development	6	183	1.67E-05
GO:0043009	Chordate embryonic development	7	344	2.63E-05
GO:0051053	Negative regulation of DNA metabolic process	4	37	2.63E-05
GO:0009792	Embryonic development ending in birth or egg hatching	7	348	2.64E-05
GO:0010628	Positive regulation of gene expression	8	578	4.53E-05
GO:0034984	Cellular response to DNA damage stimulus	7	382	4.53E-05
GO:0050790	Regulation of catalytic activity	9	851	6.49E-05
GO:0006974	Response to DNA damage stimulus	7	422	7.55E-05
GO:0006366	Transcription from RNA polymerase II promoter	9	882	7.90E-05
GO:0000087	M phase of mitotic cell cycle	6	269	8.95E-05
GO:0016481	Negative regulation of transcription	7	450	1.00E-04
GO:0016568	Chromatin modification	6	282	1.07E-04
GO:0006461	Protein complex assembly	8	682	1.12E-04
GO:0031328	Positive regulation of cellular biosynthetic process	8	700	1.25E-04
GO:0006275	Regulation of DNA replication	4	65	1.25E-04
GO:0010629	Negative regulation of gene expression	7	491	1.46E-04
GO:0000075	Cell cycle checkpoint	4	77	2.16E-04
GO:0008156	Negative regulation of DNA replication	3	26	4.36E-04
GO:0051259	Protein oligomerization	5	217	4.91E-04
GO:0051716	Cellular response to stimulus	8	865	4.99E-04
GO:0033554	Cellular response to stress	7	623	5.80E-04
GO:0032259	Methylation	4	106	6.07E-04
GO:0006260	DNA replication	5	232	6.07E-04
GO:0006306	DNA methylation	3	33	7.06E-04
GO:0051096	Positive regulation of helicase activity	2	3	8.39E-04
GO:0032206	Positive regulation of telomere maintenance	2	3	8.39E-04

GO:0030521	Androgen receptor signaling pathway	3	37	8.96E-04
GO:0007067	Mitosis	5	260	8.96E-04
GO:0051128	Regulation of cellular component organization	6	458	9.51E-04
GO:0043086	Negative regulation of catalytic activity	5	266	9.51E-04

GO, gene ontology; C, number of genes annotated by the given term in the test set; G, number of genes annotated by the given term in the reference set.
Only GO terms with $P \leq 0.001$ (Two-tailed Fisher´s exact test) are shown.

Cluster 2 (n = 4) comprised genes that showed relatively constant expression and likely represent the bulk of transcripts inherited from the gametes since they were detected at the pronuclear stage, but were also present at similar levels at later stages **(Figure 25)**. By avoiding mRNA degradation, or if degraded, compensated for by new synthesis from the embryonic genome, these genes are able to maintain stable levels throughout development. The genes whose regressions were constant and statistically significant ($P<0.05$, ANOVA test) in this cluster were v-akt murine thymoma viral oncogene homolog 1 *(AKT1)*, breast cancer 1 *(BRCA1)*, *GAPDH*, and NLR family, pyrin domain containing 5 *(NLRP5)* **(Figure 25)**.

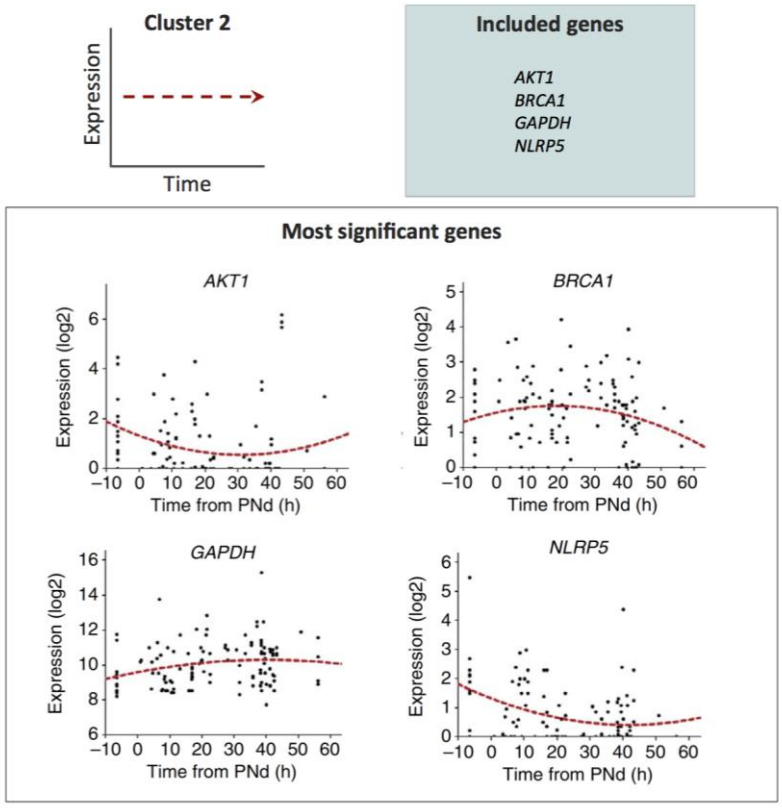

Figure 25 | Gene expression patterns for cluster 2 genes.
Significant quadratic regressions were classified into four different clusters according to the expression trend versus time. Cluster 2 (n = 4) comprised genes that showed relatively constant expression as defined by an increase or decrease in expression of less than 1 point. All regressions for this cluster were significant (P<0.05, ANOVA test). Each expression data point corresponds to the mean value obtained from three technical replicates. A baseline of C_t = 28 was used to obtained the shown expression values.

As a group, these genes have known functions in monosaccharide metabolism and lipid biosynthesis as well as food and stress response or RNA stability (**Table 7).** Notably, we detected high variability in *BRCA1* expression between cells from the same embryo**,** which could explain the discordance with previous findings since these studies detected differences between stages by using the average expression of all equivalent samples (Wells *et al.*, 2005; Giscard d'Estaing *et al.*, 2005).

Table 7 | Most represented gene ontology terms for cluster 2.

GO:Term	Term name	C	G	Adjusted *P* value
GO:0006006	Glucose metabolic process	3	163	6.65E-04
GO:0010907	Positive regulation of glucose metabolic process	2	12	6.65E-04
GO:0019318	Hexose metabolic process	3	201	6.65E-04
GO:0032094	Response to food	2	15	6.65E-04
GO:0032369	Negative regulation of lipid transport	2	13	6.65E-04
GO:0032770	Positive regulation of monooxygenase activity	2	17	6.65E-04
GO:0034405	Response to fluid shear stress	2	8	6.65E-04
GO:0045598	Regulation of fat cell differentiation	2	13	6.65E-04
GO:0048009	Insulin-like growth factor receptor signaling pathway	2	16	6.65E-04
GO:0050995	Negative regulation of lipid catabolic process	2	17	6.65E-04
GO:0050999	Regulation of nitric-oxide synthase activity	2	13	6.65E-04
GO:0051000	Positive regulation of nitric-oxide synthase activity	2	7	6.65E-04
GO:0043487	Regulation of RNA stability	2	14	6.65E-04
GO:0005996	Monosaccharide metabolic process	3	236	7.07E-04
GO:0008633	Activation of pro-apoptotic gene products	2	19	7.08E-04
GO:0043029	T cell homeostasis	2	20	7.30E-04
GO:0015909	Long-chain fatty acid transport	2	22	8.21E-04
GO:0043491	Protein kinase B signaling cascade	2	23	8.43E-04
GO:0046889	Positive regulation of lipid biosynthetic process	2	25	9.34E-04
GO:0002260	Lymphocyte homeostasis	2	28	1.00E-03
GO:0045862	Positive regulation of proteolysis	2	28	1.00E-03
GO:0051353	Positive regulation of oxidoreductase activity	2	28	1.00E-03

GO, gene ontology; C, number of genes annotated by the given term in the test set; G, number of genes annotated by the given term in the reference set.
Only GO terms with $P \leq 0.001$ (Two-tailed Fisher´s exact test) are shown.

Cluster 3 (n = 10) included genes that were activated during embryo development, but were not originally expressed in the zygote **(Figure 26)**. Genes with an expression lower than 2 at time zero and at least a two-fold difference at the final time point were selected for this cluster.

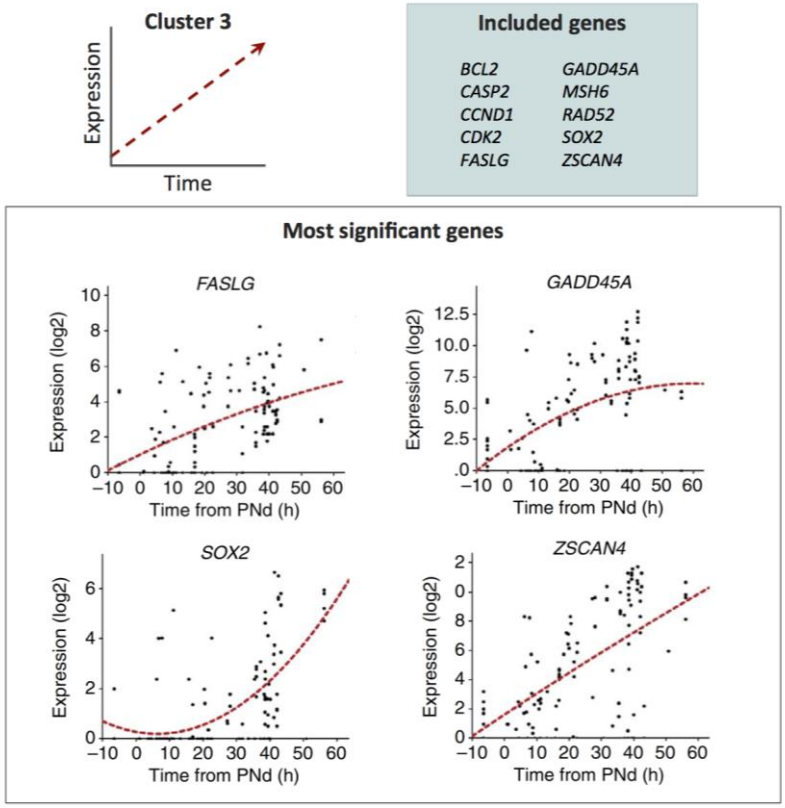

Figure 26 | Gene expression patterns for cluster 3 genes.
Significant quadratic regressions were classified into four different clusters according to the expression trend versus time. Cluster 3 (n = 10) comprised genes with an expression value lower than 2 at time zero and at least a two-fold difference at the final time point. The most significant regressions from the cluster were selected with $P<1x10^{-6}$ (ANOVA test) and fold change>10. Each expression data point corresponds to the mean value obtained from three technical replicates. A baseline of $C_t = 28$ was used to obtained the shown expression values. For the rest of genes from this cluster see Supplementary Fig. 1.

Gene ontology (GO) analysis showed that these genes were associated with regulation of the cell cycle, particularly interphase, but were also involved in other biological process such as the stress response ($P\leq0.001$, Fisher´s exact test; **Table 8).** The most relevant genes in this cluster were Fas ligand *(FASLG),* growth arrest and DNA-damage-inducible alpha *(GADD45A),* SRY-box 2 *(SOX2),* and zinc finger and SCAN domain containing 4 *(ZSCAN4;* fold change>10 and $P<1x10^{-6}$, ANOVA test; **Figure 26).** *FASLG* is a death receptor ligand whose expression has been shown to correlate with cellular fragmentation in human embryos at the two- and four-cell stage (Kawamura *et al.*, 2001). We observed

a gradual increase in *FASLG* expression with development starting with basal levels at the pronuclear stage to suggest that embryos do not undergo apoptosis until later in development as previously described(Hardy, 1999). In addition, *ZSCAN4*, which is involved in telomere maintenance, exhibited the greatest increase in expression of all the genes in this cluster (fold change = 211), with considerably lower levels observed before PNd. This was also in accordance with previous studies showing *ZSCAN4* expression in eight-cell embryos and no expression in zygotes (Shaw *et al.*, 2012).

Table 8 | Most represented gene ontology terms for cluster 3.

GO:Term	Term name	C	G	Adjusted *P* value
GO:0022402	Cell cycle process	6	643	9.19E-05
GO:0051325	Interphase	4	115	9.19E-05
GO:0051329	Interphase of mitotic cell cycle	4	109	9.19E-05
GO:0007049	Cell cycle	6	948	4.28E-04
GO:0009411	Response to UV	3	55	7.31E-04
GO:0033554	Cellular response to stress	5	625	9.57E-04
GO:0033273	Response to vitamin	3	69	9.57E-04
GO:0046661	Male sex differentiation	3	71	9.57E-04

GO, gene ontology; C, number of genes annotated by the given term in the test set; G, number of genes annotated by the given term in the reference set.
Only GO terms with $P \leq 0.001$ (Two-tailed Fisher´s exact test) are shown.

Cluster 4 (n = 12) genes also increased in expression on embryonic genome activated (EGA), but unlike cluster 3, were also detected at the pronuclear stage to suggest both a gametic and embryo source of transcripts. *CCNA1*, myeloid cell leukemia 1 (*MCL1*), and zygote arrest 1 (*ZAR1*) showed the most significant difference for this group (fold change>10 and $P<1x10^{-6}$, ANOVA test; **Figure 27).** We detected low expression of *CCNA1* at the pronuclear stage with significantly increased expression on EGA as previously described (Kiessling *et al.*, 2010) and increasingly high levels of *ZAR1* beginning at the pronuclear stage. While *CCNA1* binds particular cell cycle regulators, *ZAR1* is thought to function as a maternal effect gene in mouse and human embryos (Wu *et al.*, 2003). However, GO analysis did not show any statistically significant annotations for this cluster.

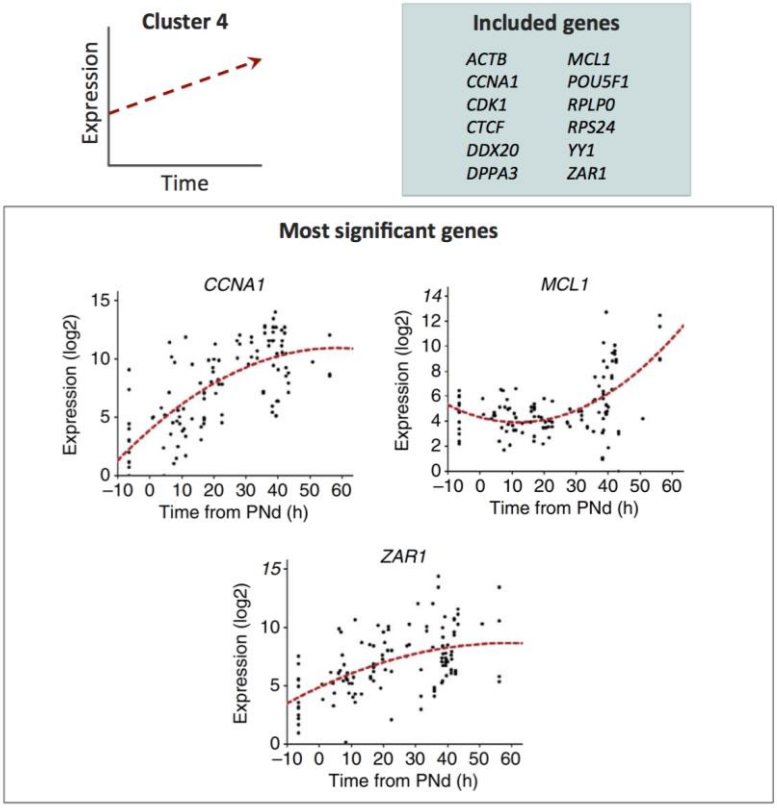

Figure 27 | Gene expression patterns for cluster 4 genes.
Significant quadratic regressions were classified into four different clusters according to the expression trend versus time. Cluster 4 (n = 12) comprised genes with expression higher than 2 at time zero and two-fold or more at the last time point. The most significant regressions were selected with $P<1x10^{-6}$ (ANOVA test) and fold change>10. Each expression data point corresponds to the mean value obtained from three technical replicates. A baseline of C_t = 28 was used to obtained the shown expression values. For the rest of gene charts from this cluster see Supplementary Figure 1.

Although some of the genes in our study have been previously described in relation to human embryo viability, most of these studies examined expression patterns in whole embryos (Kawamura *et al.*, 2001; Dobson *et al.*, 2004; Giscard d'Estaing *et al.*, 2005; Wells *et al.*, 2005; Vassena *et al.*, 2011; Shaw *et al.*, 2012; Shaw *et al.*, 2013), in pools of whole embryos (Jurisicova *et al.*, 2003; Jaroudi *et al.*, 2009; Zhang *et al.*, 2009; Kiessling *et al.*, 2010; Bazrgar *et al.*, 2014), and/or only at a single stage of preimplantation development (Giscard d'Estaing *et al.*, 2005; Kiessling *et al.*, 2010; Bazrgar *et al.*, 2014). In

contrast, we evaluated gene expression at the single-cell level throughout multiple stages of early embryogenesis and showed that considerable variability is observed among samples, which complicate the identification of potential differences in embryos from the same stage. Note that we analyzed gene expression profiling in cryopreserved embryos and that some transcripts may be affected by the freezing-thawing procedures despite similar developmental timing and genome activation as fresh embryos (Shaw *et al.*, 2012). However, we addressed this limitation by calculating expression levels in each blastomere, a method preferable to normalization to a housekeeping gene(s) due to individual gene variation as previously described (Warren *et al.*, 2006).

4.4.3 Activation times for EGA transcripts

For genes that showed clear activation in EGA (clusters 3 and 4), we sought to determine the exact time in which activation occurs **(Figure 28).** The minimum of each quadratic function was calculated for this purpose, and 8 of the 22 genes exhibited an increase in expression starting from PNd. Interestingly, most of the cluster 3 genes were activated earlier in development than cluster 4 genes. This can be explained by the finding that they were not originally expressed in the gametes and thus needed to be activated by the EGA at the earliest stage. In contrast, we observed that the majority of the cluster 4 genes did not need such early activation by the embryo, as there was already an initial pool of transcripts inherited by the zygote. Further, genes with the observed stable expression pattern (cluster 2) could be the result of a balance between mRNA degradation and new mRNA synthesis. Therefore, although these genes could be transcriptionally activated as well, the activation time could not be established for this cluster.

The major wave of human embryonic genome activation occurs at the six- to eight-cell stage; however, other studies suggest that there is minor transcription of certain genes beginning at the two-cell stage (Dobson *et al.*, 2004; Zhang *et al.*, 2009; Galan *et al.*, 2010; Vassena *et al.*, 2011). In accordance with more recent findings (Xue *et al.*, 2013), here we show the potential activation of a subset of genes as early as the zygote stage. More importantly, we also determined that this unique group of genes is associated with cell cycle regulation and shows nearly non-existent expression before

embryonic activation, to confirm that they were unlikely inherited from the gametes. Further studies should probe the role of these early-activated genes and their function in proper human preimplantation development.

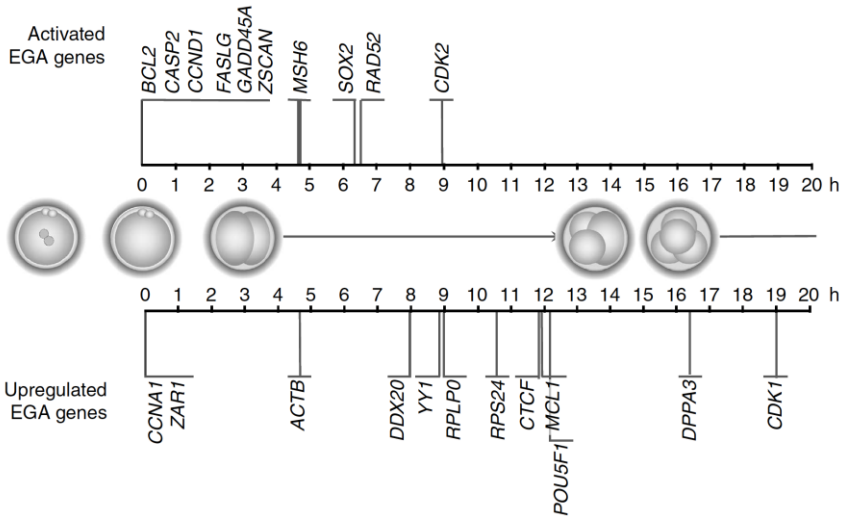

Figure 28 | Activation times of embryonic genes.
EGA timing is shown in hours (h) after PNd. Two groups were identified according to the basal levels at the pronuclear stage: "Activated EGA genes" (*n* = 10) that were originally absent at the zygote stage and corresponded to cluster 3 genes, and "Upregulated genes" (*n* = 12) that were already present at the pronuclear stage were designated for cluster 4 genes. A schematic representation of embryo development with normal mitotic divisions was included as a guide.

4.5 Correlation between morphology and kinetics

The correlation between the different morphology parameters and the kinetic behavior of the embryos was studied to elucidate a possible relationship between them. All possible combinations were analyzed among every kinetic parameter or the irregular division existence versus fragmentation degree, multinucleation or vacuole existence.

4.5.1 Morphology versus kinetic parameters

Fragmentation was the first morphological parameter studied to detect a possible effect on kinetics. We differentiated between low degree of fragmentation, which represented less than 25% of the cytoplasmic volume, and high degree, which represented 25% or higher. The only kinetic parameter that was statistically significant among fragmentation groups was the time between the PNd and the first cytokinesis (P<0.05, Mann-Whitney U-test), which was longer in those embryos with higher fragmentation degree (3.0 h vs. 2.6 h) **(Table 9)**. This finding should be taken into consideration with the data reported in section 1.1, in which we showed how most of the embryos in this study become fragmented during the first division **(Figure 17b)**. Therefore, we could deduce that the fragment extrusion slows down the embryo development at the moment in which they originate.

According to multinucleation, we observed important differences in most of the kinetic parameters analyzed **(Table 9).** The time between two and three cells was the first parameter that was highly different between groups (presence and absence of multinucleation), being shorter in the multinucleated embryos (1.6 h vs. 11.7 h), although it was not statistically significant. The next two parameters, time between three and four cells and time between four and five cells, were both statistically significant between multinucleated and non-multinucleated embryos (P<0.05, Mann-Whitney U-test). The first one was longer in multinucleated embryos (10.9 h vs. 1.0 h) and the second one was shorter (0.8 h vs. 11.3 h). These results support previous published data showing that morphokinetic parameters are affected by multinucleation (Ergin *et al.*, 2014; Balakier *et al.*, 2016).

Table 9 | Kinetic parameters under the effect of different morphological events.

		High fragmentation			Multinucleation			Vacuoles		
		N	Median	IQR	N	Median	IQR	N	Median	IQR
PNd to 1st cytokinesis (h)	No	45	**2.6**[a]	(2.1;3.0)	54	2.6	(2.3;3.1)	57	2.6	(2.2;3.1)
	Yes	21	**3.0**[a]	(2.6;4.6)	12	3.0	(2.5;4.3)	9	3	(2.7;3.8)
First cytokinesis (min)	No	46	15.0	(10.0;35.0)	55	15.0	(10.0;35.0)	57	20.0	(15.0;32.5)
	Yes	21	20.0	(15.0;30.0)	12	25.0	(16.2;30.0)	10	20.0	(10.0;31.2)
Two to three cells (h)	No	33	11.6	(0.9;12.5)	36	11.7	(1.7;12.6)	41	11.6	(1.3;12.7)
	Yes	14	8.8	(1.4;12.9)	11	1.6	(0.0;12.3)	6	2.1	(0.4;12.2)
Three to four cells (h)	No	28	1.1	(0.4;4.0)	30	**1.0**[b]	(0.4;2.5)	36	1.2	(0.5;7.3)
	Yes	11	1.3	(0.8;8.3)	9	**10.9**[b]	(1.0;12.3)	3	2.4	(0.8;NA)
Four to five cells (h)	No	15	2.7	(0.5;12.3)	14	**11.3**[c]	(4.5;13.6)	18	5.0	(0.6;12.1)
	Yes	6	9.3	(5.1;15.7)	7	**0.8**[c]	(0.5;4.8)	3	13.3	(8.1;NA)
Five to six cells (h)	No	12	2.3	(0.2;10.2)	13	1.3	(0.3;5.6)	14	2.5	(0.6;8.4)
	Yes	5	2.3	(0.6;5.8)	4	8.1	(2.4;14.4)	3	0.5	(0.1;NA)
Six to seven cells (h)	No	11	1.3	(0.6;4.3)	12	1.8	(0.6;6.4)	13	1.3	(0.8;3.6)
	Yes	5	1.8	(1.0;8.0)	4	1.5	(1.0;9.6)	3	7.2	(0.4;NA)
Seven to eight cells (h)	No	10	0.8	(0.4;1.4)	10	0.8	(0.5;2.2)	12	0.7	(0.5;1.1)
	Yes	4	1.7	(0.5;4.3)	4	0.6	(0.3;4.9)	2	2.4	(1.9;NA)
Eight to nine cells (h)	No	3	1.6	(0.5;NA)	1	0.5	(0.5;0.5)	3	1.6	(0.5;NA)
	Yes	0	NA	(NA;NA)	2	2.5	(1.6;NA)	0	NA	(NA;NA)

IQR, interquartile range (Q1; Q3); NA, not applicable; PNd, pronuclear disappearance.
Kinetic parameters medians were calculated according to if high fragmentation, multinucleation, or vacuoles were existent or absent (Yes/No). Fragmentation was considered high when equal or higher than 25%. [a,b,c] $P<0.05$ (Mann-Whitney *U*-test).

We did not observe any statistically significant differences between the kinetic parameters of embryos with or without vacuoles **(Table 9).** This could be due to the lower number of embryos that were detected with vacuoles in this study. Nevertheless, some parameters did exhibit a trend toward difference between groups, such as the time between two and three cells or the time between four and five cells, being the first one longer in embryos without vacuoles, and the second one shorter in embryos without vacuoles.

Finally, we should highlight that the number of embryos decreased gradually with development as we were taking out some of them for analysis, and this affected the statistical power for the analysis of later kinetic parameters

4.5.2 Morphology versus irregular divisions

As an important event in the kinetic behavior of the human embryo, we also analyzed the existence of irregular divisions in relation to some morphological parameters **(Table 10).** In the correlation study with the fragmentation degree, 35.4% of the embryos with regular divisions and 25.0% of the embryos with irregular divisions showed a high percentage of fragmentation, without statistical differences between groups. Nevertheless, 40.0% of the embryos with irregular divisions had multinucleation at some stage; this value was statistically significant compared with the percentage in embryos with regular divisions (8.3%; $P<0.05$, Fisher's exact test). This correlation between irregular divisions and multinucleation supports the previous results in section 5.1, in which we observed that multinucleated embryos showed significant differences in the duration of most of the morphokinetic parameters versus those embryos without multinucleation **(Table 9).** This finding would support again the importance of analyzing kinetics in embryos with regular and irregular division separately. Finally, we did not observe any statistically significant correlation between the existence of vacuoles and irregular divisions and, as we mentioned before, this could be due to the low sample size in this group ($n = 10$).

Table 10 | Contingency table to analyze the relationship between division type and morphological events.

		Fragmentation		Multinucleation		Vacuoles	
	Total	Low	High	No	Yes	No	Yes
Embryos with regular divisions (%)	48 (100)	31 (64.6)	17 (35.4)	**44[a] (91.7)**	**4[b] (8.3)**	42 (87.5)	6 (12.5)
Embryos with irregular divisions (%)	20 (100)	15 (75.0)	5 (25.0)	**12[a] (60.0)**	**8[b] (40.0)**	6 (80.0)	4 (20.0)

High fragmentation was considered when ≥25%. Pearson Chi-square test was performed in the fragmentation comparison, and Fisher's exact test was performed to determine differences in multinucleation and vacuoles comparison since in both there was one cell with less than 5 cases. [a,b] $P<0.05$ (Fisher's exact test).

4.6 Correlation between morphology and aneuploidy

We determined if there was a correlation between the presence of aneuploidy and the incidence of cellular fragmentation on the basis of previous observations up to the four-cell stage (Chavez *et al.*, 2012), in which DNA fragments were observed by 4',6-diamino-2-fenilindol (DAPI) staining in fragments from embryos at cleavage stage. We examined whether there was an association between aneuploidy and fragmentation degree considering embryos with low (<25%) versus high (≥25%) fragmentation. While 46.3% of the embryos with low fragmentation were aneuploid (19/41), the incidence of aneuploidy in highly fragmented embryos was 62.5% (10/16). Although we observed a general association trend between higher fragmentation degree and aneuploidy incidence, this was not statistically significant.

We aimed to find the relationship between aneuploidy and multinucleation at any stage of the embryo development, as previous work has been contradictory about this correlation (Hardarson *et al.*, 2001; Ambroggio *et al.*, 2011; Balakier *et al.*, 2016). In the embryos that did not show multinucleation, 42.6% were aneuploid (20/47); in embryos with multinucleation the percentage of aneuploid embryos was 90% (9/10). This difference is statistically significant ($P<0.05$, Fisher´s exact test), supporting previous studies (Ambroggio *et al.*, 2011). Surprisingly, one embryo showing multinucleation in one of the blastomeres at the two-cell stage was euploid. We did not find any differences in the number of chromosomes affected between multinucleated and not multinucleated embryos, which supports previous reports (Balakier *et al.*, 2016).

Finally, we also assessed a possible correlation between the existence of vacuoles and aneuploidy, since vacuoles could affect spindle dynamics. No statistically significant differences were found between embryos with vacuoles versus those without, regarding aneuploidy or the number of chromosomes affected in case of aneuploidy. This supports a previous study that showed no spindle displacement in oocytes and embryos with big vacuoles (Wallbutton and Kasraie, 2010).

4.7 Correlation between morphology and gene expression

Changes in gene expression can be correlated with changes in the morphology of the embryos. To study this, we analyzed the expression of all genes in the different morphological groups for the most frequent parameters: fragmentation, multinucleation and vacuole existence. To avoid bias during analysis due to expression differences in embryos collected at different developmental times, we used a discrete time variable. To ensure an adequate number of embryos in each group for drawing relevant conclusions, two different groups were created using a cutoff of 30 h after PNd, with both groups having the same time range: from 0 to 30 h after PNd and from 30 to 60 h after PNd.

4.7.1 Gene expression in fragmented embryos

As we had information about fragmentation degree from all embryos with gene expression data, the sample size for the analysis was 78 embryos, with 119 analyzed blastomeres in total. We differentiated two degrees of fragmentation: low when fragmentation was below 25%, and high if fragmentation was 25% or higher. We used *Babelomics* to compare gene expression levels between the groups and estimate the false discovery rate. In the embryos collected before 30 h after PNd (n = 65), none of the 86 analyzed genes showed statistically significant differences between low-fragmented and high-fragmented embryos. Nevertheless, we found significant expression differences in embryos that were collected after 30 h post PNd. First, we compared the average collection time between groups. In total, 29 out 86 genes were differentially expressed between embryos with low and high fragmentation (P<0.05, limma test; **Figure 29a**). The two most differentially downregulated genes in high-fragmented embryos after 30 h post PNd were *GADD45A* and *ZSCAN4* (**Figure 29b**) *GADD45A* is related to DNA damage arrest, the low mRNA levels in high fragmented embryos could be related to the origin of fragmentation. Our hypothesis is that embryos with low *GADD45A* levels would not arrest even if they have some damage and would create fragments in those chaotic divisions. *ZSCAN4* is telomere maintenance gene, and its low expression in high fragmentation could be related to the high proportion of aneuploid embryos in the high-fragmented

group. This finding would be in concordance with previous studies showing low telomere length in embryos with high fragmentation at day 3 of development (Keefe *et al.*, 2005). In contrast, the two most upregulated genes in embryos with high fragmentation were *FASLG* and *YBX2* (**Figure 29c**). *FASLG* is a death receptor, which would correlate fragmentation with apoptosis processes, and *YBX2* is a maternal gene that has been showed to protect the maternal mRNA from degradation in mouse embryos (Yu *et al.*, 2003). More interestingly, it has been reported that arrested embryos have lower expression of *YBX2* mRNA (Wong *et al.*, 2010), thus its high expression in the high-fragmented embryos of our study would be in concordance with the low levels of *GADD45A* transcripts, and would highlight once again fragmentation as an alternative to cell cycle arrest.

In addition, we detected that all blastomeres from the embryo *6B1* had an expression profile more similar to those embryos with low fragmentation (**Figure 29a**). We observed that the exact percentage of fragmentation was 25%, which is the threshold value to define the fragmentation groups.

There was only one other embryo with 25% fragmentation, *3B1*, but in this case its expression profile was similar to embryos in the high fragmentation group. It is important to note that the evaluation of fragmentation degree could be difficult in some cases, as the fragments are distributed in the whole embryo and, although we use the multiplane capture to increase the accuracy of the measure, some small error margin is expected. For the same reason, for future studies we propose to compare extreme degrees of fragmentation, such as <10% versus >40%, that, due to the small sample size, we were not able to perform.

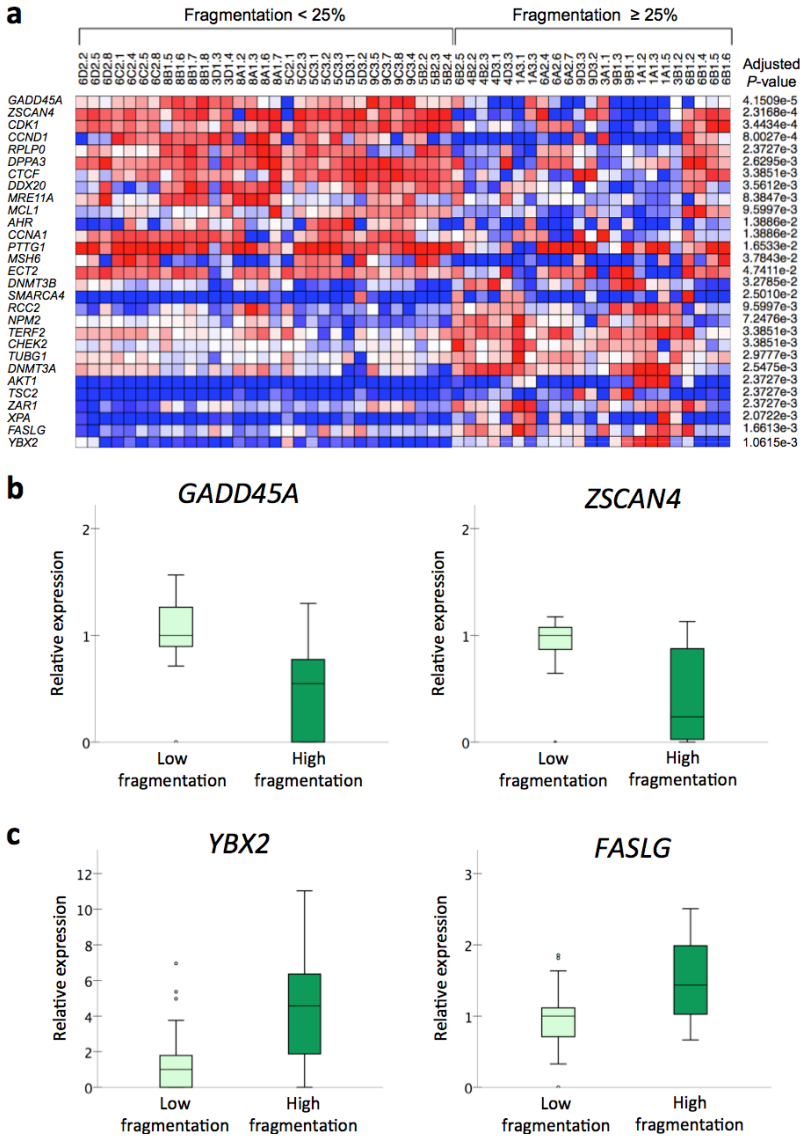

Figure 29 | Differential gene expression between low- and high-fragmented embryos. Heatmap of genes showing significant differential expression (P<0.05, limma test, n = 29) in low- and high-fragmented embryos collected after 30 h post PNd **(a)**. Each column represents a single blastomere. Blue colored squares show low expression, red color represents high levels of gene expression, and white squares indicate moderate expression (log2). Box plots from the top downregulated **(b)** and upregulated genes **(c)** in embryos with high fragmentation (≥25%) compared with low fragmentation (<25%) after 30 h following PNd. A plot represents gene expression values between quartile 1 and 3, the black line inside the box is the median value, and the black circles are outliers. Relative expression was obtained by dividing by the median expression value in embryos with low fragmentation.

4.7.2 Gene expression in multinucleated embryos

Another morphological parameter that we studied and correlated with gene expression was multinucleation. We collected gene expression data corresponding to 65 blastomeres from embryos retrieved during the first 30 hours after PNd and 54 blastomeres from embryos retrieved later. The differential analysis showed no differences in any of the timing groups between multinucleated and non-multinucleated embryos for the studied genes. It remains unknown if this result was produced for the low number of multinucleated embryos in our sample group, as there was a total of 12 embryos, 6 collected during the first time range and 6 embryos during the second one.

4.7.3 Gene expression in vacuolated embryos

According to vacuole formation, none of the 86 selected genes was previously correlated with this morphology feature. Nevertheless, taking advantage of the deepness of our study, we wanted to include this correlation study to see if embryos with vacuoles were expressing some genes differentially. For the group of embryos collected between the PNd and the next 30 hours, we found 4 differentially expressed genes between those blastomeres that had vacuoles (n = 6; P<0.05, limma test) compared with those that did not (n = 59, P<0.05, limma test; **Figure 30a**). Two genes, *YY1* and Cofilin 1 *(CFL1),* were the most upregulated in embryos with vacuoles in comparison to embryos without (**Figure 30b**), whereas AURKA and POU Class 5 Homeobox 1 *(POU5F1)* were the two most downregulated (**Figure 30c**).

In the embryos that were collected after the first 30 h post PNd we found just one differentially expressed gene, RB transcriptional corepressor 1 *(RB1),* that was downregulated in those blastomeres from embryos with vacuoles (n = 12) compared with embryos without vacuoles (n = 42; P<0.05, limma test; **Figure 31a**).

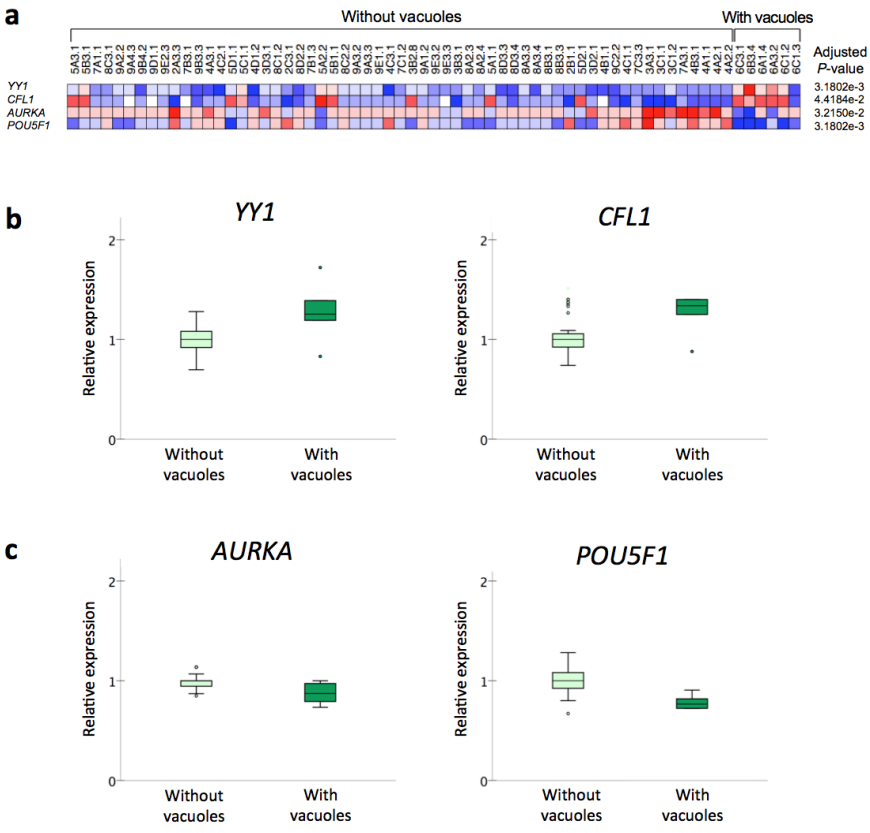

Figure 30 | Differential gene expression between embryos with and without vacuoles during the first 30 h after pronuclear disappearance.
Heatmap of genes showing significant differential expression (n = 4; P<0.05, limma test) in embryos without vacuoles and with vacuoles collected during the first 30 h after PNd (**a**). Each column represents a single blastomere. Blue colored squares show low expression, red color represents high levels of gene expression, and white squares indicate moderate expression (log2). Box plots from the upregulated **(b)** and downregulated **(c)** genes in embryos with vacuoles collected during the first 30 h of development after PNd. A plot represents gene expression values between quartile 1 and 3, the black line inside the box is the median value, and the black circles are outliers. Relative expression was obtained by dividing by the median expression value in embryos without vacuoles.

We noted that all nine embryos with vacuoles were from the same woman, with only one more embryo from the same woman not containing vacuoles (6D2). This embryo was collected after the first 30 hours post PNd and showed low *RB1* expression (**Figure 31b**), similar to those embryos with vacuoles collected at similar time, pointing to a new dimension of individual expression differences. This is in accordance with a previously published case report that support that the vacuole existence is a patient-dependent feature with a probable genetic cause (Wallbutton and Kasraie, 2010).

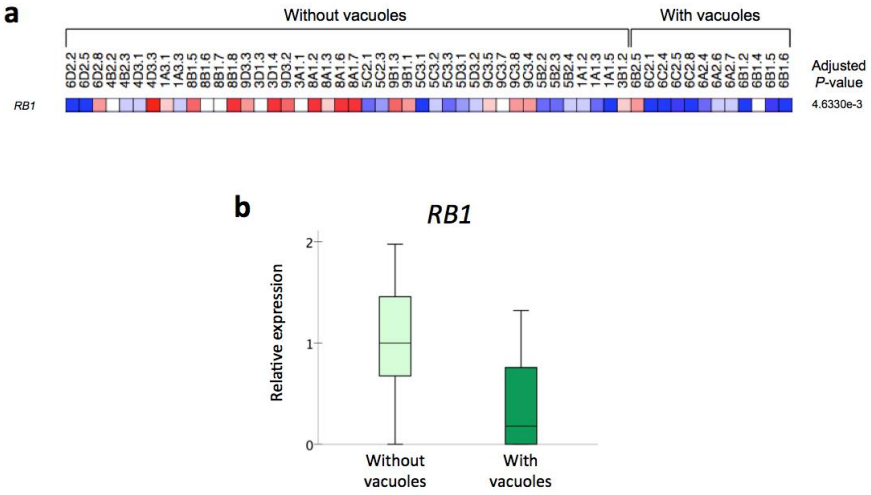

Figure 31 | Differential gene expression between embryos with and without vacuoles during the 30 h and 60 h after pronuclear disappearance.
Heatmap of genes showing significant differential expression (n = 1; P<0.05, limma test) in embryos without vacuoles and with vacuoles collected between 30 h and 60 h post PNd (**a**). Each column represents a single blastomere. Blue colored squares show low expression, red color represents high levels of gene expression, and white squares indicate moderate expression (log2). Box plot from differential RB1 expression between embryos with vacuoles and without **(b)**. A plot represents gene expression values between quartile 1 and 3, the black line inside the box is the median value, and the black circles are outliers. Relative expression was obtained by dividing by the median expression value in embryos without vacuoles.

4.8 Correlation between kinetics and aneuploidy

4.8.1 Kinetic parameters versus aneuploidy

We next evaluated the developmental kinetics of euploid versus aneuploid embryos to determine which parameter(s) may be correlated with the presence of aneuploidy. We found that two parameters were statistically significant between aneuploid and euploid embryos (**Table 11**). Since embryos were taken out for analysis at different developmental times, it is important to note that the sample size gradually decreased as development proceeded, making the analysis of statistically significant differences for later parameters difficult. The most significant parameter was the time between the PNd and the start of the first cytokinesis (P=0.025, Mann-Whitney U-test), which was longer in aneuploid embryos compared with euploid embryos. This finding suggests that chromosome missegregation may have occurred to influence the length of this first mitotic cycle and that further consideration should be given to the competency of the sperm used for fertilization since several mitotic spindle components for the first cell division are paternally inherited in human embryos (Sathananthan *et al.*, 1991; Palermo *et al.*, 1994). In addition, although this parameter has been recently found predictive of which embryos will reach the blastocyst stage (Desai *et al.*, 2014), no study to our knowledge has defined this parameter for assessing chromosomal status in embryos. Just one recent publication studied a similar parameter, the time between PNd and the two-cell stage, between euploid and aneuploid embryos (Patel *et al.*, 2016). Their results did not show statistically significant differences between groups, although it is important to note that their parameter, unlike ours, includes the duration of the first cytokinesis, and that could be masking the results. We suspect that the time between PNd and the start of the first cytokinesis will be particularly useful as it may potentially help in the selection against chromosomal abnormalities of gametic origin, whether maternal or paternal; is independent of the irregular divisions, as they will not affect its duration; and can be measured in non-ICSI and vitrified zygotes, in contrast to other parameters that require the exact time of fertilization as a reference point.

Table 11 | Kinetic parameters in euploid versus aneuploid embryos.

		All embryos			Regular divisions			Irregular divisions		
		N	Median	IQR	N	Median	IQR	N	Median	IQR
PNd to first cytokinesis (h)	Euploid	22	**2.4**[a]	(2.1;2.9)	18	**2.3**[c]	(2.1;2.9)	4	2.9	(0.9;3.1)
	Aneuploid	26	**2.8**[a]	(2.5;3.3)	14	**2.8**[c]	(2.5;3.3)	12	2.9	(2.5;7.9)
First cytokinesis (min)	Euploid	22	15.0	(13.8;26.3)	18	15.0	(10.0;21.3)	4	25.0	(16.3;60.0)
	Aneuploid	26	20.0	(13.8;31.3)	14	20.0	(10.0;31.3)	12	22.5	(15.0;37.5)
Two to three cells (h)	Euploid	14	11.3	(1.4;12.2)	10	11.7	(11.1;12.6)	4	1.3	(0.5;4.3)
	Aneuploid	23	11.4	(0.8;12.6)	11	12.5	(11.8;12.9)	12	0.8	(0.1;2.4)
Three to four cells (h)	Euploid	12	**0.8**[b]	(0.2;1.3)	10	0.8	(0.4;1.3)	2	5.4	(0.1;NA)
	Aneuploid	20	**2.4**[b]	(0.9;8.4)	11	1.7	(0.8;2.7)	9	4.4	(1.6;12.3)
Four to five cells (h)	Euploid	5	5.3	(1;13.8)	4	8.8	(2.9;14.6)	1	0	(0;11.2)
	Aneuploid	25	9.9	(0.8;12.3)	6	12.8	(11.7;15.7)	9	2.7	(0.3;9)
Five to six cells (h)	Euploid	5	7.2	(1.4;9.3)	4	4.9	(0.7;7.4)	1	11.2	(11.2;4.3)
	Aneuploid	12	1.6	(0.4;3.8)	6	1.6	(0.5;2.7)	6	1.6	(0.3;13.8)
Six to seven cells (h)	Euploid	4	1	(0.6;3.5)	3	0.8	(0.5;NA)	1	4.3	(4.3;0.8)
	Aneuploid	12	2	(1;8.5)	6	1.5	(0.5;3.9)	6	5.1	(1.2;13.2)
Seven to eight cells (h)	Euploid	4	0.8	(0.6;1.1)	3	0.8	(0.5;NA)	1	0.8	(0.8;0.5)
	Aneuploid	10	0.7	(0.4;3.4)	6	1.5	(0.4;3.4)	4	0.6	(0.3;4.9)
Eight to nine cells (h)	Euploid	1	0.5	(0.5;0.5)	0	NA	(NA;NA)	1	0.5	(0.5;NA)
	Aneuploid	2	2.5	(1.6;NA)	0	NA	(NA;NA)	2	2.5	(1.6;NA)

IQR, interquartile range (Q1;Q3); NA, not applicable; PNd, pronuclear disappearance.
Kinetic parameters were first calculated for every euploid and aneuploid embryo ('All embryos'). In addition, they were classified according to the type of divisions ('Regular divisions' and 'Irregular divisions'), since one irregular division may alter all subsequent kinetic parameters, which are calculated base on the cell stage of the embryo. [a,b,c] $P<0.05$ (Mann-Whitney *U*-test).

As **Table 11** demonstrates, the time between the three- and four-cell stages was also statistically different between aneuploid and euploid embryos (*P*=0.048, Mann-Whitney *U*-test), and approximately three times longer in aneuploid embryos. We thus used both significant parameters, PNd to first cytokinesis and time between the three- and four-cell stages, to visually differentiate euploid from aneuploid embryos (**Figure 32**).

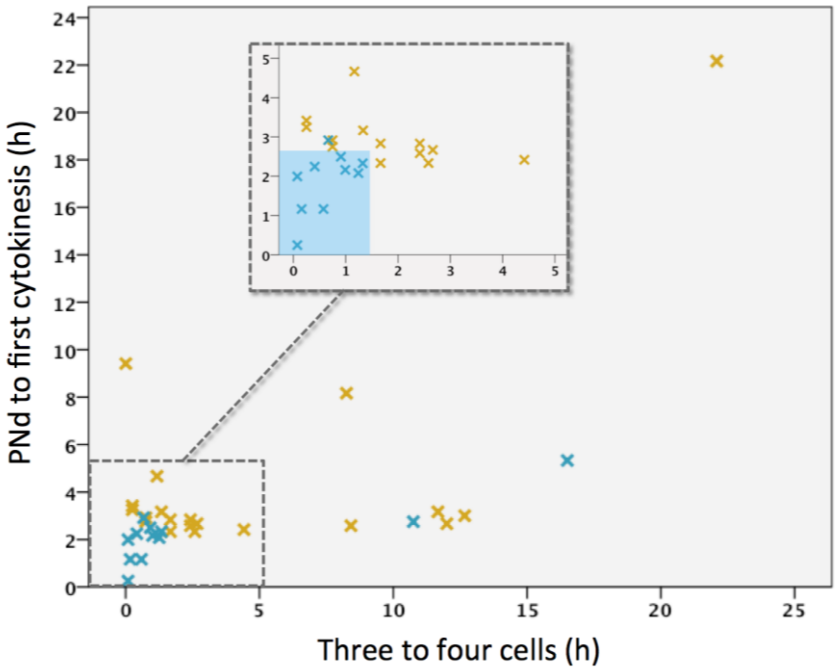

Figure 32 | Distribution of embryos according to the most differential kinetic parameters for aneuploidy.
Euploid embryos (blue) are clustered in the lower left corner, compared with aneuploid embryos (orange), which are scattered over the chart. A zoom window has been to better detect possible overlapping between ploidy groups.

Whereas it was clear that euploid embryos had shorter values of these two parameters, we could still observe some overlapping or outliers that did not allow the complete differentiation of euploid embryos (**Figure 32**). For this reason, although we consider that kinetic parameters can help to increase the

probability of selecting a euploid embryo, they should not be used as a replacement for genetic screening in the clinical routine since they have a low predictive value for ploidy (60-70%) (Chavez *et al.*, 2012; Campbell *et al.*, 2013; Basile *et al.*, 2014). Also, it is important to consider that embryo kinetic behaviors can be affected by several factors, such as different clinical settings, different time-lapse instruments or interpatient variability (Kaser and Racowsky, 2014; Kramer *et al.*, 2014). In any case, even if kinetics should not be applied for aneuploidy prediction in a clinical program, we should take them into consideration, as a complementary test to predict blastocyst formation and implantation (Wong *et al.*, 2010; Meseguer *et al.*, 2011).

4.8.2 Irregular divisions versus aneuploidy

We observed that the number of embryos with irregular divisions in the aneuploid group was considerably higher (12/26) when compared with the euploid group (4/22), although not statistically significant. To determine whether there were differences in the aneuploidy frequency owing to this phenomenon, we analyzed the developmental kinetics of regular versus irregular embryo divisions separately (**Table 11**), since irregular divisions directly influence the parameter timing.

When we separated the embryos solely on the basis of regular and irregular divisions, we did not detect a significant difference in the timing from three- to four-cell stages between ploidy groups to confirm that the previous detected difference was due to the division type (regular/irregular), instead of the ploidy status. Nevertheless, we still detected statistically significant differences in the time between PNd and the start of the first cytokinesis between ploidy groups in embryos with regular divisions (P = 0.049, Mann-Whitney U-test), but not in embryos with irregular divisions. Thus, we would like to emphasize once again the importance of analyzing embryos with irregular division separately. Otherwise, significant differences between the study groups may be masked by this phenomenon since they have very different kinetic patterns creating very scattered data, or vice versa, that the finding differences originate from the type of division, instead of the study variable, as has occurred in our data with ploidy.

Surprisingly, 4 out of 20 embryos that underwent irregular divisions were euploid. Three of these embryos were analyzed immediately after the first mitosis—the irregular one—and only one blastomere from each embryo was analyzed using aCGH. The fourth embryo also exhibited an abnormal first division, but was removed for analysis at the nine-cell stage and the three blastomeres examined using aCGH were euploid male. No multinucleation was detected in any of the four embryos and, notably, three of the four embryos were from the same couple, indicating an individual dimension of embryo development.

It is not new that euploid embryos can also have irregular divisions (Campbell *et al.*, 2013), although it still remains unclear if these type of divisions work as a correction mechanism in polyploid embryos resulting in euploid embryos, or if they result in mosaic embryos with a mix of cells that are euploid and aneuploid, or both.

4.9 Correlation between kinetics and gene expression

As we have kinetic information for all of the embryos analyzed we aimed to look for some trends in gene expression related with altered kinetic patterns. To avoid bias during analysis due to expression differences in embryos collected at different developmental times, we created two groups using a cutoff of 30 hours.

4.9.1 Kinetic parameters versus gene expression

To study the effect of kinetics on gene expression, we first determined the median value of each parameter to create two comparison groups: embryos with a parameter shorter than the median and embryos with the parameter longer. In the analysis, we only included parameters with data for a minimum of ten embryos, to assure the sample size to detect statistical significant differences. For those embryos analyzed before 30 h post PNd, we found differences in gene expression for one kinetic parameter, the time between the PNd and the first cytokinesis (P<0.05, limma test; **Table 12**).

Table 12 | Statistically differentially expressed genes between embryos with different kinetics.

		N	Median	N under median	N above median	Differential genes
Before 30 h post PNd	*PNd to 1st cytokinesis (h)*	48	2.38	25	23	**5**
	First cytokinesis (min)	49	15.0	26	23	0
	Two to three cells (h)	31	10.83	15	16	0
	Three to four cells (h)	23	0.92	12	11	0
After 30 h post PNd	*PNd to 1st cytokinesis (h)*	49	2.75	27	22	**13**
	First cytokinesis (min)	51	0.42	25	26	0
	Two to three cells (h)	50	10.75	25	25	0
	Three to four cells (h)	50	2.42	27	23	0
	Four to five cells (h)	46	11.29	23	23	**6**
	Five to six cells (h)	43	2.25	22	21	0
	Six to seven cells (h)	43	1.25	23	20	0
	Seven to eight cells (h)	40	0.83	23	17	0

PNd, pronuclear disappearance.
Number of statistical differential genes (P<0.05, limma test) between embryos with shorter and longer kinetics parameters during the first 30 h and the time after 30 h post PNd.

Five genes were differentially expressed (P<0.05, limma test) between the embryos with this parameter shorter than the median (2.38h) and embryos with a longer parameter. Three of the differential genes—*OOEP*, cryptochrome circadian clock 1 (*CRY1*) and *RB1*—were highly expressed in the embryos with shorter time between PNd and the start of the first cytokinesis, whereas two genes –*FASLG* and diaphanous related formin 1 (*DIAPH1*)- were highly expressed in embryos with longer time between PNd and the start of the first cytokinesis (**Figure 33**).

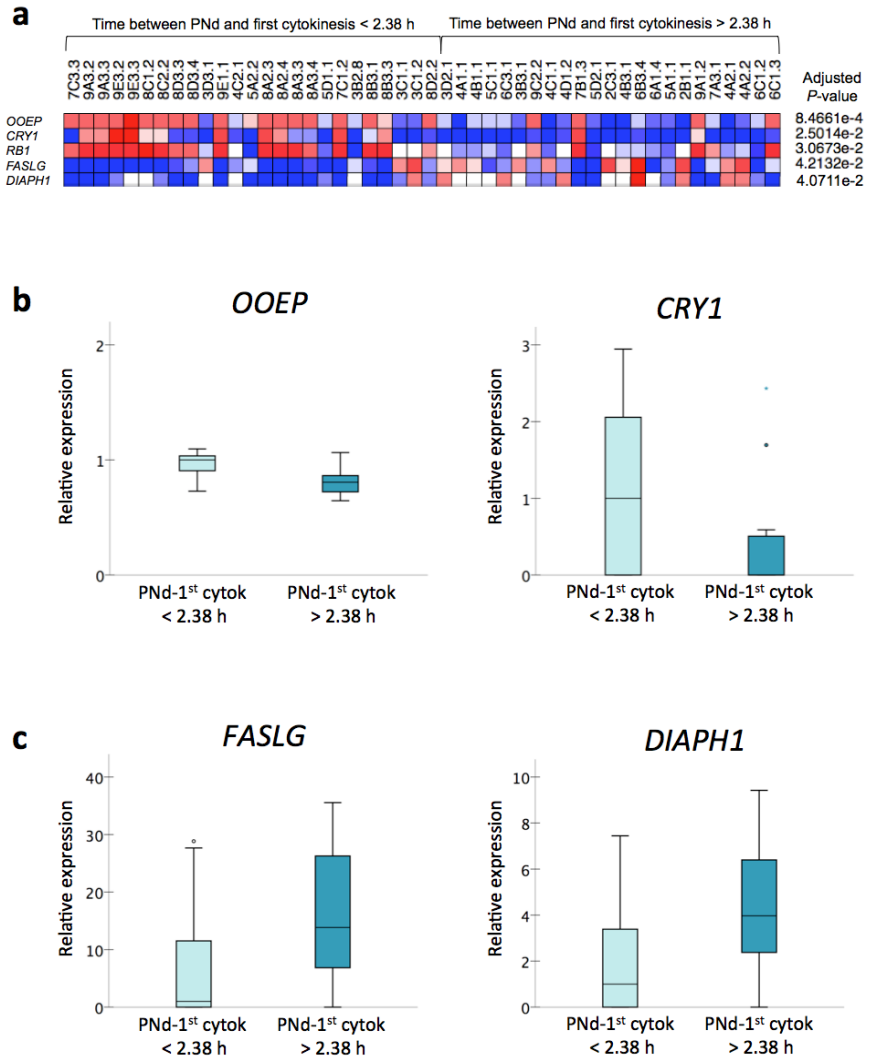

Figure 33 | Differential expression for embryos with shorter versus longer time between the PNd and first cytokinesis during the first 30 h post PNd.
(a) Statistically significant gene expression differences between embryos with the shorter time between PNd and the start of the first cytokinesis and embryos with the longer time (n = 5; P<0.05, limma test). Each column represents a single blastomere. Blue colored squares show low expression, red color represents high levels of gene expression, and white squares indicate moderate expression (log2). Box plots from the top downregulated **(b)** and upregulated genes **(c)** during the first 30 h post PNd in embryos with a time between the PNd and 1st cytokinesis longer than the median (2.38 h) compared with embryos with a time between the PNd and the 1st cytokinesis shorter. A plot represents gene expression values between quartile 1 and 3, the black line inside the box is the median value, and the black circles are outliers. Relative expression was obtained by dividing the data between the median value from embryos with the shorter parameter (<2.38 h).

For the embryos analyzed between 30 and 60 h post PNd, there were two kinetic parameters that affected the transcriptomic profile: the time between the PNd and the start of the first cytokinesis, as in the previous group, and the time between the four- and the five-cell stages (**Table 12**). For the time between the PNd and the start of the first cytokinesis, a total of 13 genes were expressed differentially between the 27 embryos with the parameter shorter than the median (2.75h) and the 22 embryos with this parameter longer (P<0.05, limma test; **Table 12**). The genes that were highly expressed in the embryos with a parameter shorter were mutS homolog 6 (*MSH6*), mutS homolog 2 (*MSH2*), *MCL1*, *CFL1*, and *YY1*; the genes period circadian clock 1 (*PER1*), RB1, nucleophosmin/nucleoplasmin 2 (NPM2), DEAD-box helicase 4 (*DDX4*), regulator of chromosome condensation 2 (*RCC2*), mutS homolog 3 (*MSH3*), DNA damage recognition and repair factor (*XPA*), and *FASLG*, showed a lower expression in these embryos (**Figure 34**).

Note that *FASLG* and *RB1* were differentially expressed also in embryos during the first 30 h after PNd for the same parameter, the time between PNd and the start of the first cytokinesis. More importantly, *FASLG* showed lower levels of expression in all embryos with a shorter time of the parameter, independent of the time of collection. It is known that *FASLG* is an apoptosis receptor that had been related to cell fragmentation at the two- and four-cell stages (Kawamura *et al.*, 2001), which indicates that a shorter time between the PNd and the first cytokinesis may be related with better embryo development. This is also in concordance with our previous results (see sections 1.1, 5.1 and 7.1), where *FASLG* levels were upregulated in high-fragmented embryos and, at the same time, this group of embryos showed longer time between PNd and the first cytokinesis, as the first division is when most of the fragmentation takes place.

Finally, the differential genes found in embryos with shorter versus longer time between the four- and the five-cell stages were discarded as we found statistically significant differences in the average collection time of the samples of each group that could bias the findings (average collection time of embryos with short time between four- and five-cell stages: 42.6±6.7 h and average collection time of embryos with long time between four- and five-cell stages: 38.1±4.5 h; P<0.05, t-test).

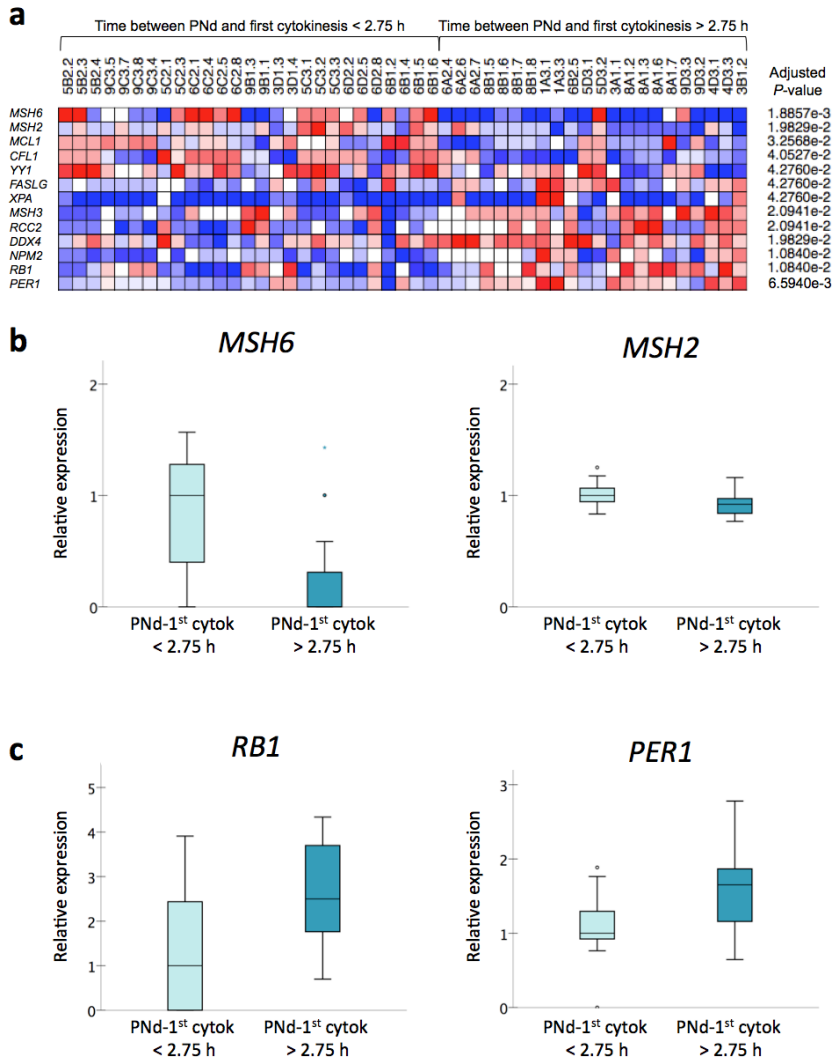

Figure 34 | Differential expression for embryos with shorter versus longer time between the pronuclear disappearance and first cytokinesis between 30 h and 60 h post PNd.

Statistically differentially expressed genes between embryos with shorter time between PNd and the start of the first cytokinesis and embryos with longer time (n = 13; P<0.05, limma test). Each column represents a single blastomere. Blue colored squares show low expression, red color represents high levels of gene expression, and white squares indicate moderate expression (log2). Box plots from the top downregulated **(b)** and upregulated genes **(c)** between the 30 h and 60 h post PNd in embryos with a time between the PNd and 1st cytokinesis longer than the median (2.75 h) compared with embryos with a shorter time between the PNd and the 1st cytokinesis. A plot represents gene expression values between quartile 1 and 3, the black line inside the box is the median value, and the black circles are outliers. Relative expression was obtained by dividing between the median expression value in embryos with short parameter (<2.75 h).

4.9.2 Irregular divisions versus gene expression

We analyzed the expression of all genes in embryos with regular divisions versus irregular divisions. For the group of embryos analyzed between the PNd time and the next 30 h we found one significantly differentially expressed gene, *GADD45A* (*P*<0.05, limma test; **Figure 35**) between embryos with at least one irregular division (*n* =15) and embryos with all regular divisions (*n* = 34). Whereas for the group from 30 h to 60 h post PNd, we did not find any differentially expressed genes between the embryos with irregular divisions (*n* = 17) and embryos with regular divisions (*n* = 37).

Since there is a strong link between the irregular divisions and aneuploidies, it remains unknown if *GADD45A* expression difference in the first time range group is due to the high proportion of aneuploid embryos in the group of irregular divisions (72.7%) compared with the group with embryos with regular divisions, in which the percentage of aneuploid embryos was as low as 22.7%.

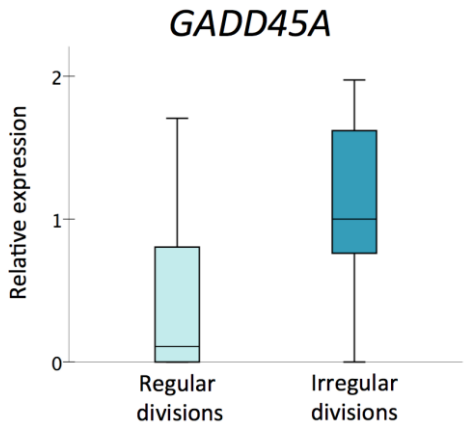

Figure 35 | GADD45A expression between embryos with regular or irregular divisions during the first 30 h post PNd.
GADD45A was the only gene differentially expressed between embryos that showed one irregular division during the first 30 h after PNd (*n* = 15) and embryos with all regular divisions during the same time (*n* = 34; *P*<0.05, limma test). Relative expression was obtained by dividing between the median expression value in embryos with regular divisions.

4.10 Correlation between aneuploidy and gene expression

Via a combination of single-cell gene expression and whole chromosomal data analysis within a single embryo, we also uncovered gene expression patterns indicative of ploidy status. Ploidy and gene expression information was obtained from a total of 53 embryos with 92 cells analyzed using RT-qPCR and 76 cells assessed via aCGH. To compare the expression profiles between ploidy groups without introducing bias due to differences in developmental time, two different groups were created using a cutoff of 30 h post PNd. For the first group, we obtained 41 expression profiles from 33 embryos with an incidence of aneuploidy of 39.4%; in the second group, we collected 52 gene expression profiles from 20 embryos with a 75.0% aneuploidy incidence. We determined that the incidence of aneuploidy was higher in the second group because of the increased frequency of mitotic errors identified by aneuploid blastomere mosaicism compared with the first group. We then used Babelomics (Medina *et al.*, 2010) to compare gene expression levels between the two. In the embryos collected before 30 h, 20 of 86 analyzed genes showed statistically significant differences between euploid versus aneuploid embryos (P<0.05, limma test; **Figure 36a**).

More specifically, we identified a set of genes highly expressed in aneuploid embryos and almost undetectable in euploid embryos, such as caspase 2 (*CASP2)*, cyclin D1 (*CCND1)*, *CCNA1*, DEAD-box helicase 20 *(DDX20)* and *GADD45A*, that further increases in expression as development proceeds (**Figure 36b**). This distinct pattern of expression may be explained by the propagation of chromosomal errors that occurred early in preimplantation development with each subsequent mitotic division.

In contrast, the expression of the catenin beta 1 (*CTNNB1*), *YBX2* and tuberous sclerosis 2 (*TSC2*) were tremendously downregulated in aneuploid embryos compared with euploid embryos (P=0.01, limma test; **Figure 36c**). We determined that most of the transcripts with decreased expression in aneuploid embryos belonged to Cluster 1, which contains genes expressed at high levels in the zygote before embryonic activation and thus, likely of gametic origin.

An analysis of gene expression 30 h after PNd, however, did not show statistically significant differences between aneuploid and euploid embryos. This was possibly due to an increase in the transcriptomic variability between embryos from the same stage in late development. Recently, it has been shown that four-cell stage embryos show the highest variability compared to oocytes and blastocysts (Shaw *et al.*, 2013). The main reason for this phenomenon is that during this stage, as at the eight-cell stage, there is a gradual degradation of maternal transcripts overlapping with the new synthesis by the embryonic genome. This highly dynamic process could take place with different rhythms between embryos from the same developmental stage, and even in cells from the same embryo, as it has been shown for individual blastomeres from eight-cell embryos (Yan *et al.*, 2013). Another reason for the non-detected differences between ploidy groups at later stages could be a hypothetical asymmetric distribution of the transcripts throughout development caused by irregular divisions. Uneven blastomere size is correlated with a high aneuploidy incidence (Magli *et al.*, 2001; Hardarson *et al.*, 2001) and, at the same time, uneven blastomere size has been hypothesized to be related to an irregular transcript distribution (Hardarson *et al.*, 2001; Prados *et al.*, 2012).

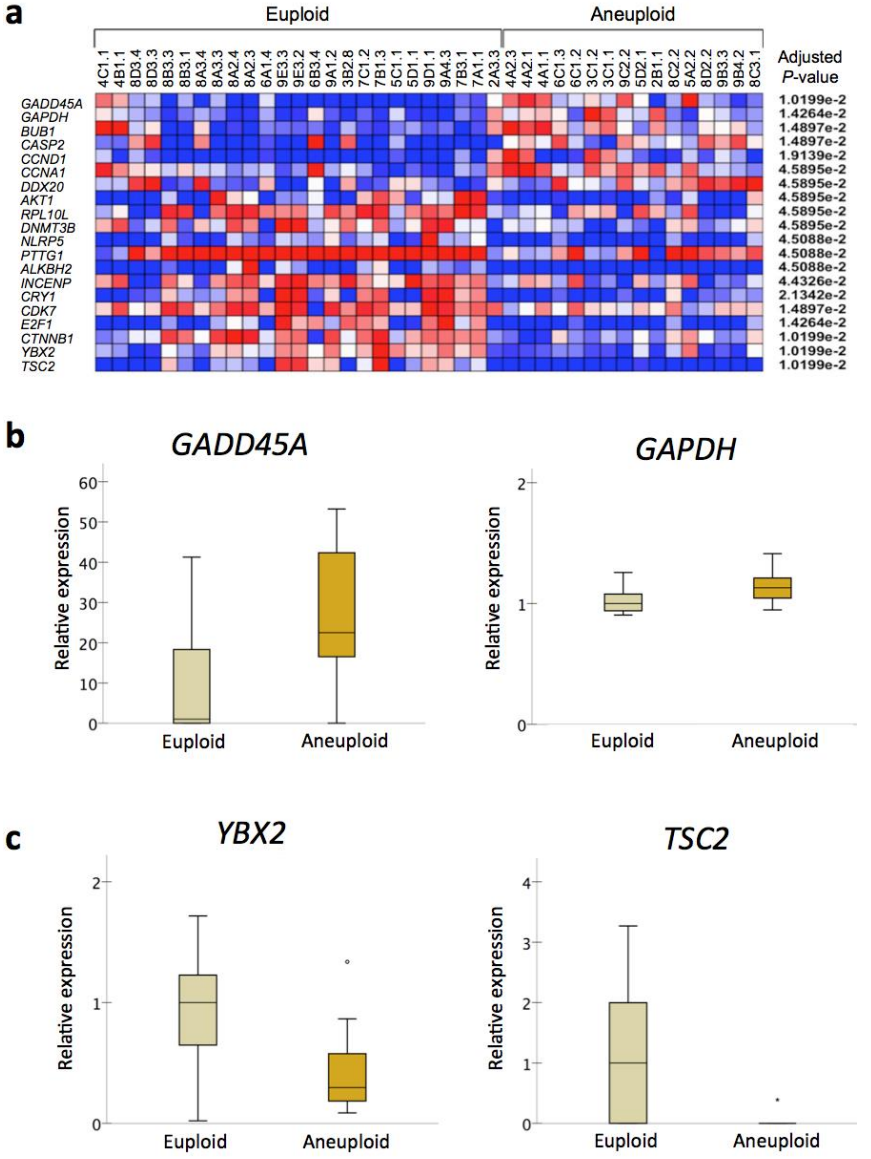

Figure 36 | Differential gene expression in euploid versus euploid embryos.
(a) Heatmap of genes showing significant differential expression (P<0.05, limma test) in euploid versus aneuploid embryos during the first 30 h post PNd. Each column represents a single blastomere. Blue colored squares show low expression, red color represents high levels of gene expression, and white squares indicate moderate expression (log2). **(b)** Box plots from the most upregulated in aneuploid embryos before 30 h post PNd. **(c)** Box plots from the most downregulated genes in aneuploid embryos before 30 h post PNd. A plot represents gene expression values between quartile 1 and 3, the black line inside the box is the median value, and the black circles are outliers. Relative expression was obtained by dividing between the median expression value in euploid embryos.

We also evaluated the significant GO terms in these 20 genes, to determine which molecular pathways were influenced by aneuploid generation (**Table 13**). We observed that the most significant GO terms (n = 16; P<0.001, Fisher´s exact test) were related to cell cycle (7/16) or DNA damage (5/16).

Table 13 | Significant gene ontology terms for genes differentially expressed between aneuploid and euploid embryos.

GO:Term	Term name	C	G	Adjusted *P* value
GO:0007049	Cell cycle	11	941	1.14E-07
GO:0022402	Cell cycle process	9	640	1.19E-06
GO:0000278	Mitotic cell cycle	8	470	1.98E-06
GO:0051726	Regulation of cell cycle	7	314	2.94E-06
GO:0051301	Cell division	6	281	4.51E-05
GO:0051716	Cellular response to stimulus	8	865	1.05E-04
GO:0006259	DNA metabolic process	7	640	1.56E-04
GO:0033554	Cellular response to stress	7	623	1.56E-04
GO:0034984	Cellular response to DNA damage stimulus	6	383	1.56E-04
GO:0006974	Response to DNA damage stimulus	6	423	2.38E-04
GO:0051329	Interphase of mitotic cell cycle	4	109	4.29E-04
GO:0019953	Sexual reproduction	6	484	4.29E-04
GO:0051325	Interphase	4	115	4.52E-04
GO:0051246	Regulation of protein metabolic process	6	508	4.52E-04
GO:0048609	Reproductive process in a multicellular organism	6	506	4.52E-04
GO:0006281	DNA repair	5	330	9.96E-04

GO, gene ontology; C, number of genes annotated by the given term in the test set; G, number of genes annotated by the given term in the reference set.
Only GO terms with P≤0.001 (Two-tailed Fisher´s exact test) are shown.

What is the possible significance of those genes differentially expressed between aneuploid and euploid embryos and their possible roles in aneuploidy generation? Indeed, the most difficult, but also the most interesting question for us was what is first, the aneuploidy or the transcriptomic modification? To address this question, we took the 20 differentially expressed genes and disregarded those maternally inherited and, at the same time, activated by the

embryonic genome, since it was not possible to know if those changes were a cause or an effect of aneuploidies. Thus, we focused exclusively on 7 genes. Four of them—*AKT1*, *CRY1*, DNA methyltransferase 3b (*DNMT3B)*, *YBX2*—were maternally inherited and did not show any embryonic activation during the time of the study; and the other 3 genes—*CASP2*, *CCND1*, *GADD45A*—were exclusively activated by the embryo genome and did not show any expression levels before PNd.

Starting with the maternal genes, all four were downregulated in the aneuploid embryos, and we considered them useful to study the possible cause of the aneuploidies.

The first maternal gene, *AKT1*, is an initiator gene of the G2/M transition and is essential for promoting the first mitosis after fertilization in mouse (Wu *et al.*, 2011; Baran *et al.*, 2013). *AKT1* is also the main agent responsible for mediating the anti-apoptotic signal in the zygote (Wu *et al.*, 2011; Baran *et al.*, 2013). Based on these findings, low *AKT1* levels inherited from the oocyte could lead to errors during the first embryo mitosis, and/or could end in an apoptotic process that would avoid most of these embryos to go further in development.

Our aneuploid embryos also had low *CRY1* transcript levels. *CRY1* synthetizes a circadian regulator protein that has been described to have a function during female meiosis (Amano *et al.*, 2009). More specifically, low expression of *CRY1* seems to slows meiotic progression in mouse oocytes (Amano *et al.*, 2009). From our results, we could hypothesize that this effect of *CRY1* in meiosis could lead to the generation of meiotic aneuploidies, but even if does not, altered transcripts levels may have an effect in the subsequent mitotic division after fertilization.

DNMT3B synthetizes a protein involved in *de novo* methylation during mammalian development and has been identified in human oocytes (Kocabas *et al.*, 2006). One recent study showed that *DNMT3B* has lower expression in human embryos arrested at the one- or two-cell stages (Wong *et al.*, 2010). We also found low *DNMT3B* levels in aneuploid embryo, suggesting that a altered mRNA inheritance of this gene could lead to chromosomal abnormalities during development.

Finally, we found *YBX2* to be a crucial gene to study in early embryo development. The mouse Y-box protein (*MSY2*) is the *YBX2* homologous gene in mouse and it has been shown to bind maternal transcripts to avoid degradation during the first stages of the embryo development (Yu *et al.*, 2003). In addition, *MSY2* knockout mice showed a 25% mRNA reduction in their oocytes as well as aberrant spindle formation (Medvedev *et al.*, 2011). Thus, low *YBX2* expression could impede the proper maternal mRNA inheritance and the embryo development could be adversely affected, not only in the division machinery producing aneuploidies, but also in any other crucial process of early stages. In fact, a previous study in human embryos showed that YBX2 mRNA levels were significantly lower in arrested embryos (Wong *et al.*, 2010).

After analyzing those maternal genes that we hypothesized are involved in the origin of aneuploidies, we moved to the analyses of those genes that were not expressed in the oocyte and showed differential expression levels in the aneuploid embryos compared to the euploid embryos. These three genes were highly expressed in the aneuploid embryos, meaning that they are crucial to understand which are the first changes that occur inside the embryo and that are driven by its own genome as a response to the existence of chromosomal abnormalities.

Two of these three genes, *CASP2* and *GADD45A*, are DNA damage response genes that activate cell cycle arrest. This finding would be in concordance with previous studies showing that around 90% of the arrested embryos are aneuploidy (Magli *et al.*, 2007; Qi *et al.*, 2014).

Finally, *CCND1* was also found at high levels in the aneuploid embryos. This gene encodes a protein involved in the G1/S transition in the mitotic cell cycle. The overexpression of this gene would have an effect on cell cycle progression, opposite to the function of the other two activated genes, but consistent with the still high aneuploidy incidence found in human blastocysts, which is more than 50% (Fragouli and Wells, 2011).

In summary, our findings suggest that aneuploidies in the human embryo are mainly the consequence of the inheritance of an abnormal pool of transcripts, which could cause either a meiotic error during gametogenesis or a mitotic

error during the first cleavages of the embryo development. In any case, the embryo response includes the activation of genes involved in development arrest and those genes that contribute to cell cycle progression. The final balance of transcript levels will define the destiny of the aneuploid embryo.

4.10.1 Model to predict ploidy status in early embryos

Taking advantage of the difference in transcript expression observed between euploid and aneuploid embryos during the first 30 h of development, our next aim was to create a prediction model for embryo ploidy on the basis of a specific gene expression signature (**Figure 37**). To accomplish this, cells from which both ploidy and gene expression data were obtained with a collection time before 30 h post PNd were selected (n = 41). Although expression values from all 86 genes were available, we focused on the most informative genes to improve the functionality of the predictor. The Mann-Whitney U-test was performed on the aneuploid and euploid samples to obtain 31 differentially expressed genes (P<0.05). Before model construction, samples were randomly split into a training group (n = 27) and a validation group (n = 14). Only the samples from the training group were used for the model design. To assess model accuracy, a five-fold cross-validation was performed and repeated 20 times to estimate the misclassification rate. From this, several models were generated depending on the number of closest neighbors evaluated for the test step and the number of genes selected for the training step. To obtain the most reliable predictor, we applied additional restrictive parameters and only selected genes with a P<0.005 (Mann-Whitney U-test, n = 12). Cross-validation showed that the model with k = 7 was the most stringent [accuracy 85.2%, Matthews correlation coefficient (MCC) 0.62, root mean squared error (RMSE) 0.31, AUC 0.92]. Once selected, the predictor model was tested using the validation sample group. The confirmation rate was 85.7% (12/14) with two of the euploid samples being misclassified as aneuploid and no aneuploid samples inappropriately called as euploid. Finally, we tested the prediction model in a different group of samples collected at the same time as the training samples, but for which no results from aneuploidy screening were obtained (n = 25). The prediction model classified 11 of the samples as aneuploid and 14 as euploid with an incidence of aneuploidy of 44.0%, which is similar to the observed

aneuploidy rate in the samples with known ploidy results at the same stage (39.0%). We also compared the time intervals between the PNd and the start of the first cytokinesis in each embryo since this was the most relevant parameter related to chromosome status. As expected, the median time was much longer in the embryos classified as aneuploid versus those predicted to be euploid (2.58 h versus 1.09 h).

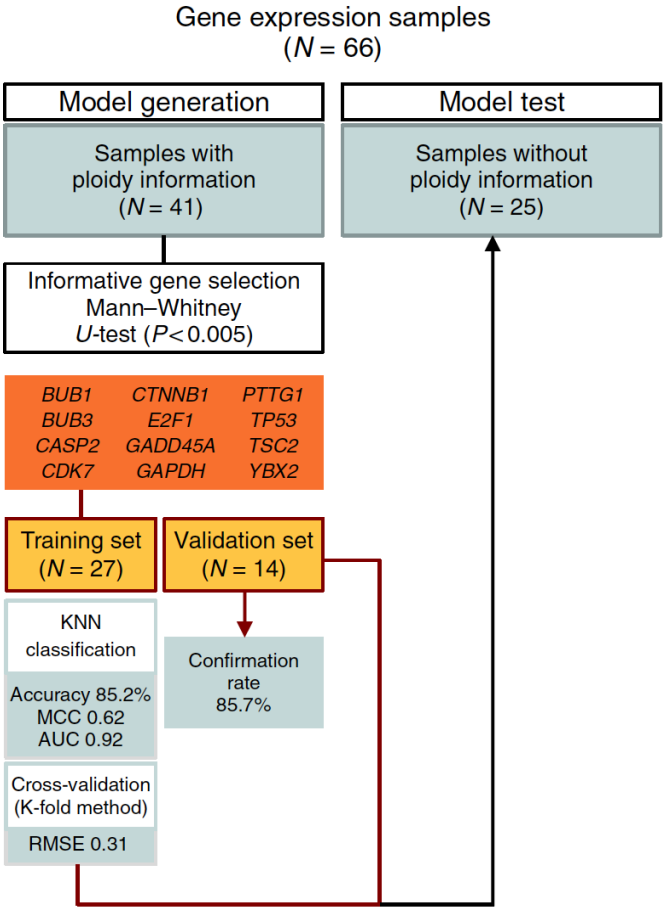

Figure 37 | Embryo aneuploidy prediction model.
A diagram of each phase of the aneuploidy prediction model. All samples with gene expression data were used in this process. Samples with ploidy results were selected for model generation and validation. Samples without ploidy information became the prediction group. KNN, k-nearest neighbors; MCC, Matthews correlation coefficient; AUC, area under the curve; RMSE, root mean squared error.

The predictor model identified 12 genes as applicable for the classification of euploid versus aneuploid samples: *BUB1* mitotic checkpoint serine/threonine kinase (*BUB1*), *BUB3*, *CASP2*, *CDK7*, *CTNNB1*, E2F transcription factor 1 (*E2F1*), *GADD45A*, *GAPDH*, pituitary tumor-transforming 1 (*PTTG1*), *TP53*, *TSC2*, and *YBX2*. With the exception of *BUB1*, *CASP2*, *GAPDH*, and *GADD45A*, which were more highly expressed in aneuploid embryos, the majority of genes were upregulated in euploid embryos (**Figure 36a**).

The vast majority of these genes were expressed at lower levels in aneuploid embryos compared to euploid embryos such as *BUB3*, *CDK7*, *PTTG1*, *TSC2*, and *YBX2*, and all of them appeared to be inherited from one, or possibly both gametes. This supports the idea that embryos that receive an abnormal pool or levels of certain transcripts proceed from an aneuploid oocyte or are destined to be aneuploid later in development. Taken together, these data identify a gene subset that are differentially regulated in euploid versus aneuploid embryos and suggests that mathematical modeling on the basis of the expression of this key group of genes may provide a useful tool to largely predict the ploidy status of embryos (**Figure 38**).

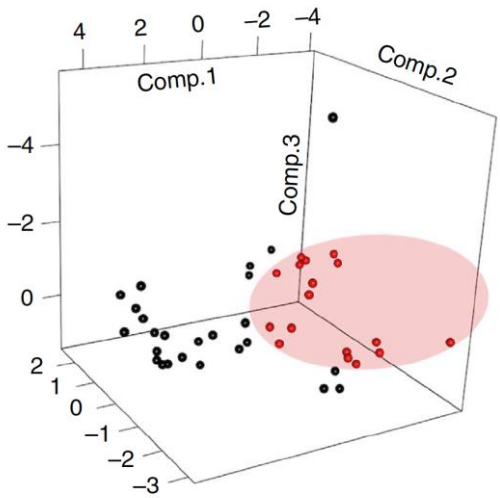

Figure 38 | Distribution of embryos according to the aneuploidy prediction signature. Principal component analysis of cells (*n* = 41) from embryos at early stages (before 30 h post PNd) on the basis of expression of the 12 genes selected in the prediction model. Cells from euploid embryos are shown in black (*n* = 25), and samples from aneuploid embryos are designated red (*n* = 16).

While previous time-lapse studies have provided methods for the enrichment in the selection of euploid embryos following early cleavage divisions or blastocyst formation (Chavez *et al.*, 2012; Campbell *et al.*, 2013; Basile *et al.*, 2014), our data suggest that euploid embryos may be distinguished from aneuploid embryos before the first mitotic division. Due to the limited number of human samples available for research, this should be considered as a pilot study and further work would be necessary to confirm the ploidy predictor model in case of clinical use. Although our results can be considered robust, since they have been obtained from a very diverse population of embryos coming from different clinics, with different culture conditions and different stimulation protocols, they would need to be replicated in fresh embryos, as the timing intervals and/or the expression levels may be displaced. In addition, because of data protection, we did not have access to possible relevant patient information, such as, semen quality, or infertility status that could help to find different patterns in future studies.

Although we did not consider the clinical application as the aim of our study since other invasive techniques, such as aCGH or NGS, are currently available for chromosomal analysis with a very high efficiency. We would like to highlight that our model was designed for the first 30 h after PNd in which embryos have between 1 and 4 cells and should not be biopsied at these stages for clinical purposes. Rather, we consider our study as a keystone in the knowledge of human embryo development that should contribute to the establishment of non-invasive diagnostic tools that could reliably predict aneuploidy generation at the zygote stage via detection of surrogate molecules in the embryo culture media.

4.11 Descriptive atlas of human embryo development

To integrate all descriptive analysis of this study, morphology, kinetics, aneuploidy screening and gene expression data, we aimed to create a unique atlas of the early human embryo development **(Figure 39)**. We focused on grouping embryos with similar morphokinetic patterns to better understand all variations of the human embryo development and their effects on the chromosome status. Our atlas shows the high variability underlying human embryo development, with 18 groups being the minimal number of patterns that we were able to differentiate in our sample size. Euploid embryos were clustered into 3 groups, whereas aneuploid embryos, including those that were mosaic, could be classified in 11 groups. We have to note that 16 embryos could not be classified in any of the previous groups because to their chromosome status, creating 4 additional groups, called "OVERLAPPING", with common patterns for euploid and aneuploid embryos.

It is important to understand that while human euploid embryos seem to follow a unique way to succeed without high variability, aneuploid embryos may follow different pathways, overlapping and camouflaging with euploid embryos in some cases. The variability in the behavior of aneuploid embryos could be related to different types of aneuploid embryos that can be observed, starting with embryos with single or multiple aneuploidies and combinations of monosomies and trisomies for any of the 23 pairs of chromosomes. This would be the reason why all the attempts to purely separate the populations based on visual or behavior characteristics have failed.

In the atlas, four parameters were used for the clustering of the embryos according to their chromosomal status, two kinetic (PNd to 1st cytokinesis and PNd to three-cell stage) and two morphologic parameters (fragmentation and multinucleation). The time between PNd and the first cytokinesis was used in combination with the percentage of fragmentation. When embryos started the first cytokinesis in less than 2.5 h after PNd and, in addition, showed less than 10% fragmentation, they were all euploid (n = 6), even in one case showing one irregular division from 1 to 3 cells. In contrast, embryos that took more than 6 hours to divide from the PNd and, in addition, showed more than 35%

fragmentation, were all aneuploid (*n* = 7). Those embryos that did not follow the previous patterns were classified according to the time from PNd to the three-cell stage. If the time until the three-cell stage was between 13 and 14 h from the PNd, the embryos were euploid (*n* = 6); when the time was between 14.4 and 17 h the embryos were all aneuploid (*n* = 10) or mosaic (*n* = 2). We then analyzed those embryos that did not follow any of the previous patterns, and we selected those ones showing multinucleation at any stage (*n* = 8). All of them were aneuploid or, in one case, mosaic. The leftover embryos were a mix of euploid (*n* = 11) and aneuploid embryos (*n* = 5) that could not be differentiated attending to their morphokinetic behavior.

Although the irregular divisions were not helpful in classifying behaviors from euploid versus aneuploid embryos, we considered them to be included in the atlas since they are an uncommon phenomenon whose origin has not been yet well described. Interestingly, there was one euploid embryo that underwent one irregular division during the first mitosis from the one to the four-cell stage.

Finally, a gene expression descriptive was also included to complete the human embryo atlas. We showed which genes were upregulated and downregulated in aneuploid embryos at four different stages. A high number of genes were differentially expressed in aneuploid embryos during the three first divisions studied, which would represent cleavage until the four-cell stage in embryos with regular divisions, whereas after the 7^{th} division only four genes were differentially expressed.

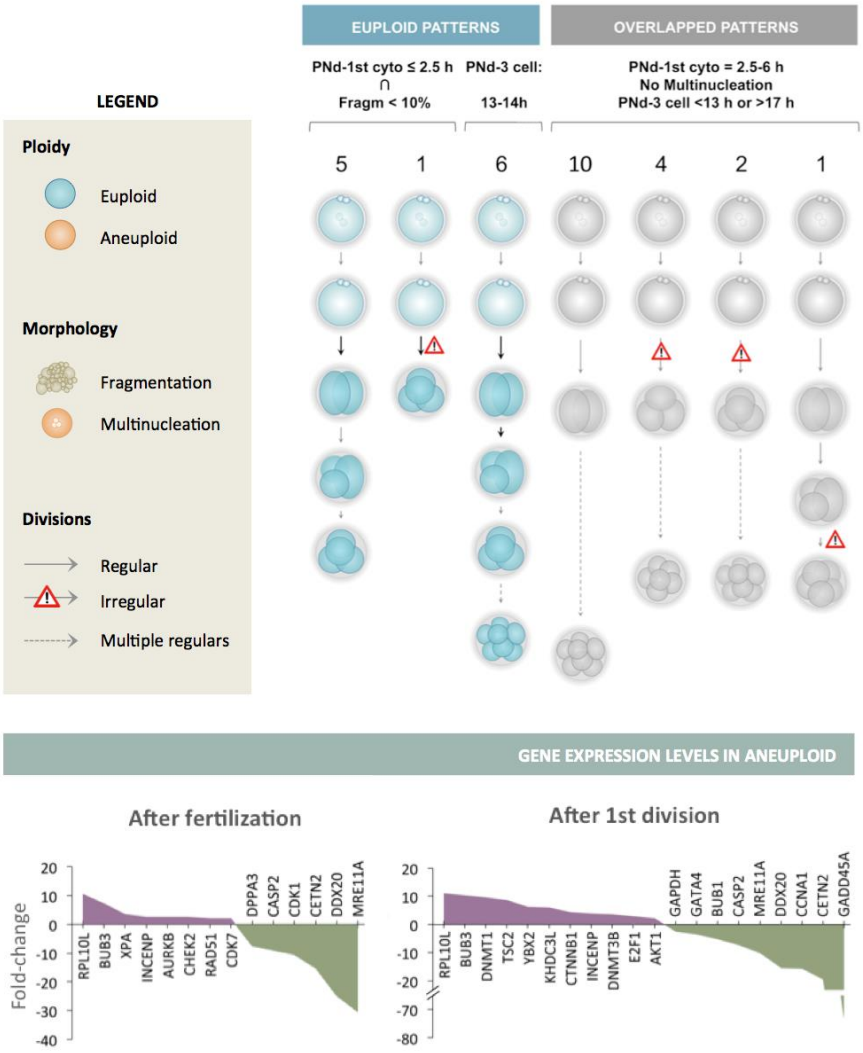

Figure 39 | Atlas of the human embryo development.
All analyzed embryos have been represented and grouped together according to morphology, kinetics and chromosome patterns. Numbers on the top of each pattern column represent the number of embryos that were grouped. The overlapped patterns represent both euploid and aneuploid embryos that were indistinguishable by morphokinetics. Embryos at one-cell stage were not included in the morphokinetic pattern classification, as they did not have any division-related information (n=8). Nevertheless, a same embryo could be included in two groups, in case it followed the criteria for both. For fold-change calculation in gene expression charts, euploid embryos expression levels were taken as a reference. PNd, pronuclear disappearance; cyto, cytokinesis; Fragm, fragmentation; ∩, logical intersection.

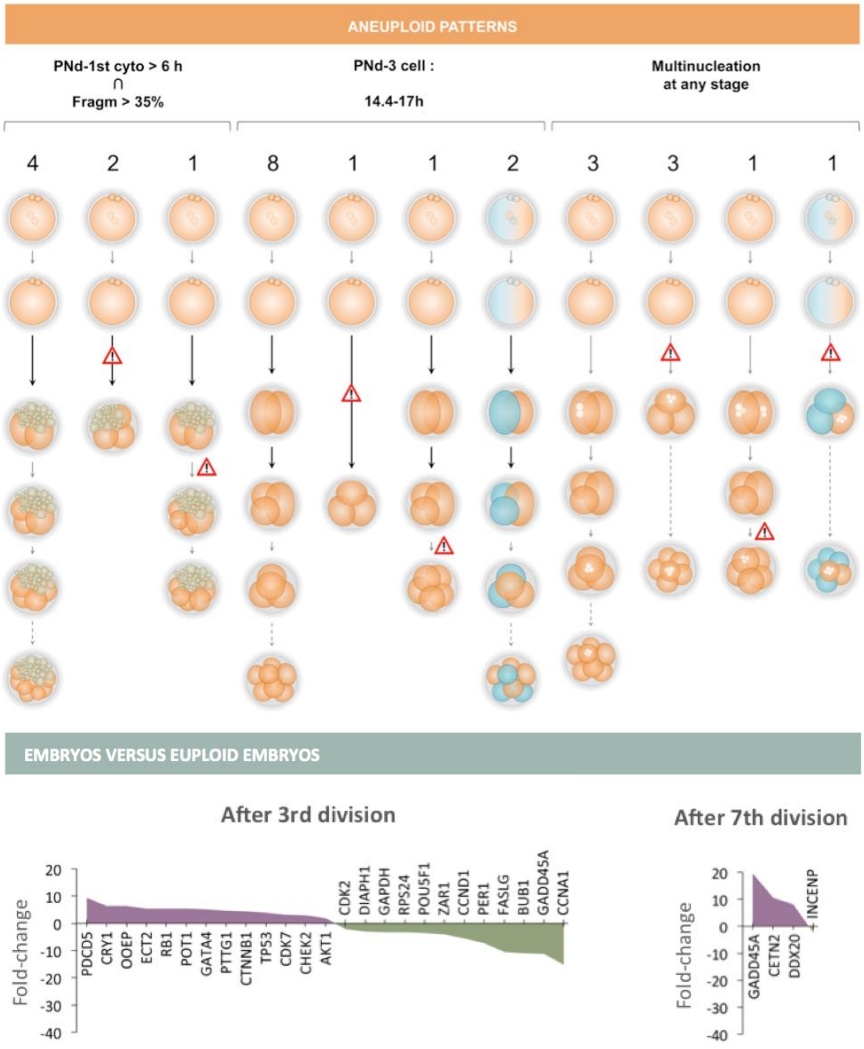

Figure 39 (Continued)

CONCLUSIONS

5 | Conclusions

C1. Morphological parameters can display a dynamic behavior during embryo development. Specifically, most of the cellular fragmentation appears during the first mitotic division, and fragments can be reabsorbed, divided or fused with other fragments or blastomeres.

C2. Kinetic parameters are sensitive to the existence of irregular divisions, thus they should be always calculated according to the division type to avoid drawing misleading conclusions.

C3. More than half of the human embryos from IVF patients are aneuploid. Aneuploidy incidence is correlated with multinucleation, but not with fragmentation or vacuole existence.

C4. The gene expression patterns during embryo development follow different patterns according to the origin: maternal, embryonic or both. In addition, we have observed that embryonic genome activation starts as early as at zygote stage.

C5. The kinetics of aneuploid embryos are altered in comparison to the euploid. More specifically, the time between the pronuclear disappearance and the start of the first cytokinesis is longer in aneuploid embryos. Similarly, the time between the three- and the four-cell stage is longer in aneuploid embryos, although this is caused by the higher proportion of aneuploid embryos with irregular divisions, which alter the kinetic behavior.

C6. The transcriptomics of aneuploid embryos show significant differences during the first 30 hours of development in comparison to euploid embryos. Taking this into account, the ploidy status of cleavage-stage embryos can be predicted by a transcriptomic signature.

C7. The atlas generated from the embryos analyzed in this study shows the high variability underlying human embryo development. While the euploid embryos seem to follow a uniform development without high variability for morphokinetics, aneuploid embryos may follow different pathways, overlapping with and mimicking euploid embryos in some cases, making them hard to differentiate.

REFERENCES

6 | References

Abdelhadi, I., Colls, P., Sandalinas, M., Escudero, T., and Munne, S. (2003). Preimplantation genetic diagnosis of numerical abnormalities for 13 chromosomes. Reprod. Biomed. Online *2,* 226-231.

Aguilar, J., Rubio, I., Munoz, E., Pellicer, A., and Meseguer, M. (2016). Study of nucleation status in the second cell cycle of human embryo and its impact on implantation rate. Fertil. Steril. *2,* 291-299.e2.

Al-Asmar, N., Peinado, V., Vera, M., Remohi, J., Pellicer, A., Simon, C., Hassold, T., and Rubio, C. (2012). Chromosomal abnormalities in embryos from couples with a previous aneuploid miscarriage. Fertil. Steril. *1,* 145-150.

Alfarawati, S., Fragouli, E., Colls, P., Stevens, J., Gutierrez-Mateo, C., Schoolcraft, W.B., Katz-Jaffe, M.G., and Wells, D. (2011). The relationship between blastocyst morphology, chromosomal abnormality, and embryo gender. Fertil. Steril. *2,* 520-524.

Alikani, M., Calderon, G., Tomkin, G., Garrisi, J., Kokot, M., and Cohen, J. (2000). Cleavage anomalies in early human embryos and survival after prolonged culture in-vitro. Hum. Reprod. *12,* 2634-2643.

Alikani, M., Cohen, J., Tomkin, G., Garrisi, G.J., Mack, C., and Scott, R.T. (1999). Human embryo fragmentation in vitro and its implications for pregnancy and implantation. Fertil. Steril. *5,* 836-842.

Alikani, M., Schimmel, T., and Willadsen, S.M. (2005). Cytoplasmic fragmentation in activated eggs occurs in the cytokinetic phase of the cell cycle, in lieu of normal cytokinesis, and in response to cytoskeletal disorder. Mol. Hum. Reprod. *5,* 335-344.

Alpha Scientists in Reproductive Medicine and ESHRE Special Interest Group of Embryology. (2011). The Istanbul consensus workshop on embryo assessment: proceedings of an expert meeting. Hum. Reprod. *6,* 1270-1283.

Alvarez, C., Garcia-Garrido, C., Taronger, R., and Gonzalez de Merlo, G. (2013). In vitro maturation, fertilization, embryo development & clinical outcome of human metaphase-I oocytes retrieved from stimulated intracytoplasmic sperm injection cycles. Indian J. Med. Res. *2,* 331-338.

Amano, T., Matsushita, A., Hatanaka, Y., Watanabe, T., Oishi, K., Ishida, N., Anzai, M., Mitani, T., Kato, H., Kishigami, S. *et al*. (2009). Expression and functional analyses of circadian genes in mouse oocytes and preimplantation embryos: Cry1 is involved in the meiotic process independently of circadian clock regulation. Biol. Reprod. *3,* 473-483.

Ambroggio, J., Gindoff, P.R., Dayal, M.B., Khaldi, R., Peak, D., Frankfurter, D., and Dubey, A.K. (2011). Multinucleation of a sibling blastomere on day 2 suggests unsuitability for embryo transfer in IVF-preimplantation genetic screening cycles. Fertil. Steril. *4,* 856-859.

Aparicio-Ruiz, B., Basile, N., Perez Albala, S., Bronet, F., Remohi, J., and Meseguer, M. (2016). Automatic time-lapse instrument is superior to single-point morphology observation for selecting viable embryos: retrospective study in oocyte donation. Fertil. Steril. *6,* 1379-1385.e10.

Ata, B., Kaplan, B., Danzer, H., Glassner, M., Opsahl, M., Tan, S.L., and Munne, S. (2012). Array CGH analysis shows that aneuploidy is not related to the number of embryos generated. Reprod. Biomed. Online *6,* 614-620.

Athayde Wirka, K., Chen, A.A., Conaghan, J., Ivani, K., Gvakharia, M., Behr, B., Suraj, V., Tan, L., and Shen, S. (2014). Atypical embryo phenotypes identified by time-lapse microscopy: high prevalence and association with embryo development. Fertil. Steril. *6,* 1637-48.e1-5.

Azzarello, A., Hoest, T., and Mikkelsen, A.L. (2012). The impact of pronuclei morphology and dynamicity on live birth outcome after time-lapse culture. Hum. Reprod. *9,* 2649-2657.

Balakier, H., and Cadesky, K. (1997). The frequency and developmental capability of human embryos containing multinucleated blastomeres. Hum. Reprod. *4,* 800-804.

Balakier, H., Sojecki, A., Motamedi, G., and Librach, C. (2016). Impact of multinucleated blastomeres on embryo developmental competence, morphokinetics, and aneuploidy. Fertil. Steril. *3,* 608-614.e2.

Baltz, J.M. (2012). Media composition: salts and osmolality. Methods Mol. Biol. 61-80.

Baran, V., Fabian, D., and Rehak, P. (2013). Akt/PKB plays role of apoptosis relay on entry into first mitosis of mouse embryo. Zygote *4,* 406-416.

Basile, N., Nogales Mdel, C., Bronet, F., Florensa, M., Riqueiros, M., Rodrigo, L., Garcia-Velasco, J., and Meseguer, M. (2014). Increasing the probability of selecting chromosomally normal embryos by time-lapse morphokinetics analysis. Fertil. Steril. *3,* 699-704.

Bazrgar, M., Gourabi, H., Yazdi, P.E., Vazirinasab, H., Fakhri, M., Hassani, F., and Valojerdi, M.R. (2014). DNA repair signalling pathway genes are overexpressed in poor-quality pre-implantation human embryos with complex aneuploidy. Eur. J. Obstet. Gynecol. Reprod. Biol. 152-156.

Bernardini, L.M., Costa, M., Bottazzi, C., Gianaroli, L., Magli, M.C., Venturini, P.L., Francioso, R., Conte, N., and Ragni, N. (2004). Sperm aneuploidy and recurrent pregnancy loss. Reprod. Biomed. Online *3,* 312-320.

Bhattacharya, S., Hamilton, M.P., Shaaban, M., Khalaf, Y., Seddler, M., Ghobara, T., Braude, P., Kennedy, R., Rutherford, A., Hartshorne, G., and Templeton, A. (2001). Conventional in-vitro fertilisation versus intracytoplasmic sperm injection for the treatment of non-male-factor infertility: a randomised controlled trial. Lancet *9274,* 2075-2079.

Bond, D.J., and Chandley, A.C. (1983). Aneuploidy Oxford University Press).

Bultman, S.J., Gebuhr, T.C., Pan, H., Svoboda, P., Schultz, R.M., and Magnuson, T. (2006). Maternal BRG1 regulates zygotic genome activation in the mouse. Genes Dev. *13,* 1744-1754.

Burruel, V., Klooster, K., Barker, C.M., Pera, R.R., and Meyers, S. (2014). Abnormal early cleavage events predict early embryo demise: sperm oxidative stress and early abnormal cleavage. Sci. Rep. 6598.

Campbell, A., Fishel, S., Bowman, N., Duffy, S., Sedler, M., and Hickman, C.F. (2013). Modelling a risk classification of aneuploidy in human embryos using non-invasive morphokinetics. Reprod. Biomed. Online *5,* 477-485.

Campos-Galindo, I., Garcia-Herrero, S., Martinez-Conejero, J.A., Ferro, J., Simon, C., and Rubio, C. (2015). Molecular analysis of products of conception obtained by hysteroembryoscopy from infertile couples. J. Assist. Reprod. Genet. *5,* 839-848.

Capalbo, A., Bono, S., Spizzichino, L., Biricik, A., Baldi, M., Colamaria, S., Ubaldi, F.M., Rienzi, L., and Fiorentino, F. (2013a). Sequential comprehensive chromosome analysis on polar bodies, blastomeres and trophoblast: insights into female meiotic errors and chromosomal segregation in the preimplantation window of embryo development. Hum. Reprod. *2,* 509-518.

Capalbo, A., Wright, G., Elliott, T., Ubaldi, F.M., Rienzi, L., and Nagy, Z.P. (2013b). FISH reanalysis of inner cell mass and trophectoderm samples of previously array-CGH screened blastocysts shows high accuracy of diagnosis and no major diagnostic impact of mosaicism at the blastocyst stage. Hum. Reprod. *8,* 2298-2307.

Carbone, L., and Chavez, S.L. (2015). Mammalian pre-implantation chromosomal instability: species comparison, evolutionary considerations, and pathological correlations. Syst. Biol. Reprod. Med. *6,* 321-335.

Cetinkaya, M., Pirkevi, C., Yelke, H., Colakoglu, Y.K., Atayurt, Z., and Kahraman, S. (2015). Relative kinetic expressions defining cleavage synchronicity are better predictors of blastocyst formation and quality than absolute time points. J. Assist. Reprod. Genet. *1,* 27-35.

Chavez, S.L., Loewke, K.E., Han, J., Moussavi, F., Colls, P., Munne, S., Behr, B., and Reijo Pera, R.A. (2012). Dynamic blastomere behaviour reflects human embryo ploidy by the four-cell stage. Nat. Commun. 1251.

Chavez, S.L., McElroy, S.L., Bossert, N.L., De Jonge, C.J., Rodriguez, M.V., Leong, D.E., Behr, B., Westphal, L.M., and Reijo Pera, R.A. (2014). Comparison of epigenetic mediator expression and function in mouse and human embryonic blastomeres. Hum. Mol. Genet. *18,* 4970-4984.

Chawla, M., Fakih, M., Shunnar, A., Bayram, A., Hellani, A., Perumal, V., Divakaran, J., and Budak, E. (2015). Morphokinetic analysis of cleavage stage embryos and its relationship to aneuploidy in a retrospective time-lapse imaging study. J. Assist. Reprod. Genet. *1,* 69-75.

Chen, A.A., Tan, L., Suraj, V., Reijo Pera, R., and Shen, S. (2013). Biomarkers identified with time-lapse imaging: discovery, validation, and practical application. Fertil. Steril. *4,* 1035-1043.

Chi, H.J., Koo, J.J., Choi, S.Y., Jeong, H.J., and Roh, S.I. (2011). Fragmentation of embryos is associated with both necrosis and apoptosis. Fertil. Steril. *1,* 187-192.

Choi, K.S., Kim, J.Y., Lim, S.K., Choi, Y.W., Kim, Y.H., Kang, S.Y., Park, T.J., and Lim, I.K. (2012). TIS21(/BTG2/PC3) accelerates the repair of DNA double strand breaks by enhancing Mre11 methylation and blocking damage signal transfer to the Chk2(T68)-p53(S20) pathway. DNA Repair (Amst) *12,* 965-975.

Chow, J.F., Yeung, W.S., Lau, E.Y., Lee, V.C., Ng, E.H., and Ho, P.C. (2014). Array comparative genomic hybridization analyses of all blastomeres of a cohort of embryos from young IVF patients revealed significant contribution of mitotic errors to embryo mosaicism at the cleavage stage. Reprod. Biol. Endocrinol. 105-7827-12-105.

Christopikou, D., Tsorva, E., Economou, K., Shelley, P., Davies, S., Mastrominas, M., and Handyside, A.H. (2013). Polar body analysis by array comparative genomic hybridization accurately predicts aneuploidies of maternal meiotic origin in cleavage stage embryos of women of advanced maternal age. Hum. Reprod. *5,* 1426-1434.

Collodel, G., Capitani, S., Baccetti, B., Pammolli, A., and Moretti, E. (2007). Sperm aneuploidies and low progressive motility. Hum. Reprod. *7,* 1893-1898.

Cruz, M., Garrido, N., Herrero, J., Perez-Cano, I., Munoz, M., and Meseguer, M. (2012). Timing of cell division in human cleavage-stage embryos is linked with blastocyst formation and quality. Reprod. Biomed. Online *4,* 371-381.

Dal Canto, M., Coticchio, G., Mignini Renzini, M., De Ponti, E., Novara, P.V., Brambillasca, F., Comi, R., and Fadini, R. (2012). Cleavage kinetics analysis of human embryos predicts development to blastocyst and implantation. Reprod. Biomed. Online *5,* 474-480.

Demko, Z.P., Simon, A.L., McCoy, R.C., Petrov, D.A., and Rabinowitz, M. (2016). Effects of maternal age on euploidy rates in a large cohort of embryos analyzed with 24-chromosome single-nucleotide polymorphism-based preimplantation genetic screening. Fertil. Steril. *5,* 1307-1313.

Desai, N., Ploskonka, S., Goodman, L.R., Austin, C., Goldberg, J., and Falcone, T. (2014). Analysis of embryo morphokinetics, multinucleation and cleavage anomalies using continuous time-lapse monitoring in blastocyst transfer cycles. Reprod. Biol. Endocrinol. 54-7827-12-54.

Destouni, A., Zamani Esteki, M., Catteeuw, M., Tsuiko, O., Dimitriadou, E., Smits, K., Kurg, A., Salumets, A., Van Soom, A., Voet, T., and Vermeesch, J.R. (2016). Zygotes segregate entire parental genomes in distinct blastomere lineages causing cleavage-stage chimerism and mixoploidy. Genome Res. *5,* 567-578.

Diaz-Gimeno, P., Horcajadas, J.A., Martinez-Conejero, J.A., Esteban, F.J., Alama, P., Pellicer, A., and Simon, C. (2011). A genomic diagnostic tool for human endometrial receptivity based on the transcriptomic signature. Fertil. Steril. *1,* 50-60, 60.e1-15.

Diez-Juan, A., Rubio, C., Marin, C., Martinez, S., Al-Asmar, N., Riboldi, M., Diaz-Gimeno, P., Valbuena, D., and Simon, C. (2015). Mitochondrial DNA content as a viability score in human euploid embryos: less is better. Fertil. Steril. *3,* 534-41.e1.

Dobson, A.T., Raja, R., Abeyta, M.J., Taylor, T., Shen, S., Haqq, C., and Pera, R.A. (2004). The unique transcriptome through day 3 of human preimplantation development. Hum. Mol. Genet. *14,* 1461-1470.

Ebner, T., Moser, M., Sommergruber, M., Gaiswinkler, U., Shebl, O., Jesacher, K., and Tews, G. (2005). Occurrence and developmental consequences of vacuoles throughout preimplantation development. Fertil. Steril. *6,* 1635-1640.

Egozcue, S., Blanco, J., Vendrell, J.M., Garcia, F., Veiga, A., Aran, B., Barri, P.N., Vidal, F., and Egozcue, J. (2000). Human male infertility: chromosome anomalies, meiotic disorders, abnormal spermatozoa and recurrent abortion. Hum. Reprod. Update *1,* 93-105.

Ergin, E.G., Caliskan, E., Yalcinkaya, E., Oztel, Z., Cokelez, K., Ozay, A., and Ozornek, H.M. (2014). Frequency of embryo multinucleation detected by time-lapse system and its impact on pregnancy outcome. Fertil. Steril. *4,* 1029-1033.e1.

Escrich, L., Grau, N., de los Santos, M.J., Romero, J.L., Pellicer, A., and Escriba, M.J. (2012). The dynamics of in vitro maturation of germinal vesicle oocytes. Fertil. Steril. *5,* 1147-1151.

ESHRE Guideline Group on Good practice in IVF. (December, 2015). Revised guidelines for good practice in IVF laboratories (2015).

Fasano, G., Fontenelle, N., Vannin, A.S., Biramane, J., Devreker, F., Englert, Y., and Delbaere, A. (2014). A randomized controlled trial comparing two vitrification methods versus slow-freezing for cryopreservation of human cleavage stage embryos. J. Assist. Reprod. Genet. *2,* 241-247.

Fauque, P., Audureau, E., Leandri, R., Delaroche, L., Assouline, S., Epelboin, S., Jouannet, P., and Patrat, C. (2013). Is the nuclear status of an embryo an independent factor to predict its ability to develop to term? Fertil. Steril. *5,* 1299-1304.e3.

Flaherty, S.P., Payne, D., and Matthews, C.D. (1998). Fertilization failures and abnormal fertilization after intracytoplasmic sperm injection. Hum. Reprod. 155-164.

Fragouli, E., Alfarawati, S., Goodall, N.N., Sanchez-Garcia, J.F., Colls, P., and Wells, D. (2011). The cytogenetics of polar bodies: insights into female meiosis and the diagnosis of aneuploidy. Mol. Hum. Reprod. *5,* 286-295.

Fragouli, E., and Wells, D. (2011). Aneuploidy in the human blastocyst. Cytogenet. Genome Res. *2-4,* 149-159.

Franasiak, J.M., Forman, E.J., Hong, K.H., Werner, M.D., Upham, K.M., Treff, N.R., and Scott, R.T. (2014). Aneuploidy across individual chromosomes at the embryonic level in trophectoderm biopsies: changes with patient age and chromosome structure. J. Assist. Reprod. Genet. *11,* 1501-1509.

Fukuda, Y., and Chang, M.C. (1978). Relationship between sperm concentration and polyspermy in intact and zona-free mouse eggs inseminated in vitro. Arch. Androl. *3,* 267-273.

Galan, A., Diaz-Gimeno, P., Poo, M.E., Valbuena, D., Sanchez, E., Ruiz, V., Dopazo, J., Montaner, D., Conesa, A., and Simon, C. (2013). Defining the genomic signature of totipotency and pluripotency during early human development. PLoS One *4,* e62135.

Galan, A., Montaner, D., Poo, M.E., Valbuena, D., Ruiz, V., Aguilar, C., Dopazo, J., and Simon, C. (2010). Functional genomics of 5- to 8-cell stage human embryos by blastomere single-cell cDNA analysis. PLoS One *10,* e13615.

Gardner, D.K., Lane, M., Stevens, J., Schlenker, T., and Schoolcraft, W.B. (2000). Blastocyst score affects implantation and pregnancy outcome: towards a single blastocyst transfer. Fertil. Steril. *6,* 1155-1158.

Geraedts, J., Montag, M., Magli, M.C., Repping, S., Handyside, A., Staessen, C., Harper, J., Schmutzler, A., Collins, J., Goossens, V. *et al.* (2011). Polar body array CGH for prediction of the status of the corresponding oocyte. Part I: clinical results. Hum. Reprod. *11,* 3173-3180.

Gianaroli, L., Racowsky, C., Geraedts, J., Cedars, M., Makrigiannakis, A., and Lobo, R.A. (2012). Best practices of ASRM and ESHRE: a journey through reproductive medicine. Fertil. Steril. *6,* 1380-1394.

Giscard d'Estaing, S., Perrin, D., Lenoir, G.M., Guerin, J.F., and Dante, R. (2005). Upregulation of the BRCA1 gene in human germ cells and in preimplantation embryos. Fertil. Steril. *3,* 785-788.

Guo, G., Huss, M., Tong, G.Q., Wang, C., Li Sun, L., Clarke, N.D., and Robson, P. (2010). Resolution of cell fate decisions revealed by single-cell gene expression analysis from zygote to blastocyst. Dev. Cell. *4,* 675-685.

Gutierrez-Mateo, C., Colls, P., Sanchez-Garcia, J., Escudero, T., Prates, R., Ketterson, K., Wells, D., and Munne, S. (2011). Validation of microarray comparative genomic hybridization for comprehensive chromosome analysis of embryos. Fertil. Steril. *3,* 953-958.

Hardarson, T., Hanson, C., Sjogren, A., and Lundin, K. (2001). Human embryos with unevenly sized blastomeres have lower pregnancy and implantation rates: indications for aneuploidy and multinucleation. Hum. Reprod. *2,* 313-318.

Hardarson, T., Lofman, C., Coull, G., Sjogren, A., Hamberger, L., and Edwards, R.G. (2002). Internalization of cellular fragments in a human embryo: time-lapse recordings. Reprod. Biomed. Online *1,* 36-38.

Hardy, K. (1999). Apoptosis in the human embryo. Rev. Reprod. *3,* 125-134.

Harton, G.L., Magli, M.C., Lundin, K., Montag, M., Lemmen, J., Harper, J.C., and European Society for Human Reproduction and Embryology (ESHRE) PGD Consortium/Embryology Special Interest Group. (2011). ESHRE PGD Consortium/Embryology Special Interest Group--best practice guidelines for polar body and embryo biopsy for preimplantation genetic diagnosis/screening (PGD/PGS). Hum. Reprod. *1,* 41-46.

Hassold, T. (1982). Mosaic trisomies in human spontaneous abortions. Hum. Genet. *1,* 31-35.

Hassold, T., and Hunt, P. (2001). To err (meiotically) is human: the genesis of human aneuploidy. Nat. Rev. Genet. *4,* 280-291.

Herrero, J., Tejera, A., Albert, C., Vidal, C., de los Santos, M.J., and Meseguer, M. (2013). A time to look back: analysis of morphokinetic characteristics of human embryo development. Fertil. Steril. *6,* 1602-9.e1-4.

Hlinka, D., Kalatova, B., Uhrinova, I., Dolinska, S., Rutarova, J., Rezacova, J., Lazarovska, S., and Dudas, M. (2012). Time-lapse cleavage rating predicts human embryo viability. Physiol. Res. *5,* 513-525.

Hnida, C., Engenheiro, E., and Ziebe, S. (2004). Computer-controlled, multilevel, morphometric analysis of blastomere size as biomarker of fragmentation and multinuclearity in human embryos. Hum. Reprod. *2,* 288-293.

Hutt, K.J., Shi, Z., Petroff, B.K., and Albertini, D.F. (2010). The environmental toxicant 2,3,7,8-tetrachlorodibenzo-p-dioxin disturbs the establishment and maintenance of cell polarity in preimplantation rat embryos. Biol. Reprod. *5,* 914-920.

Hyun, C.S., Cha, J.H., Son, W.Y., Yoon, S.H., Kim, K.A., and Lim, J.H. (2007). Optimal ICSI timing after the first polar body extrusion in in vitro matured human oocytes. Hum. Reprod. *7,* 1991-1995.

Jackson, K.V., Ginsburg, E.S., Hornstein, M.D., Rein, M.S., and Clarke, R.N. (1998). Multinucleation in normally fertilized embryos is associated with an accelerated ovulation induction response and lower implantation and pregnancy rates in in vitro fertilization-embryo transfer cycles. Fertil. Steril. *1,* 60-66.

Jaroudi, S., Kakourou, G., Cawood, S., Doshi, A., Ranieri, D.M., Serhal, P., Harper, J.C., and SenGupta, S.B. (2009). Expression profiling of DNA repair genes in human oocytes and blastocysts using microarrays. Hum. Reprod. *10,* 2649-2655.

Jaroudi, S., and SenGupta, S. (2007). DNA repair in mammalian embryos. Mutat. Res. *1,* 53-77.

Johnson, D.S., Cinnioglu, C., Ross, R., Filby, A., Gemelos, G., Hill, M., Ryan, A., Smotrich, D., Rabinowitz, M., and Murray, M.J. (2010a). Comprehensive analysis of karyotypic mosaicism between trophectoderm and inner cell mass. Mol. Hum. Reprod. *12,* 944-949.

Johnson, D.S., Gemelos, G., Baner, J., Ryan, A., Cinnioglu, C., Banjevic, M., Ross, R., Alper, M., Barrett, B., Frederick, J. *et al*. (2010b). Preclinical validation of a microarray method for full molecular karyotyping of blastomeres in a 24-h protocol. Hum. Reprod. *4,* 1066-1075.

Jurisicova, A., Antenos, M., Varmuza, S., Tilly, J.L., and Casper, R.F. (2003). Expression of apoptosis-related genes during human preimplantation embryo development: potential roles for the Harakiri gene product and Caspase-3 in blastomere fragmentation. Mol. Hum. Reprod. *3,* 133-141.

Jurisicova, A., Varmuza, S., and Casper, R.F. (1996). Programmed cell death and human embryo fragmentation. Mol. Hum. Reprod. *2,* 93-98.

Kaser, D.J., and Racowsky, C. (2014). Clinical outcomes following selection of human preimplantation embryos with time-lapse monitoring: a systematic review. Hum. Reprod. Update *5,* 617-631.

Kawamura, K., Fukuda, J., Kodama, H., Kumagai, J., Kumagai, A., and Tanaka, T. (2001). Expression of Fas and Fas ligand mRNA in rat and human preimplantation embryos. Mol. Hum. Reprod. *5,* 431-436.

Keefe, D.L., Franco, S., Liu, L., Trimarchi, J., Cao, B., Weitzen, S., Agarwal, S., and Blasco, M.A. (2005). Telomere length predicts embryo fragmentation after in vitro fertilization in women--toward a telomere theory of reproductive aging in women. Am. J. Obstet. Gynecol. *4,* 1256-60; discussion 1260-1.

Keltz, M.D., Skorupski, J.C., Bradley, K., and Stein, D. (2006). Predictors of embryo fragmentation and outcome after fragment removal in in vitro fertilization. Fertil. Steril. *2,* 321-324.

Kiessling, A.A., Bletsa, R., Desmarais, B., Mara, C., Kallianidis, K., and Loutradis, D. (2010). Genome-wide microarray evidence that 8-cell human blastomeres over-express cell cycle drivers and under-express checkpoints. J. Assist. Reprod. Genet. *6,* 265-276.

Kirkegaard, K., Agerholm, I.E., and Ingerslev, H.J. (2012). Time-lapse monitoring as a tool for clinical embryo assessment. Hum. Reprod. *5,* 1277-1285.

Kirkegaard, K., Kesmodel, U.S., Hindkjaer, J.J., and Ingerslev, H.J. (2013). Time-lapse parameters as predictors of blastocyst development and pregnancy outcome in embryos from good prognosis patients: a prospective cohort study. Hum. Reprod. *10,* 2643-2651.

Kocabas, A.M., Crosby, J., Ross, P.J., Otu, H.H., Beyhan, Z., Can, H., Tam, W.L., Rosa, G.J., Halgren, R.G., Lim, B., Fernandez, E., and Cibelli, J.B. (2006). The transcriptome of human oocytes. Proc. Natl. Acad. Sci. U. S. A. *38,* 14027-14032.

Kola, I., Trounson, A., Dawson, G., and Rogers, P. (1987). Tripronuclear human oocytes: altered cleavage patterns and subsequent karyotypic analysis of embryos. Biol. Reprod. *2,* 395-401.

Kramer, Y.G., Kofinas, J.D., Melzer, K., Noyes, N., McCaffrey, C., Buldo-Licciardi, J., McCulloh, D.H., and Grifo, J.A. (2014). Assessing morphokinetic parameters via time lapse microscopy (TLM) to predict euploidy: are aneuploidy risk classification models universal? J. Assist. Reprod. Genet. *9,* 1231-1242.

Kuliev, A., Zlatopolsky, Z., Kirillova, I., Spivakova, J., and Cieslak Janzen, J. (2011). Meiosis errors in over 20,000 oocytes studied in the practice of preimplantation aneuploidy testing. Reprod. Biomed. Online *1,* 2-8.

Labarta, E., Bosch, E., Alama, P., Rubio, C., Rodrigo, L., and Pellicer, A. (2012). Moderate ovarian stimulation does not increase the incidence of human embryo chromosomal abnormalities in in vitro fertilization cycles. J. Clin. Endocrinol. Metab. *10,* E1987-94.

Le Caignec, C., Spits, C., Sermon, K., De Rycke, M., Thienpont, B., Debrock, S., Staessen, C., Moreau, Y., Fryns, J.P., Van Steirteghem, A., Liebaers, I., and Vermeesch, J.R. (2006). Single-cell chromosomal imbalances detection by array CGH. Nucleic Acids Res. *9,* e68.

Leese, H.J., Baumann, C.G., Brison, D.R., McEvoy, T.G., and Sturmey, R.G. (2008). Metabolism of the viable mammalian embryo: quietness revisited. Mol. Hum. Reprod. *12,* 667-672.

Li, L., Zheng, P., and Dean, J. (2010). Maternal control of early mouse development. Development *6,* 859-870.

Lin, D.P., Huang, C.C., Wu, H.M., Cheng, T.C., Chen, C.I., and Lee, M.S. (2004). Comparison of mitochondrial DNA contents in human embryos with good or poor morphology at the 8-cell stage. Fertil. Steril. *1,* 73-79.

Liu, H.C., He, Z.Y., Mele, C.A., Veeck, L.L., Davis, O., and Rosenwaks, Z. (2000). Expression of apoptosis-related genes in human oocytes and embryos. J. Assist. Reprod. Genet. *9,* 521-533.

Liu, L., and Keefe, D.L. (2002). Ageing-associated aberration in meiosis of oocytes from senescence-accelerated mice. Hum. Reprod. *10,* 2678-2685.

Ma, J., Zeng, F., Schultz, R.M., and Tseng, H. (2006). Basonuclin: a novel mammalian maternal-effect gene. Development *10,* 2053-2062.

Madissoon, E., Tohonen, V., Vesterlund, L., Katayama, S., Unneberg, P., Inzunza, J., Hovatta, O., and Kere, J. (2014). Differences in Gene Expression between Mouse and Human for Dynamically Regulated Genes in Early Embryo. PLoS One *8,* e102949.

Magli, M.C., Gianaroli, L., and Ferraretti, A.P. (2001). Chromosomal abnormalities in embryos. Mol. Cell. Endocrinol. S29-34.

Magli, M.C., Gianaroli, L., Ferraretti, A.P., Lappi, M., Ruberti, A., and Farfalli, V. (2007). Embryo morphology and development are dependent on the chromosomal complement. Fertil. Steril. *3,* 534-541.

Mantikou, E., Wong, K.M., Repping, S., and Mastenbroek, S. (2012). Molecular origin of mitotic aneuploidies in preimplantation embryos. Biochim. Biophys. Acta *12,* 1921-1930.

Marquard, K., Westphal, L.M., Milki, A.A., and Lathi, R.B. (2010). Etiology of recurrent pregnancy loss in women over the age of 35 years. Fertil. Steril. *4,* 1473-1477.

Mastenbroek, S., Twisk, M., van der Veen, F., and Repping, S. (2011). Preimplantation genetic screening: a systematic review and meta-analysis of RCTs. Hum. Reprod. Update *4,* 454-466.

McLernon, D.J., Harrild, K., Bergh, C., Davies, M.J., de Neubourg, D., Dumoulin, J.C.M., Gerris, J., Kremer, J.A.M., Martikainen, H., Mol, B.W. *et al*. (2010). Clinical effectiveness of elective single versus double embryo transfer: meta-analysis of individual patient data from randomised trials. BMJ

Medina, I., Carbonell, J., Pulido, L., Madeira, S.C., Goetz, S., Conesa, A., Tarraga, J., Pascual-Montano, A., Nogales-Cadenas, R., Santoyo, J. *et al*. (2010). Babelomics: an integrative platform for the analysis of transcriptomics, proteomics and genomic data with advanced functional profiling. Nucleic Acids Res. *Web Server issue,* W210-3.

Medvedev, S., Pan, H., and Schultz, R.M. (2011). Absence of MSY2 in mouse oocytes perturbs oocyte growth and maturation, RNA stability, and the transcriptome. Biol. Reprod. *3,* 575-583.

Mertzanidou, A., Wilton, L., Cheng, J., Spits, C., Vanneste, E., Moreau, Y., Vermeesch, J.R., and Sermon, K. (2013). Microarray analysis reveals abnormal chromosomal complements in over 70% of 14 normally developing human embryos. Hum. Reprod. *1,* 256-264.

Meseguer, M., Herrero, J., Tejera, A., Hilligsoe, K.M., Ramsing, N.B., and Remohi, J. (2011). The use of morphokinetics as a predictor of embryo implantation. Hum. Reprod. *10,* 2658-2671.

Meseguer, M., Martinez-Conejero, J.A., O'Connor, J.E., Pellicer, A., Remohi, J., and Garrido, N. (2008). The significance of sperm DNA oxidation in embryo development and reproductive outcome in an oocyte donation program: a new model to study a male infertility prognostic factor. Fertil. Steril. *5,* 1191-1199.

Milewski, R., Kuc, P., Kuczynska, A., Stankiewicz, B., Lukaszuk, K., and Kuczynski, W. (2015). A predictive model for blastocyst formation based on morphokinetic parameters in time-lapse monitoring of embryo development. J. Assist. Reprod. Genet. *4,* 571-579.

Mir, P., Rodrigo, L., Mateu, E., Peinado, V., Milan, M., Mercader, A., Buendia, P., Delgado, A., Pellicer, A., Remohi, J., and Rubio, C. (2010). Improving FISH diagnosis for preimplantation genetic aneuploidy screening. Hum. Reprod. *7,* 1812-1817.

Mir, P., Rodrigo, L., Mercader, A., Buendia, P., Mateu, E., Milan-Sanchez, M., Peinado, V., Pellicer, A., Remohi, J., Simon, C., and Rubio, C. (2013). False positive rate of an arrayCGH platform for single-cell preimplantation genetic screening and subsequent clinical application on day-3. J. Assist. Reprod. Genet. *1,* 143-149.

Munne, S. (2006). Chromosome abnormalities and their relationship to morphology and development of human embryos. Reprod. Biomed. Online *2,* 234-253.

Munne, S., Alikani, M., Tomkin, G., Grifo, J., and Cohen, J. (1995). Embryo morphology, developmental rates, and maternal age are correlated with chromosome abnormalities. Fertil. Steril. *2,* 382-391.

Munne, S., Ary, J., Zouves, C., Escudero, T., Barnes, F., Cinioglu, C., Ary, B., and Cohen, J. (2006). Wide range of chromosome abnormalities in the embryos of young egg donors. Reprod. Biomed. Online *3,* 340-346.

Munne, S., Sandalinas, M., Magli, C., Gianaroli, L., Cohen, J., and Warburton, D. (2004). Increased rate of aneuploid embryos in young women with previous aneuploid conceptions. Prenat. Diagn. *8,* 638-643.

Neganova, I.E., Sekirina, G.G., and Eichenlaub-Ritter, U. (2000). Surface-expressed E-cadherin, and mitochondrial and microtubule distribution in rescue of mouse embryos from 2-cell block by aggregation. Mol. Hum. Reprod. *5,* 454-464.

Niakan, K.K., and Eggan, K. (2013). Analysis of human embryos from zygote to blastocyst reveals distinct gene expression patterns relative to the mouse. Dev. Biol. *1,* 54-64.

Niakan, K.K., Han, J., Pedersen, R.A., Simon, C., and Pera, R.A. (2012). Human pre-implantation embryo development. Development *5,* 829-841.

Nogales, M.C., Bronet, F., Basile, N., Martinez, E.M., Linan, A., Rodrigo, L., and Meseguer, M. (2017). Type of chromosome abnormality affects embryo morphology dynamics. Fertil. Steril. *1,* 229-235.e2.

Norppa, H., and Falck, G.C. (2003). What do human micronuclei contain? Mutagenesis *3,* 221-233.

Nybo Andersen, A.M., Wohlfahrt, J., Christens, P., Olsen, J., and Melbye, M. (2000). Maternal age and fetal loss: population based register linkage study. BMJ *7251,* 1708-1712.

Obradors, A., Rius, M., Daina, G., Ramos, L., Benet, J., and Navarro, J. (2011). Whole-chromosome aneuploidy analysis in human oocytes: focus on comparative genomic hybridization. Cytogenet. Genome Res. *2-4,* 119-126.

Pagidas, K., Ying, Y., and Keefe, D. (2008). Predictive value of preimplantation genetic diagnosis for aneuploidy screening in repeated IVF-ET cycles among women with recurrent implantation failure. J. Assist. Reprod. Genet. *2-3,* 103-106.

Palermo, G., Munne, S., and Cohen, J. (1994). The human zygote inherits its mitotic potential from the male gamete. Hum. Reprod. *7,* 1220-1225.

Patel, D.V., Shah, P.B., Kotdawala, A.P., Herrero, J., Rubio, I., and Banker, M.R. (2016). Morphokinetic behavior of euploid and aneuploid embryos analyzed by time-lapse in embryoscope. J. Hum. Reprod. Sci. *2,* 112-118.

Pavone, M.E., Innes, J., Hirshfeld-Cytron, J., Kazer, R., and Zhang, J. (2011). Comparing thaw survival, implantation and live birth rates from cryopreserved zygotes, embryos and blastocysts. J. Hum. Reprod. Sci. *1,* 23-28.

Payne, D., Flaherty, S.P., Barry, M.F., and Matthews, C.D. (1997). Preliminary observations on polar body extrusion and pronuclear formation in human oocytes using time-lapse video cinematography. Hum. Reprod. *3,* 532-541.

Pickering, S.J., Taylor, A., Johnson, M.H., and Braude, P.R. (1995). An analysis of multinucleated blastomere formation in human embryos. Hum. Reprod. *7,* 1912-1922.

Prados, F.J., Debrock, S., Lemmen, J.G., and Agerholm, I. (2012). The cleavage stage embryo. Hum. Reprod. i50-71.

Qi, S.T., Liang, L.F., Xian, Y.X., Liu, J.Q., and Wang, W. (2014). Arrested human embryos are more likely to have abnormal chromosomes than developing embryos from women of advanced maternal age. J. Ovarian Res. 65-2215-7-65. eCollection 2014.

R Core Team. (2013). R: A language and Environment for Statistical Computing (Vienna, Austria: R Foundation for Statistical Computing).

Racowsky, C., Combelles, C.M., Nureddin, A., Pan, Y., Finn, A., Miles, L., Gale, S., O'Leary, T., and Jackson, K.V. (2003). Day 3 and day 5 morphological predictors of embryo viability. Reprod. Biomed. Online *3,* 323-331.

Reed, M.L., Hamic, A., Caperton, C.L., and Thompson, D.J. (2010). Live birth after anonymous donation of twice-cryopreserved embryos that had been stored in liquid nitrogen for a cumulative storage time of approximately 13.5 years. Fertil. Steril. *7,* 2771.e1-2771.e3.

Rodrigo, L., Mateu, E., Mercader, A., Cobo, A.C., Peinado, V., Milan, M., Al-Asmar, N., Campos-Galindo, I., Garcia-Herrero, S., Mir, P., Simon, C., and Rubio, C. (2014). New tools for embryo selection: comprehensive chromosome screening by array comparative genomic hybridization. Biomed. Res. Int. 517125.

Rodrigo, L., Rubio, C., Peinado, V., Villamon, R., Al-Asmar, N., Remohi, J., Pellicer, A., Simon, C., and Gil-Salom, M. (2011). Testicular sperm from patients with obstructive and nonobstructive azoospermia: aneuploidy risk and reproductive prognosis using testicular sperm from fertile donors as control samples. Fertil. Steril. *3,* 1005-1012.

Rubio, C., Bellver, J., Rodrigo, L., Bosch, E., Mercader, A., Vidal, C., De los Santos, M.J., Giles, J., Labarta, E., Domingo, J. *et al*. (2013a). Preimplantation genetic screening using fluorescence in situ hybridization in patients with repetitive implantation failure and advanced maternal age: two randomized trials. Fertil. Steril. *5,* 1400-1407.

Rubio, C., Bellver, J., Rodrigo, L., Castillón, G., Guillén, A., Vidal, C., Giles, J., Ferrando, M., Cabanillas, S., Remohí, J., Pellicer, A., and Simón, C. (2017). *In Vitro* Fertilization with Preimplantation Genetic Diagnosis for Aneuploidies (PGD-A) in Advanced Maternal Age: A Randomized Controlled Study. Fertil. Steril. In press.

Rubio, C., Gil-Salom, M., Simon, C., Vidal, F., Rodrigo, L., Minguez, Y., Remohi, J., and Pellicer, A. (2001). Incidence of sperm chromosomal abnormalities in a risk population: relationship with sperm quality and ICSI outcome. Hum. Reprod. *10,* 2084-2092.

Rubio, C., Mercader, A., Alama, P., Lizan, C., Rodrigo, L., Labarta, E., Melo, M., Pellicer, A., and Remohi, J. (2010). Prospective cohort study in high responder oocyte donors using two hormonal stimulation protocols: impact on embryo aneuploidy and development. Hum. Reprod. *9,* 2290-2297.

Rubio, C., Pehlivan, T., Rodrigo, L., Simon, C., Remohi, J., and Pellicer, A. (2005). Embryo aneuploidy screening for unexplained recurrent miscarriage: a minireview. Am. J. Reprod. Immunol. *4,* 159-165.

Rubio, C., Rodrigo, L., Mir, P., Mateu, E., Peinado, V., Milan, M., Al-Asmar, N., Campos-Galindo, I., Garcia, S., and Simon, C. (2013b). Use of array comparative genomic hybridization (array-CGH) for embryo assessment: clinical results. Fertil. Steril. *4,* 1044-1048.

Rubio, I., Kuhlmann, R., Agerholm, I., Kirk, J., Herrero, J., Escriba, M.J., Bellver, J., and Meseguer, M. (2012). Limited implantation success of direct-cleaved human zygotes: a time-lapse study. Fertil. Steril. *6,* 1458-1463.

Ruttanajit, T., Chanchamroen, S., Cram, D.S., Sawakwongpra, K., Suksalak, W., Leng, X., Fan, J., Wang, L., Yao, Y., and Quangkananurug, W. (2016). Detection and quantitation of chromosomal mosaicism in human blastocysts using copy number variation sequencing. Prenat. Diagn. *2,* 154-162.

Salvaggio, C.N., Forman, E.J., Garnsey, H.M., Treff, N.R., and Scott, R.T.,Jr. (2014). Polar body based aneuploidy screening is poorly predictive of embryo ploidy and reproductive potential. J. Assist. Reprod. Genet. *9,* 1221-1226.

Sathananthan, A.H., Kola, I., Osborne, J., Trounson, A., Ng, S.C., Bongso, A., and Ratnam, S.S. (1991). Centrioles in the beginning of human development. Proc. Natl. Acad. Sci. U. S. A. *11,* 4806-4810.

Sathananthan, A.H., Ratnam, S.S., Ng, S.C., Tarin, J.J., Gianaroli, L., and Trounson, A. (1996). The sperm centriole: its inheritance, replication and perpetuation in early human embryos. Hum. Reprod. *2,* 345-356.

Schatten, H. (2016). Human Reproduction: Updates and New Horizons Wiley).

Schneider, C.A., Rasband, W.S., and Eliceiri, K.W. (2012). NIH Image to ImageJ: 25 years of image analysis. Nat. Methods *7,* 671-675.

Schoolcraft, W.B., Katz-Jaffe, M.G., Stevens, J., Rawlins, M., and Munne, S. (2009). Preimplantation aneuploidy testing for infertile patients of advanced maternal age: a randomized prospective trial. Fertil. Steril. *1,* 157-162.

Schwanhausser, B., Busse, D., Li, N., Dittmar, G., Schuchhardt, J., Wolf, J., Chen, W., and Selbach, M. (2011). Global quantification of mammalian gene expression control. Nature *7347,* 337-342.

Shamonki, M.I., Jin, H., Haimowitz, Z., and Liu, L. (2016). Proof of concept: preimplantation genetic screening without embryo biopsy through analysis of cell-free DNA in spent embryo culture media. Fertil. Steril. *6,* 1312-1318.

Shaw, L., Sneddon, S.F., Brison, D.R., and Kimber, S.J. (2012). Comparison of gene expression in fresh and frozen-thawed human preimplantation embryos. Reproduction *5,* 569-582.

Shaw, L., Sneddon, S.F., Zeef, L., Kimber, S.J., and Brison, D.R. (2013). Global gene expression profiling of individual human oocytes and embryos demonstrates heterogeneity in early development. PLoS One *5,* e64192.

Smyth, G.K. (2005). Limma: linear models for microarray data. Bioinformatics and Computational Biology Solutions using R and Bioconductor 397-420.

Stephenson, M.D., Awartani, K.A., and Robinson, W.P. (2002). Cytogenetic analysis of miscarriages from couples with recurrent miscarriage: a case-control study. Hum. Reprod. *2,* 446-451.

Strassburger, D., Goldstein, A., Friedler, S., Raziel, A., Kasterstein, E., Mashevich, M., Schachter, M., Ron-El, R., and Reish, O. (2010). The cytogenetic constitution of embryos derived from immature (metaphase I) oocytes obtained after ovarian hyperstimulation. Fertil. Steril. *3,* 971-978.

Sullivan, E.A., Zegers-Hochschild, F., Mansour, R., Ishihara, O., de Mouzon, J., Nygren, K.G., and Adamson, G.D. (2013). International Committee for Monitoring Assisted Reproductive Technologies (ICMART) world report: assisted reproductive technology 2004. Hum. Reprod. *5,* 1375-1390.

Sundvall, L., Ingerslev, H.J., Breth Knudsen, U., and Kirkegaard, K. (2013). Inter- and intra-observer variability of time-lapse annotations. Hum. Reprod. *12,* 3215-3221.

Tachataki, M., Winston, R.M., and Taylor, D.M. (2003). Quantitative RT-PCR reveals tuberous sclerosis gene, TSC2, mRNA degradation following cryopreservation in the human preimplantation embryo. Mol. Hum. Reprod. *10,* 593-601.

Tashiro, F., Kanai-Azuma, M., Miyazaki, S., Kato, M., Tanaka, T., Toyoda, S., Yamato, E., Kawakami, H., Miyazaki, T., and Miyazaki, J. (2010). Maternal-effect gene Ces5/Ooep/Moep19/Floped is essential for oocyte cytoplasmic lattice formation and embryonic development at the maternal-zygotic stage transition. Genes Cells *8,* 813-828.

Taylor, D.M., Handyside, A.H., Ray, P.F., Dibb, N.J., Winston, R.M., and Ao, A. (2001). Quantitative measurement of transcript levels throughout human preimplantation development: analysis of hypoxanthine phosphoribosyl transferase. Mol. Hum. Reprod. *2,* 147-154.

Treff, N.R., Su, J., Taylor, D., and Scott, R.T.,Jr. (2011). Telomere DNA deficiency is associated with development of human embryonic aneuploidy. PLoS Genet. *6,* e1002161.

Uher, P., Baborova, P., Kralickova, M., Zech, M.H., Verlinsky, Y., and Zech, N.H. (2009). Non-informative results and monosomies in PGD: the importance of a third round of re-hybridization. Reprod. Biomed. Online *4,* 539-546.

Van Royen, E., Mangelschots, K., De Neubourg, D., Valkenburg, M., Van de Meerssche, M., Ryckaert, G., Eestermans, W., and Gerris, J. (1999). Characterization of a top quality embryo, a step towards single-embryo transfer. Hum. Reprod. *9,* 2345-2349.

Van Royen, E., Mangelschots, K., Vercruyssen, M., De Neubourg, D., Valkenburg, M., Ryckaert, G., and Gerris, J. (2003). Multinucleation in cleavage stage embryos. Hum. Reprod. *5,* 1062-1069.

Vanneste, E., Voet, T., Le Caignec, C., Ampe, M., Konings, P., Melotte, C., Debrock, S., Amyere, M., Vikkula, M., Schuit, F. *et al*. (2009). Chromosome instability is common in human cleavage-stage embryos. Nat. Med. *5,* 577-583.

Vassena, R., Boue, S., Gonzalez-Roca, E., Aran, B., Auer, H., Veiga, A., and Izpisua Belmonte, J.C. (2011). Waves of early transcriptional activation and pluripotency program initiation during human preimplantation development. Development *17,* 3699-3709.

Vera, M., Peinado, V., Al-Asmar, N., Gruhn, J., Rodrigo, L., Hassold, T., and Rubio, C. (2012). Human Male Meiosis and Sperm Aneuploidies. In Aneuploidy in Health and Disease, Z. Storchova ed., InTech.

Vera-Rodriguez, M., Michel, C.E., Mercader, A., Bladon, A.J., Rodrigo, L., Kokocinski, F., Mateu, E., Al-Asmar, N., Blesa, D., Simon, C., and Rubio, C. (2016). Distribution patterns of segmental aneuploidies in human blastocysts identified by next-generation sequencing. Fertil. Steril. *4,* 1047-1055.e2.

Voullaire, L., Slater, H., Williamson, R., and Wilton, L. (2000). Chromosome analysis of blastomeres from human embryos by using comparative genomic hybridization. Hum. Genet. *2,* 210-217.

Wallbutton, S., and Kasraie, J. (2010). Vacuolated oocytes: fertilization and embryonic arrest following intra-cytoplasmic sperm injection in a patient exhibiting persistent oocyte macro vacuolization--case report. J. Assist. Reprod. Genet. *4,* 183-188.

Wan, L.B., Pan, H., Hannenhalli, S., Cheng, Y., Ma, J., Fedoriw, A., Lobanenkov, V., Latham, K.E., Schultz, R.M., and Bartolomei, M.S. (2008). Maternal depletion of CTCF reveals multiple functions during oocyte and preimplantation embryo development. Development *16,* 2729-2738.

Warren, L., Bryder, D., Weissman, I.L., and Quake, S.R. (2006). Transcription factor profiling in individual hematopoietic progenitors by digital RT-PCR. Proc. Natl. Acad. Sci. U. S. A. *47,* 17807-17812.

Webster, M., Witkin, K.L., and Cohen-Fix, O. (2009). Sizing up the nucleus: nuclear shape, size and nuclear-envelope assembly. J. Cell. Sci. *Pt 10,* 1477-1486.

Wells, D., Bermudez, M.G., Steuerwald, N., Malter, H.E., Thornhill, A.R., and Cohen, J. (2005). Association of abnormal morphology and altered gene expression in human preimplantation embryos. Fertil. Steril. *2,* 343-355.

Wells, D., Ravichandran, K., Alper, M., Jain, J., Penzias, A., Benadiva, C.A., Colls, P., Konstantinidis, M., and Munne, S. (2015). Aneuploidy rates in embryos produced by fertile couples. Fertil. Steril. *3,* e307.

Wong, C.C., Loewke, K.E., Bossert, N.L., Behr, B., De Jonge, C.J., Baer, T.M., and Reijo Pera, R.A. (2010). Non-invasive imaging of human embryos before embryonic genome activation predicts development to the blastocyst stage. Nat. Biotechnol. *10,* 1115-1121.

Wu, D.D., Feng, C., Xu, X.Y., Xiao, J.Y., Liu, C., Meng, J., Wang, E.H., and Yu, B.Z. (2011). Protein kinase B/Akt may regulate G2/M transition in the fertilized mouse egg by changing the localization of p21(Cip1/WAF1). Cell Biochem. Funct. *4,* 265-271.

Wu, X., Viveiros, M.M., Eppig, J.J., Bai, Y., Fitzpatrick, S.L., and Matzuk, M.M. (2003). Zygote arrest 1 (Zar1) is a novel maternal-effect gene critical for the oocyte-to-embryo transition. Nat. Genet. *2,* 187-191.

Xu, J., Fang, R., Chen, L., Chen, D., Xiao, J.P., Yang, W., Wang, H., Song, X., Ma, T., Bo, S. *et al*. (2016). Noninvasive chromosome screening of human embryos by genome sequencing of

embryo culture medium for in vitro fertilization. Proc. Natl. Acad. Sci. U. S. A. *42,* 11907-11912.

Xue, Z., Huang, K., Cai, C., Cai, L., Jiang, C.Y., Feng, Y., Liu, Z., Zeng, Q., Cheng, L., Sun, Y.E. *et al*. (2013). Genetic programs in human and mouse early embryos revealed by single-cell RNA sequencing. Nature *7464,* 593-597.

Yan, L., Huang, L., Xu, L., Huang, J., Ma, F., Zhu, X., Tang, Y., Liu, M., Lian, Y., Liu, P. *et al*. (2015). Live births after simultaneous avoidance of monogenic diseases and chromosome abnormality by next-generation sequencing with linkage analyses. Proc. Natl. Acad. Sci. U. S. A. *52,* 15964-15969.

Yan, L., Yang, M., Guo, H., Yang, L., Wu, J., Li, R., Liu, P., Lian, Y., Zheng, X., Yan, J. *et al*. (2013). Single-cell RNA-Seq profiling of human preimplantation embryos and embryonic stem cells. Nat. Struct. Mol. Biol. *9,* 1131-1139.

Yang, Z., Liu, J., Collins, G.S., Salem, S.A., Liu, X., Lyle, S.S., Peck, A.C., Sills, E.S., and Salem, R.D. (2012). Selection of single blastocysts for fresh transfer via standard morphology assessment alone and with array CGH for good prognosis IVF patients: results from a randomized pilot study. Mol. Cytogenet. *1,* 24-8166-5-24.

Yang, Z., Zhang, J., Salem, S.A., Liu, X., Kuang, Y., Salem, R.D., and Liu, J. (2014). Selection of competent blastocysts for transfer by combining time-lapse monitoring and array CGH testing for patients undergoing preimplantation genetic screening: a prospective study with sibling oocytes. BMC Med. Genomics 38-8794-7-38.

Yu, J., Hecht, N.B., and Schultz, R.M. (2003). Requirement for RNA-binding activity of MSY2 for cytoplasmic localization and retention in mouse oocytes. Dev. Biol. *2,* 249-262.

Zhang, C., Zhang, C., Chen, S., Yin, X., Pan, X., Lin, G., Tan, Y., Tan, K., Xu, Z., Hu, P. *et al*. (2013). A single cell level based method for copy number variation analysis by low coverage massively parallel sequencing. PLoS One *1,* e54236.

Zhang, P., Zucchelli, M., Bruce, S., Hambiliki, F., Stavreus-Evers, A., Levkov, L., Skottman, H., Kerkela, E., Kere, J., and Hovatta, O. (2009). Transcriptome profiling of human pre-implantation development. PLoS One *11,* e7844.

Ziebe, S., Petersen, K., Lindenberg, S., Andersen, A.G., Gabrielsen, A., and Andersen, A.N. (1997). Embryo morphology or cleavage stage: how to select the best embryos for transfer after in-vitro fertilization. Hum. Reprod. *7,* 1545-1549.

SUPPLEMENTARY MATERIAL

7 | Supplementary material

7.1 Supplementary figures

(See next page)

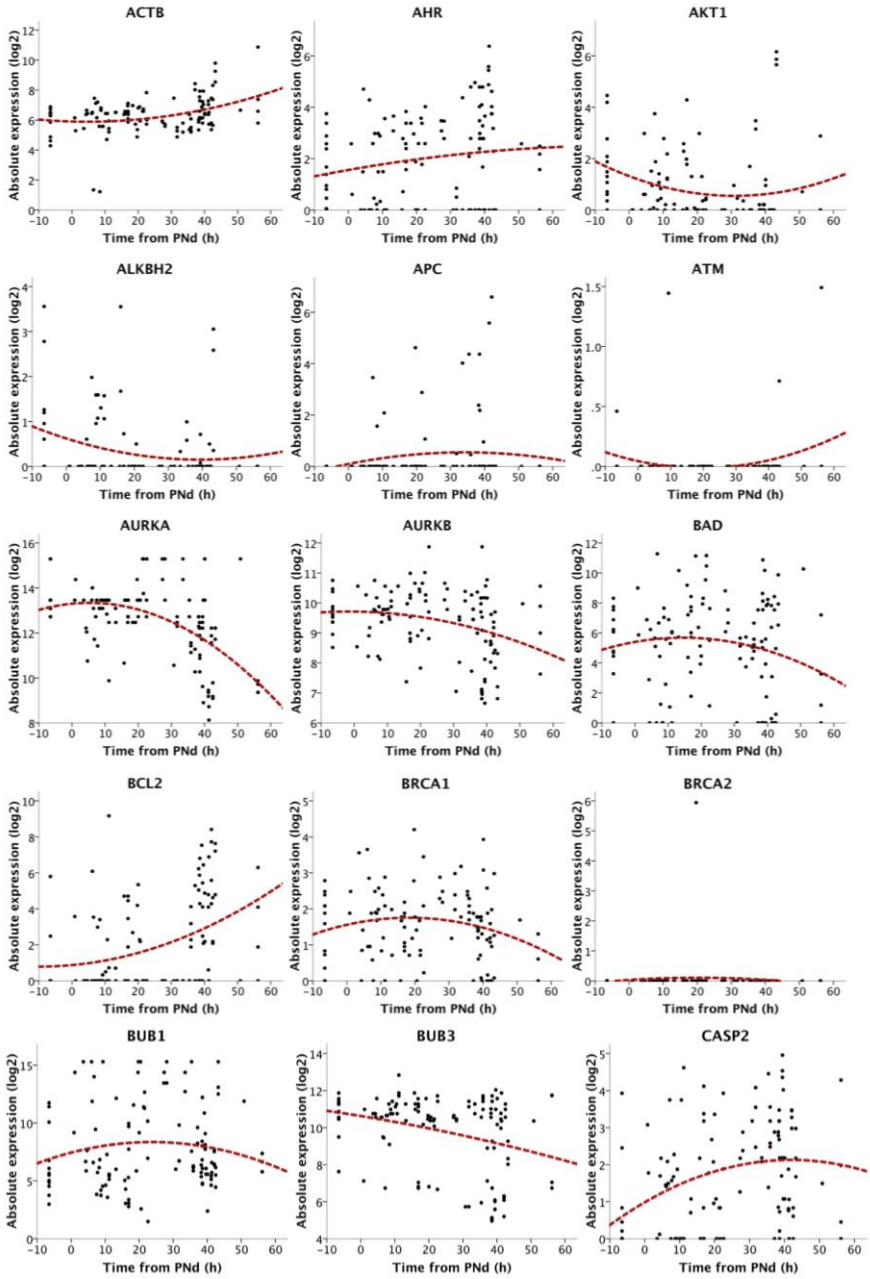

Supplementary Figure 1 | Gene expression charts with quadratic regressions.
All genes placed in alphabetic order showing expression values (28-C_t value) of single cells throughout the developmental time. PNd was established as zero and samples taken before were represented at -10 h. Quadratic regressions are with red lines.

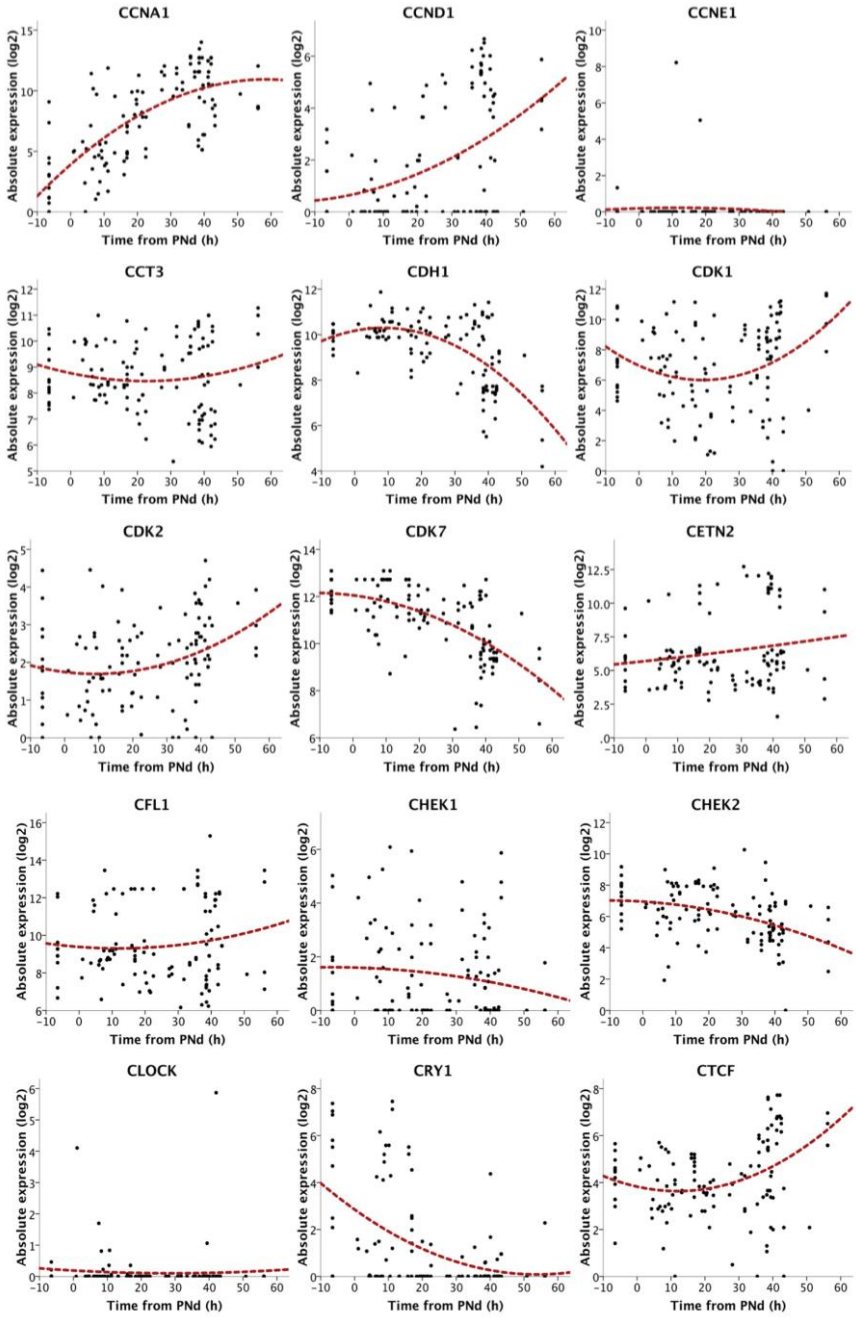

Supplementary Figure 1 (Continued)

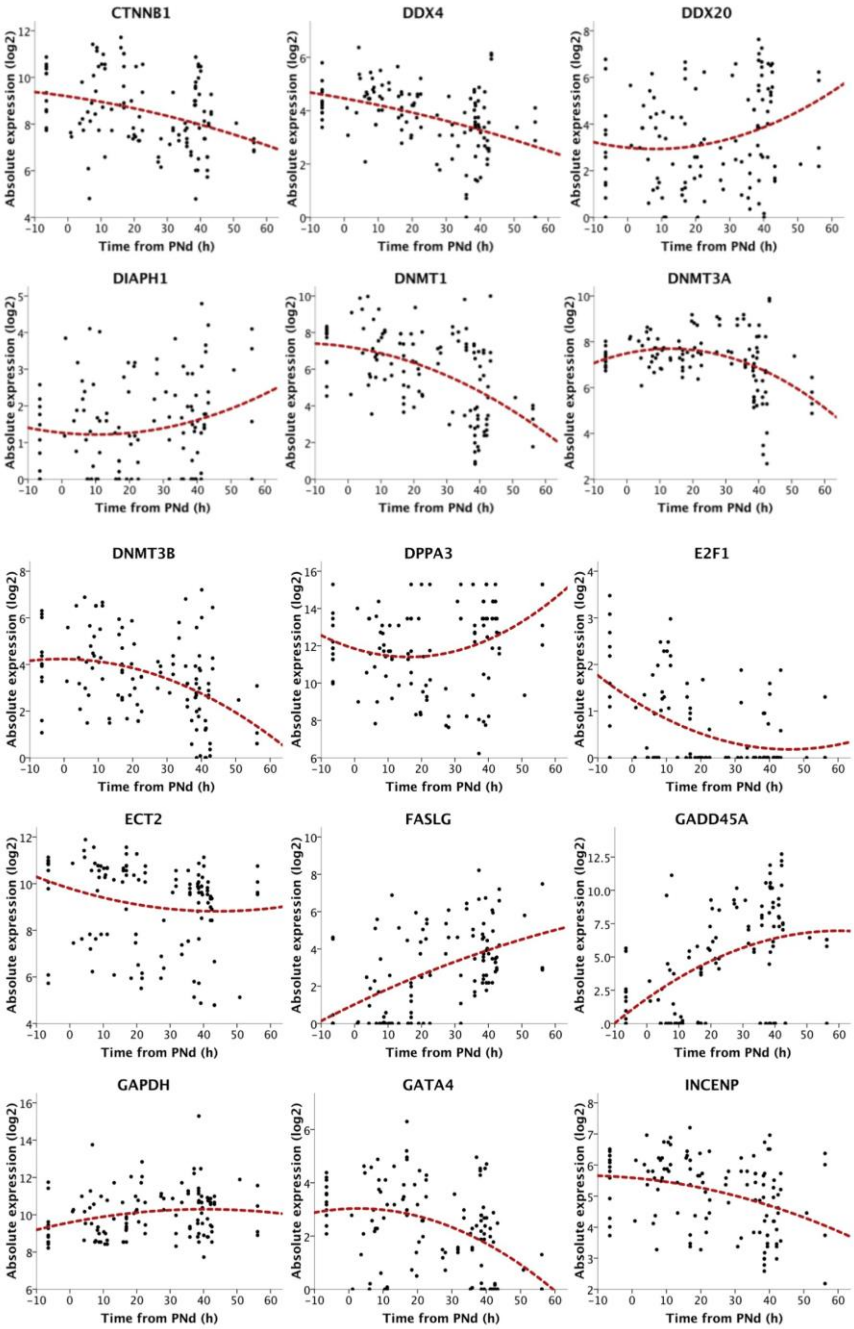

Supplementary Figure 1 (Continued)

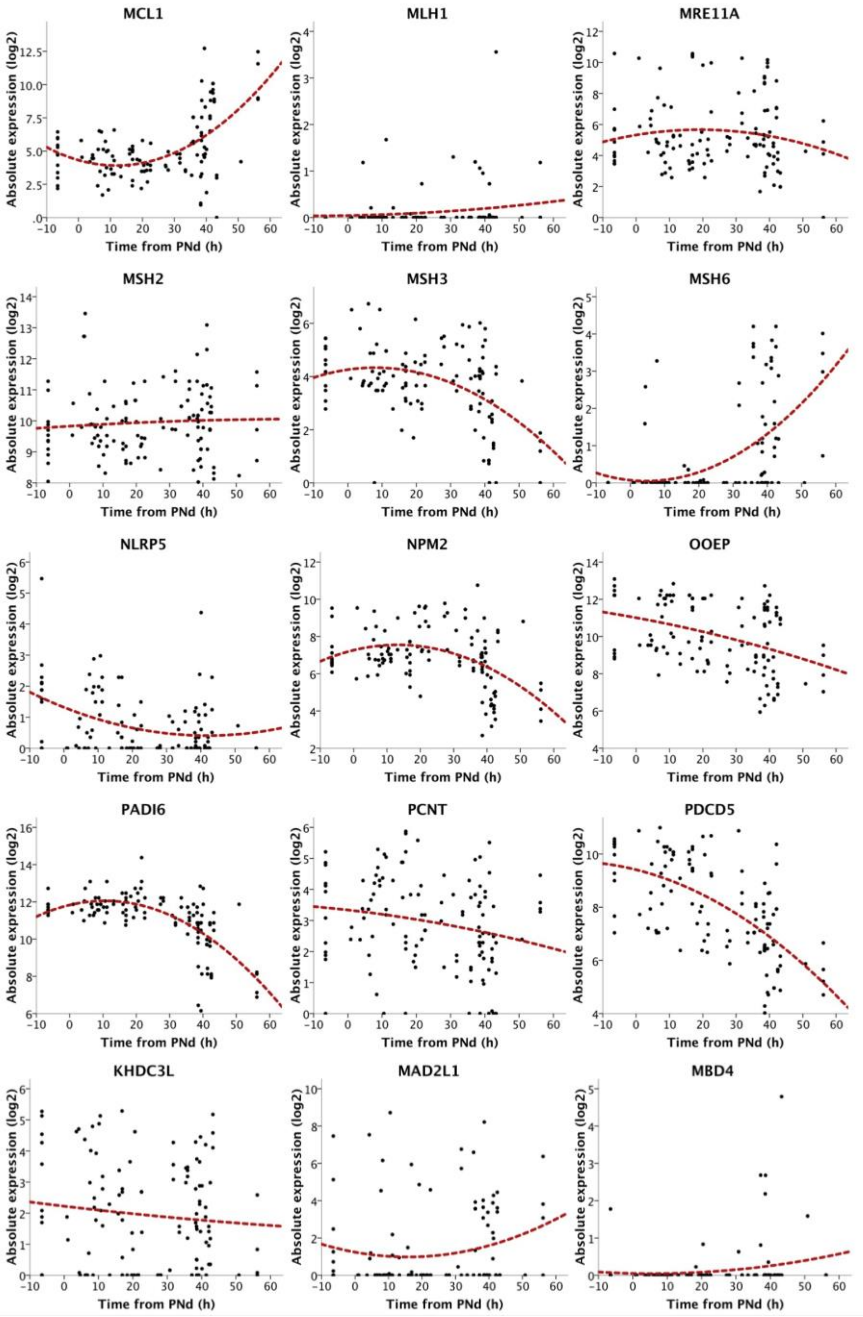

Supplementary Figure 1 (Continued)

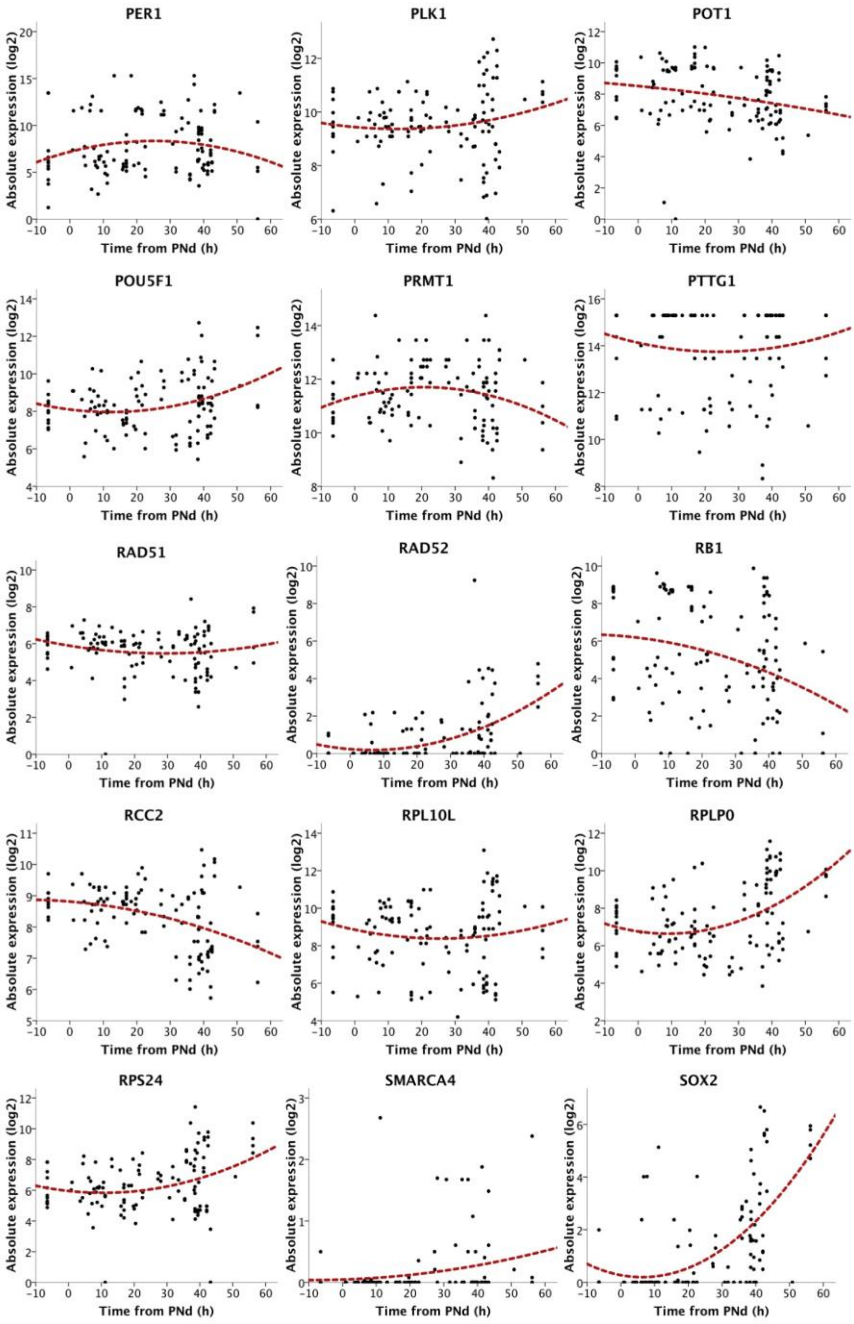

Supplementary Figure 1 (Continued)

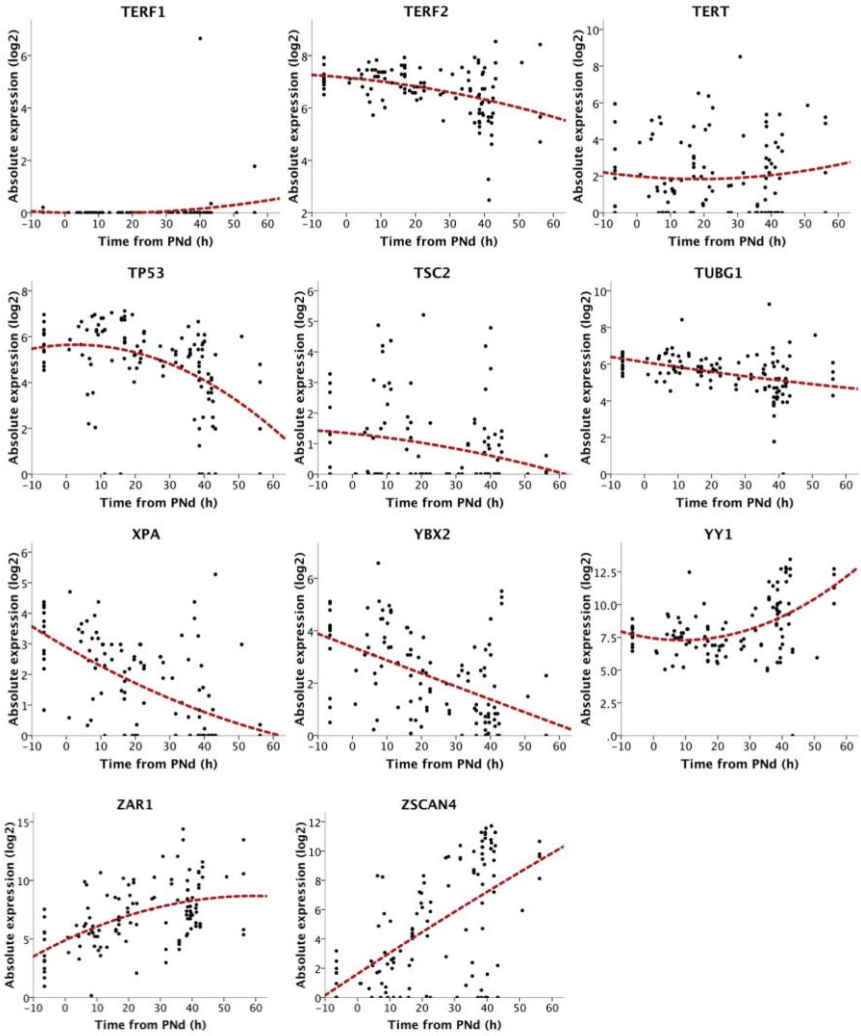

Supplementary Figure 1 (Continued)

7.2 Supplementary tables

Supplementary Table 1| Primers for gene expression analysis by RT-qPCR.

Target Gene	Gene ID	Forward primer	Reverse primer	Product Length
AHR	196	AGCCGGTGCAGAAAACAGTA	GGTCTCTATGCCGCTTGGAA	75
AKT1	207	CCATCACACCACCTGACCAA	CGAGTAGGAGAACTGGGGGA	83
ALKBH2	121642	CTGTTTGGCAAAGCTGAGGC	GGGGCCAGTTCTCTTTCATCA	127
APC	324	GGGCTTACTAATGACCACTACA	TGCAGCCTTTCATAGAGCATA	118
ATM	472	TGCTTGCTGTTGTGGACTA	ATCCAGCCAGAAAGCATCA	80
AURKA	6790	GGTGGTCAGTACATGCTCCA	GCATCCGACCTTCAATCATTTCA	90
AURKB	9212	ATGGAGAATAGCAGTGGGACAC	CAGAGGACGCCCAATCTCAA	78
BAD	572	CTCCGGAGGATGAGTGACGA	CACCAGGACTGGAAGACTCG	125
BCL2	596	AGGGTACGATAACCGGGAGAT	CATCCCACTCGTAGCCCCTC	74
BRCA1	672	AAGACTGCTCAGGGCTATCC	CCATTTCCTGCTGGAGCTTTA	96
BRCA2	675	ATGCAGCAGACCCAGCTTA	TCCTTTTGTTCAGCAGATTCCA	148
BUB1	699	ACAAGCTTCCAGTGGAGTCA	AATCCAAAGTCGCCTGGGTA	84
BUB3	9184	CTGCATACGAGCGTTTCCAAA	GGCTTGGGTCCAAATACTCAAC	86
CASP2	835	AACTGCCCAAGCCTACAGAA	TTGGTCAACCCCACGATCA	84
CCNA1	8900	GCTCGTAGGAACAGCAGCTA	CAAACTCGTCTACTTCAGGAGGATA	74
CCND1	595	ATCTACACCGACAACTCCATCC	GGTTCCACTTGAGCTTGTTCAC	79
CCNE1	898	ATACTTGCTGCTTCGGCCTT	TCAGTTTTGAGCTCCCCGTC	148
CCT3	7203	CCCGATGTGGTCATCACTGAA	CTCTGCGGATGGCTGTGATA	85
CDH1	999	CGTCACCACAAATCCAGTGAAC	TACTGCTGCTTGGCCTCAAA	78
CDK1	983	CCTAGTACTGCAATTCGGGAAA	CCTGCATAAGCACATCCTGAA	85
CDK2	1017	TGGGCCCGGCAAGATTTTAG	TGTTAGGGTCGTAGTGCAGC	91
CDK7	1022	GGGAGCCCCAATAGAGCTTATA	CTACACCATACATCCTAGCTCCA	91
CETN2	1069	GGAGTTGGGTGAGAACCTGAC	TCTTGCTCACTGACCTCTCC	90
CFL1	1072	GCTCCAAGGACGCCATCA	TCCTTGACCTCCTCGTAGCA	79
CHEK1	1111	TGGTACAACAAACCCCTCAA	CACTGGGAGACTCTGACAC	76
CHEK2	11200	GCCCTTCAGGATGGATTTGC	ACAGCTTTTGTCCCTCCCAAA	72
CLOCK	9575	CCTGAGACAGCTGCTGACAA	ACGGCCGTGTGAGATGATTT	149
CRY1	1407	AACCAGCAGATGTGTTTCCC	CCTTTCCAAAGGGCTCAGAA	87
CTCF	10664	GCGGCTTTTGTCTGTTCTAA	CTGGGCCAGCACAATTATCA	85
DDX20	11218	ATGCATCGGATTGGGAGAGC	TTTTCTTCCTCTCCCCGGCA	80
DIAPH1	1729	TCCCTTCGTGTGTCTCTCAA	TAAGGAGGCCAAGCCTTCA	75
DNMT1	1786	GCCATTGGCTTGGAGATCA	AGCAGCTTCCTCCTCCTTTA	84
DNMT3A	1788	AGCCTCAATGTTACCCTGGAAC	TACGCACACTCCAGAAAGCA	83

DNMT3B	1789	GTGAAGCACGAGGGGAATATCA	TTCCGCCAATCACCAAGTCA	100
DPPA3	359787	AAGACCAACAAACAAGGAGCC	TCCCATCCATTAGACACGCAG	90
E2F1	1869	AGCTCATTGCCAAGAAGTCCAA	TCCTGGGTCAACCCCTCAA	94
ECT2	1894	GCTGTGTCGACATGTAGCTAA	CAAAGGATTCTGGATCAGCAGTA	80
FASLG	356	CTTGGTAGGATTGGGCCTGG	TGTGTGCATCTGGCTGGTAG	91
GADD45A	1647	GCGACCTGCAGTTTGCAATA	CTTTCGGTCTTCTGCTCTCCA	63
INCENP	3619	AGCAGAAGGCTTGCCAAGAA	ATTCAGGAGCCTCTCCAGGTAA	87
MAD2L1	4085	AGATCACAGCTACGGTGACA	TGTGGTCCCGACTCTTCC	118
MBD4	8930	TGGAAGCTTCTCATCGCTAC	GCTGAAGGATACTTCTCCAGAAAC	95
MCL1	4170	TGGGTTTGTGGAGTTCTTCCA	CTCCAGCAACACCTGCAAAA	83
MRE11A	4361	AGCCAGAGAAGCCTCTTGTA	TCTGGCTAAAGCGAAGAACAC	81
MSH2	4436	GCCCAGGATGCCATTGTTAA	TTGAGTGTCTGCATTGGTTCTAC	71
MSH3	4437	TGCCATTGCCTATGCTACAC	GGCGGATAATGGGTGACAAA	78
MSH6	2956	CCAAGGCGAAGAACCTCAAC	TTGGCCCAAACCAAATCTCC	97
NPM2	10361	AAGAAGATGCAGCCGGTCAC	GGGAGAAAGCTGCACTCCTAC	84
OOEP	441161	GTGCCTGGCATGGTTTCAC	TCTGATGCATGGGCCTTCAA	87
PADI6	353238	GTACGCCACAGTGAAGATGACA	ATCCTCGTTGGGCCCATAGTA	85
PCNT	5116	TCTCTGGAAGGTTTCAGCCG	CGCACCATCTGCAGTAAAGC	88
PDCD5	9141	GGCCCAACAGGAAGCAAA	ACTGATCCAGAACTTGGGCTA	71
PER1	5187	TCTGCCGTATCAGAGGAGGT	GGTCACATACGGGGTTAGGC	77
PLK1	5347	GCAGCGTGCAGATCAACTTC	CTCGTCGATGTAGGTCACGG	83
POT1	25913	CGAGGTAGAAAGATGTCAACAGCTA	CACATAGTGGTGTCCTCTCCAAA	77
POU5F1	5460	GCTTGGGCTCGAGAAGGATG	CATAGTCGCTGCTTGATCGC	80
PRMT1	3276	AGTTCACACGCTGCCACAA	GTCTGCTTCCAGTGCGTGTA	73
PTTG1	9232	GCCTCAGATGATGCCTATCCA	TCAGGCAGGTCAAAACTCTCA	80
RAD51	5888	GGGAAGACCCAGATCTGTCA	ATGTACATGGCCTTTCCTTCAC	86
RAD52	5893	GGATCTTGGGACCTCCAAACTTA	TCTTCATGTCCTGGCTCTTCC	85
RB1	5925	CTCACCTCCCATGTTGCTCA	GGGTGTTCGAGGTGAACCAT	73
RCC2	55920	TGCCTGTACCAAACGTGGTT	GGAGAAGACTCGCTTCTGGG	86
RPL10L	140801	CGAGGTGCCTTTGGAAAACC	TTCTGAAGCTTGGTGCGGAT	86
RPS24	6229	CGAATCGTGGTTCTCTTTTCCTC	TAGTGCGGATAGTTACGGTGTC	79
SMARCA4	6597	TCCGTGGTGAAGGTGTCTTA	AGCAAGACGTTGAACTTCCC	89
TERF1	7013	CAGCTTGCCAGTTGAGAACG	GGGCTGATTCCAAGGGTGTA	117
TERF2	7014	CCACCGTTCTCAACCAACC	AACCCCATTAGAGCTGTTCCA	80
TERT	7015	CGCCTGAGCTGTACTTTGTCA	TGATGATGCTGGCGATGACC	93
TP53	7157	GTGTGGTGGTGCCCTATGAG	CGCCCATGCAGGAACTGTTA	90
TSC2	7249	GCTGAACATCATCGAACGGC	CGTGGAACTCGTTCTGGTCA	122
TUBG1	7283	GGCTCATGATGGCCAACC	CGCTTACGCAGCTTGTCATA	79

XPA	7507	ACATCATTCACAATGGGGTGATA	ACCCCAAACTTCAAGAGACC	76
YBX2	51087	GTCCTGGGCACTGTCAAA	AAAGACATCTTCCTTGGTGTCA	81
YY1	7528	CCAAGAACAATAGCTTGCCCTCA	TGTTTTCTCATGGCCGAGTTATCC	71
ZAR1	326340	TGTGTGGTGTGTACAGGGAAC	TCCTCCACTCGGTAAGGGTT	90
ZSCAN4	201516	CCCGGGATTACCCAGTCAA	AGTCTCTTGCCTTGTGTCTCTA	91
ACTB	60	NA	NA	NA
CTNNB1	1499	NA	NA	NA
DDX4	54514	NA	NA	NA
GAPDH	2597	NA	NA	NA
GATA4	2626	NA	NA	NA
KHDC3L	154288	NA	NA	NA
MLH1	4292	NA	NA	NA
NLRP5	126206	NA	NA	NA
RPLP0	6175	NA	NA	NA
SOX2	6657	NA	NA	NA

NA, DNA sequence not available.

Supplementary Table 2 | Aneuploidy screening results using single-cell aCGH.

Embryo	Cell type	aCGH result
1A1	Blast	46 XY
1A3	Blast	46 XY
1A3	PB	23 X
1B3	Blast	-1 -3 +4 -9 +10 +14 +16 +17 -18 +19 -21 -22 XY
1B3	PB	+1 +3 -4 +9 -10 -14 -16 -17 -19 +22 +X
2A3	PB	23 X
2B1	Blast	+2 +5 +6 +7 +8 +15 +17 +19 +21 XXX
2B3	Blast	46 XX
2B3	Blast	46 XX
3A1	Blast	46 X0
3B1	Blast	-1 +2 +3 -4 -5 -6 -7 +9 +11 -13 -19 +22 XY
3B2	Blast	46 XX
3C1	Blast	2p+ 2q- XY
3D1	Blast	-4 +5 +6 -7 +11 -12 -13 +14 -15 +16 -17 -18 +19 -20 -21 +22 XXY
4A1	Blast	+10 +12 +14 -16 +20 -22 XX
4A2	Blast	-1 +2 +3 +5 -9 -10 +11 +13 -15 -16 +17 XY
4B1	Blast	46 XY
4C1	Blast	46 XX
4D3	Blast	-13 XY
5A2	Blast	-1 -3 +4 +5 +6 +7 -9 +10 +11 +12 +13 -14 -15 -17 -18 -19 +20 XX
5B2	Blast	46 XX
5C1	PB	23 X
5C2	Blast	-2 +5 -9 +12 +18 +20 +21 +22 XX
5C2	Blast	-9 -15 XX
5C3	Blast	-7q -8 XXY
5D1	Blast	46 XX
5D2	Blast	-2 -5 -6 +7 +10 +13 -14 +15 +16 +17 +18 +20 +21 XX
5D3	Blast	-2 -7 -16 -19 Y0
5D3	Blast	+1 +2 +7 -9q +16 +19 XXY
6A1	Blast	46 XX
6A2	Blast	+17 XX
6A2	Blast	+17 XX
6B1	Blast	+14 XY
6B1	Blast	46 XY
6B2	Blast	-8p -13q +16 XX
6B3	PB	23 X
6C1	Blast	-16 XY
6C2	Blast	+18 XY
6C2	Blast	-10 -21 Y0
6C2	Blast	46 XY
6C2	Blast	46 XY
6D1	Blast	46 XY
6D2	Blast	46 XY
6D2	Blast	46 XY
6D2	Blast	46 XY
7A1	PB	23 X
7B1	Blast	46 XY

7B1	PB	-22 X
7B3	PB	23 X
7C1	Blast	46 XY
8A1	Blast	46 XY
8A1	Blast	46 XY
8A1	Blast	46 XY
8A1	Blast	+1 +5 -8 -9 -11 +12 +14 -15 +17 +18 -19 -20 -21 XXXYY
8A1	PB	23 X
8A2	Blast	46 XY
8A2	Blast	46 XY
8A3	Blast	46 XY
8A3	Blast	46 XY
8B1	Blast	+13 Y0
8B1	Blast	+13 Y0
8B1	Blast	+13 Y0
8B1	Blast	+13 Y0
8B2	Blast	46 XX
8B2	Blast	46 XX
8B3	Blast	46 XY
8B3	PB	23 X
8C2	Blast	-2 -4 -5 -6 -9 -13 +16 -20 XX
8C2	PB	23 X
8C3	PB	-3 -10 +12 -14 X
8D2	Blast	-6 XX
8D2	PB	+1 +12 +22 X
8D3	Blast	46 XX
8D3	Blast	46 XX
9A1	Blast	46 XY
9A4	PB	46 XX
9A4	PB	23 X
9B1	Blast	+20 XX
9B3	PB	+1 +3 +4 +5 +10 +12 +13 +19 +20 X
9B4	PB	+22 X
9C2	Blast	+2 -7 -9 -10 -11 -13 -14 +16 -17 +19 -20 -22 XY
9C2	Blast	-2 -5 +9 +10 +11 +13 +15 -16 +18 +20 -21 X0
9C3	Blast	46 XX
9C3	Blast	46 XX
9C3	Blast	46 XX
9C3	Blast	46 XX
9D1	PB	23 X
9D3	Blast	+1 +2 -3 -6 -7 -11 +15 -16 +17 -18 +19 -21 XX
9E3	Blast	46 XX

aCGH, array-comparative genomic hybridization; Blast, blastomere; PB, polar body.
Individual aCGH results from all conclusive samples have been annotated. Aneuploidies are represented by the number of the chromosome affected preceded by a minus symbol when there is a loss (Ex. -9), and a plus symbol when there is a gain (Ex. +9). The result was reported as chaotic when no individual gains or losses could be identified. The exact endowment was written for the sex chromosomes (Ex. XXXY), reporting a zero when one of the two sex chromosomes was missing (Ex. Y0).

Supplementary Table 3 | Quadratic regression analysis of individual gene expression profiles.

	Equation coefficients				Predicted Expression values	
Gene	*a*	*b(x)*	*c(x²)*	*P* value	At start time	At final time
ACTB	5.91	-0.01	6.48E-04	3.2E-04	5.91	7.60
AKT1	1.32	-0.05	8.01E-04	2.6E-02	1.32	1.05
AURKA	13.30	0.01	-1.37E-03	<1.0E-06	13.30	9.81
AURKB	9.71	-1.2E-03	-3.86E-04	4.8E-03	9.71	8.43
BCL2	0.87	0.02	8.54E-04	1.1E-04	0.87	4.50
BRCA1	1.56	0.02	-5.83E-04	4.6E-02	1.56	0.92
BUB3	10.63	-0.03	-1.69E-04	2.6E-03	10.63	8.42
CASP2	0.98	0.05	-6.55E-04	8.3E-04	0.98	2.00
CCNA1	3.92	0.24	-2.06E-03	<1.0E-06	3.92	10.93
CCND1	0.64	0.03	7.00E-04	2.0E-06	0.64	4.36
CDH1	10.17	0.03	-1.68E-03	<1.0E-06	10.17	6.50
CDK1	6.95	-0.10	2.63E-03	1.0E-02	6.95	9.60
CDK2	1.74	-0.01	6.24E-04	5.8E-03	1.74	3.07
CDK7	12.05	-0.02	-8.09E-04	<1.0E-06	12.05	8.51
CHEK2	6.95	-0.01	-6.11E-04	1.2E-05	6.95	4.28
CRY1	2.85	-0.10	9.54E-04	<1.0E-06	2.85	0.09
CTCF	3.83	-0.03	1.34E-03	4.3E-04	3.83	6.24
CTNNB1	9.19	-0.02	-2.33E-04	4.7E-04	9.19	7.28
DDX20	2.99	-0.01	9.04E-04	2.8E-02	2.99	5.02
DDX4	4.46	-0.02	-1.54E-04	8.0E-06	4.46	2.66
DNMT1	7.22	-0.03	-8.63E-04	<1.0E-06	7.22	3.03
DNMT3A	7.49	0.03	-1.17E-03	8.2E-05	7.49	5.54
DNMT3B	4.23	-1.6E-03	-8.87E-04	1.2E-05	4.23	1.36
DPPA3	11.85	-0.05	1.67E-03	1.7E-02	11.85	14.02
E2F1	1.25	-0.05	5.09E-04	<1.0E-06	1.25	0.23
FASLG	1.03	0.09	-3.23E-04	<1.0E-06	1.03	4.82
GADD45A	1.87	0.17	-1.42E-03	<1.0E-06	1.87	6.94
GAPDH	9.59	0.04	-4.36E-04	3.6E-02	9.59	10.19
GATA4	3.03	0.01	-9.43E-04	8.0E-06	3.03	0.36
INCENP	5.59	-0.01	-3.15E-04	3.6E-04	5.59	4.06

MCL1	4.32	-0.07	2.89E-03	<1.0E-06	4.32	9.55
MSH3	4.26	0.02	-1.16E-03	2.0E-06	4.26	1.65
MSH6	0.07	-0.01	1.01E-03	<1.0E-06	0.07	2.72
NLRP5	1.32	-0.04	5.22E-04	7.5E-05	1.32	0.51
NPM2	7.27	0.04	-1.65E-03	6.0E-06	7.27	4.54
OOEP	11.01	-0.03	-2.27E-04	2.4E-05	11.01	8.45
PADI6	11.83	0.04	-2.02E-03	<1.0E-06	11.83	7.89
PDCD5	9.41	-0.03	-7.92E-04	<1.0E-06	9.41	5.18
POT1	8.52	-0.02	-1.57E-04	1.8E-02	8.52	6.84
POU5F1	8.10	-0.02	9.06E-04	8.8E-03	8.10	9.70
RAD52	0.23	-0.01	1.09E-03	2.0E-06	0.23	2.85
RB1	6.20	-0.02	-6.55E-04	5.2E-03	6.20	2.99
RCC2	8.81	-0.01	-3.12E-04	4.6E-05	8.81	7.34
RPLP0	6.76	-0.03	1.49E-03	7.0E-06	6.76	9.96
RPS24	5.95	-0.02	1.09E-03	9.9E-03	5.95	8.08
SOX2	0.28	-0.02	1.88E-03	<1.0E-06	0.28	4.82
TERF2	7.16	-0.01	-2.11E-04	2.7E-05	7.16	5.81
TP53	5.64	0.01	-1.11E-03	1.0E-06	5.64	2.48
TSC2	1.33	-0.01	-1.60E-04	2.9E-02	1.33	0.17
TUBG1	6.11	-0.03	7.91E-05	1.2E-04	6.11	4.79
XPA	2.89	-0.06	2.92E-04	<1.0E-06	2.89	0.18
YBX2	3.38	-0.05	1.56E-05	<1.0E-06	3.38	0.59
YY1	7.43	-0.03	1.85E-03	2.0E-06	7.43	11.41
ZAR1	4.88	0.13	-1.08E-03	<1.0E-06	4.88	8.66
ZSCAN4	1.61	0.15	-1.37E-04	<1.0E-06	1.61	9.33

Only genes with $P<0.05$ (ANOVA test) are shown ($n = 55$).
Predicted log2 values (y) were obtained by using the quadratic equation ($y=a+bx+cx^2$) for the start time ($x = 0$) and the final time (x = 56h).

7.3 Supplementary movies

(as separate files)

Supplementary Movie 1 | Main kinetic frames for parameter calculation.
Time-lapse imaging with the identification of the annotated frames until the eight-cell stage for later parameter calculation. Multicapture images from the last frame have been included at the end of the movie.

Supplementary Movie 2 | Fragmentation appearance during zygote stage.
Embryo at the zygote stage with two visible polar bodies generating fragmentation in the top side (frames 10-28).

Supplementary Movie 3 | Fragmentation appearance during the first mitotic division.
Time-lapse imaging showing a human embryo at zygote stage with two pronuclei and two polar bodies (frames 71-86), after pronuclear disappearance (frame 87), the first mitosis starts (frame 121) and afterwards some irregularities can be detected in the membranes (frame 123) giving origin to fragments before the first mitosis is completed (frame 127).

Supplementary Movie 4 | Fragmentation appearance after the first mitotic division.
Time-lapse imaging showing a human embryo completing the first mitotic division (frame 78) and the generation of fragments in this stage (frame 93)

Supplementary Movie 5 | Fragmentation dynamics during embryo development.
A highly fragmented embryo imaging in which fusion of fragments (frames 306-316), fragment resortion for a blastomere (frames 324-332, frames 374-389), and fragment division (frames 447-458) were detected.

Supplementary Movie 6 | Multinucleation in the human embryo.
An embryo at zygote stage with 5 nuclei detected (frame 134) after a failed division attempt that generated high fragmentation.

Supplementary Movie 7 | Vacuole fusion during embryo development.
Human embryo at the zygote stage with three big vacuoles (frame 27) that are fused producing one larger one (frame 124).

Supplementary Movie 8 | Abnormal first division from 1 to 3 cells.
On the left, an embryo with normal mitotic divisions. On the right, an embryo with an abnormal first division from 1 to 3 cells. Multicapture images from the last frame have been included at the end of the movie.

Supplementary Movie 9 | Abnormal first division from 1 to 4 cells.
On the left, an embryo with normal mitotic divisions. On the right, an embryo with an abnormal first division from 1 to 4 cells. Multicapture images from the last frame have been included at the end of the movie.

Supplementary Movie 10 | Abnormal third division from 1 to 3 cells.
On the left, an embryo with normal mitotic divisions. On the right, an embryo with an abnormal third division from 1 to 3 cells. Multicapture images from the last frame have been included at the end of the movie.